# Three-Dimensional Green's Function and Its Derivatives for Anisotropic Elastic, Piezoelectric and Magnetoelectroelastic Materials

THESIS

in fulfillment of the requirements for the degree of
Doctor of Engineering (Dr.-Ing.)
at the Faculty of Science and Technology
of the University of Siegen

by

Longtao Xie

First reviewer (Advisor):     Prof. Dr.-Ing. habil. Dr. h.c. Chuanzeng Zhang

Second reviewer:     Prof. Dr.-Ing. habil. Wilfried Becker

Date of the oral examination:     July 15, 2016

Siegen, August 2016

# Abstract

This thesis mainly deals with the Green's function for linear generally anisotropic materials in the infinite three-dimensional space, also called the fundamental solution. The detailed derivations and the numerical results of the explicit expressions of the Green's function and its first and second derivatives based on the residue calculus method (RCM), Stroh formalism method (SFM) and unified explicit expression method (UEEM) are presented. The numerical examples of the three different methods are compared with each other for the anisotropic elasticity. All three methods are accurate for an arbitrary point in non-degenerate cases. For nearly degenerate cases, both the RCM and the SFM become unstable while the UEEM keeps accurate. Moreover, the SFM is more stable than the RCM. To overcome the difficulty in nearly degenerate cases and degenerate cases, some material constants are slightly changed in the RCM and the SFM. Although the UEEM has some advantages compared with the RCM and the SFM, it is difficult to be extended to the multifield coupled materials. The RCM and SFM are extended to the piezoelectric materials and compared with each other. Since the SFM has a better performance than the RCM for the piezoelectric materials, it is extended further to the magnetoelectroelastic materials. The UEEM is implemented into a Boundary Element Method (BEM) as an application. Some demonstrative anisotropic elastic problems are solved by the developed BEM.

# Zusammenfassung

Diese Arbeit behandelt hauptsächlich die Greensche Funktion für lineare allgemein anisotrope Materialien im unendlichen dreidimensionalen Raum, die auch als Fundamentallösung bezeichnet wird. Die detaillierten Herleitungen und die numerischen Auswertungen der expliziten Ausdrücke der Greenschen Funktion bzw. deren ersten und zweiten Ableitung, die auf der Methode der Residuen (RCM), dem Stroh-Formalismus (SFM) sowie der Unified Explicit Expression Method (UEEM) basieren, werden ebenfalls behandelt. Die numerischen Beispiele der drei verschiedenen Methoden werden für die Elastizitätstheorie miteinander verglichen. In nicht-degenerierten Fällen sind alle drei Methoden exakt für einen beliebigen Punkt. Bei nahezu degenerierten Fällen werden sowohl die RCM als auch die SFM instabil, während die UEEM ihre Gültigkeit behält. Ungeachtet dessen ist die SFM etwas stabiler als die RCM. Um deren Instabilität in degenerierten und nahezu degenerierten Fällen zu überwinden, werden in der RCM und der SFM einige Materialkonstanten leicht modifiziert. Trotz der Vorteile der UEEM im Vergleich zu RCM und SFM, ergeben sich Schwierigkeiten bei der Erweiterung auf Mehrfeldmaterialien. Die RCM und die SFM werden auf piezoelektrische Materialien erweitert und miteinander verglichen. Dadurch, dass die SFM bessere Ergebnisse für piezoelektrische Materialien liefert als die

RCM, wird sie zusätzlich auf magnetoelektroelastische Materialien erweitert. Darüber hinaus wird die UEEM als Anwendung in einem BEM-Programm implementiert, mit dem sich einfache Elastizitätsprobleme lösen lassen.

# Acknowledgments

This thesis was completed in the course of my research activity as a PhD candidate from 2011 to 2016 at the Chair of Structural Mechanics, Department of Civil Engineering, University of Siegen, Germany.

I would like to thank my advisor, Prof. Dr.-Ing. habil. Dr. h.c. Chuanzeng Zhang as the first reviewer of my thesis, for his supervision. His scientific vision has always inspired and motivated my research work. I am very grateful to him for his patience, immense and continuous support. His guidance helped me in the whole PhD study including the writing of this thesis. This thesis could not have been completed without his help and support.

My sincere thanks to Prof. Dr.-Ing. habil. Wilfried Becker as the second reviewer of my thesis for his precious time spent to read and check my thesis in details, and his valuable comments and suggestions to improve the thesis. I would like also to thank Prof. Dr.-Ing. Torsten Leutbecher and Prof. Dr.-Ing. Ulrich Schmitz as members of the Doctoral Commission for their time and effort.

I would like to thank Professor Chyanbin Hwu from the National Cheng Kung University, Taiwan. During his scientific visit at the Chair of Structural Mechanics of the University of Siegen we had a lot of scientific discussions especially on the powerful Stroh formalism method, which have been very helpful for my PhD work. My sincere thanks also to Professor Ernian Pan from the University of Akron, USA, for valuable discussions in the course of my PhD study.

I would like to thank my colleagues Meike Stricker, Pedro Villamil, Hui Zheng, Benjamin Ankay, Elias Perras and many our former and current international guests at the Chair of Structural Mechanics for giving me a pleasant working atmosphere.

Finally, I would like to thank my family, particularly my parents and my wife, for the continuous support, encouragement, patience and love that I have received.

This work is supported by the China Scholarship Council (CSC), which is also gratefully acknowledged.

August 2016, Siegen                                                    Longtao Xie

# Contents

# List of Figures

# List of Tables

# Chapter 1

# Introduction

## 1.1  Anisotropic materials and Green's function

A material is said to be anisotropic when the deformation behavior of the material depends upon the orientation; that is, the stress-strain response of the material in one direction is different from the others. An anisotropic material is quite different from an isotropic material whose properties keep the same along all directions. Although the isotropic material is easy to understand since most theories of elasticity are valid for isotropic materials, the anisotropic materials are more common in the nature and daily life.

Early investigations of the anisotropy were motivated by the response of the naturally anisotropic materials such as wood and crystalline solids. Anisotropic materials may have special symmetries. Metals are typical anisotropic crystalline solids. They can be divided into many classes according to their symmetry properties. Among the commonly used metals, Al, Cu, Ni and Ag are cubic materials, Mg, Zn and $Al_2O_3$ are hexagonal or transversely isotropic materials, and Sn and Zr are tetragonal materials. In the modern technology, the extensive use of the composites (Jones, 1998) has brought forward many new types of anisotropic materials. Recently, the magnetoelectroelastic coupling composite materials have attracted much attention from engineers and scientists due to the multi-physical energy conversion capacities and the design ability. Most composites are essentially anisotropic.

A proper modeling of the behaviors of the anisotropic materials is required by the designs and applications of the anisotropic materials. In the linear theory of elasticity, the anisotropic property of materials is described by a symmetric matrix establishing a relation between the stresses and the strains. For a certain type of anisotropic materials referred to a coordinate system based on the symmetry of the materials, the matrix can be of a simple form, i.e., most components of the matrix are zero and the number of the independent non-zero components of the matrix is small. For example, a transversely isotropic elastic material referred to a Cartesian coordinate system with the $x_3$-axis along the symmetry axis of the material has 12 non-zero components, among which only 5 components are independent. For a generally anisotropic material, the symmetric matrix has 21 independent components which increases the difficulty to obtain the solution of a particular problem for the anisotropic materials. Although with a proper choice on the coordinate system the matrix of many materials can be kept simple, any transformation of the coordinate system will cause the matrix to be mathematically generally anisotropic. Therefore general theory for the generally anisotropic materials is preferred.

The theoretical formulations presented in this thesis are for generally or fully anisotropic materials.

The Green's function is a powerful tool to solve the boundary value problems. It can be used to solve many anisotropic problems in the applied mechanics and solid physics such as dislocation problems, inhomogeneous problems and contact problems. The derivatives of the Green's function are usually required to obtain the internal stresses in the solids. Moreover, the Green's function and its derivatives are the basic stones of the boundary integral equation method or the boundary element method (BEM), which several has advantages in the numerical analysis of many engineering problems such as fracture mechanics problems and acoustic problems especially in the infinite domain.

Physically speaking, the Green's function is the response at an observation point due to a point source applied at a particular point. When the domain is infinite, the Green's function is also referred to as the *displacement fundamental solution* of the problem. The static Green's function in the infinite domain is simply called the Green's function throughout this thesis unless special statement is given. In elasticity, the Green's function for the isotropic materials has a simple form, while it is complicated for the generally anisotropic materials. The analytical or exact Green's function is only available for special cases of anisotropic materials such as the transversely isotropic materials (Dederichs and Liebfried, 1969; Pan and Chou, 1976). The study on the anisotropic Green's function can be traced back to the works of Fredholm (1900), Lifshitz and Rozenzweig (1947) and Synge (1957). In the early research of the Green's function, many approximate solutions of the Green's function were presented (Barnett, 1972; Gundersen and Lothe, 1987; Lie and Koehler, 1968; Mura, 1987). Recently, Shiah et al. (2012) presented an efficient evaluation of the Green's function and its derivatives by representing the Green's function as a Fourier series and Tan et al. (2013) applied the evaluation technique in the BEM. Wang (1997) re-investigated the explicit expression of the Green's function for generally anisotropic materials and suggested a mall perturbation on the material constants for the practical applications. Since then many efforts have been made to derive the explicit expressions of the Green's function and its derivatives. The works of Malén (1971), Lavagnino (1995), Ting and Lee (1997), Sales and Gray (1998), Lee (2003) and Buroni and Sáez (2013) should be cited here among others. Here the word *explicit* means that no numerical integration or differentiation method is needed in the calculation.

The main topic of this thesis is the derivation of the explicit expressions of the Green's function and its first and second derivatives for the three-dimensional (3D) generally anisotropic materials including linear elastic, piezoelectric and magnetoelectroelastic materials. Although the Green's function for 3D anisotropic elastic materials has been investigated very comprehensively since many years, it is still a highly demanding issue especially in the BEM community where an accurate and efficient numerical evaluation of the Green's function and its derivatives is especially important.

## 1.2   State of the art and objectives

The line integral expression of the Green's function was first presented by Fredholm (1900). There are mainly two ways to evaluate the Green's function explicitly. A straightforward way is to apply the residue calculus to the line integral, which leads to an expression in terms of the roots of a polynomial equation. The other way is using the so called Stroh

formalism method, in which the expression is constructed from the eigenvectors of the Stroh eigenvalue problem (Malén, 1971). The relation between the two approaches is that the roots of the polynomial equation in the first approach is identical to the eigenvalues of the Stroh eigenvalue problem in the second approach. The roots and the eigenvalues are both called *the Stroh eigenvalues*. In these two approaches, the expression for distinct Stroh eigenvalues is different from that for the repeated or degenerated Stroh eigenvalues. For the general application, additional numerical treatments should be made, for example by a small perturbation on the material constants. To overcome the degeneracy problem with repeated Stroh eigenvalues, Ting and Lee (1997) proposed a unified explicit expression of the Green's function. Here the word *unified* means that after a rewritten of the expression for distinct Stroh eigenvalues, the expression remains applicable even when the Stroh eigenvalues are identical. The word *unified* is used to emphasize the difference from the explicit expression which changes when the multiplicity of the Stroh eigenvalues changes.

Due to their applications in the BEM for the analysis of the anisotropic elastic boundary value problems, many efforts have been made to derive the explicit expressions for the first and second derivatives of the Green's function. Most existing expressions are obtained by taking the derivatives of the Green's function with respect to the spherical coordinates, which can be transformed to the Cartesian coordinate system if necessary. Some representative examples of the previous investigations on the topic are the works by Sales and Gray (1998), Lavagnino (1995), Phan et al. (2004, 2005), Lee (2009), Shiah et al. (2010) and Buroni and Sáez (2013). The explicit expressions with high-order tensors in the Cartesian coordinate system were presented by Lee (2003) and Buroni and Sáez (2010). Different from the other works, Buroni and Sáez (2013) suggested a way to find unified expressions which remain applicable even when the Stroh eigenvalues degenerate or become identical.

The main aim of this thesis is to derive and investigate several explicit expressions of the Green's function and its first and second derivatives for the generally anisotropic linear elastic, piezoelectric and magnetoelectroelastic materials and their numerical evaluations. With the explicit expressions given in the Cartesian coordinate system, the main objectives of this thesis are

- to present alternative explicit expressions of the derivatives of the Green's function by using the residue calculus method, the Stroh formalism method and the method similar to that suggested by Ting and Lee (1997);

- to give a comparison of the three explicit expressions regarding their accuracy and efficiency in the numerical calculations for the anisotropic linear elastic materials;

- to obtain new explicit expressions for the linear piezoelectric and magnetoelectroelastic materials; and finally,

- to implement the unified explicit expressions into a BEM and conduct the verification tests by numerical examples.

## 1.3  Overview of the thesis

Throughout this thesis a vector, a tensor or a matrix is given either in index notation or represented by a bold letter. The summation convention is applied over repeated indices unless otherwise explicitly declared. The lowercase Latin indices take the values 1, 2, 3, while the capital Latin indices take the values 1, 2, 3, 4 for piezoelectric materials, and 1, 2, 3, 4, 5 for magnetoelectroelastic materials. A comma after a quantity $()_{,i}$ denotes spatial derivatives.

After a brief introduction in this chapter, Chapter 2 presents some theoretical foundations which are essential to the study of the Green's function for anisotropic materials. In particular, the basic equations for the anisotropic linear elastic, piezoelectric and magnetoelectroelastic materials, the classical Stroh formalism and the basic concepts of the Green's function are introduced. In addition, the boundary integral equations for 3D generally anisotropic and linear elastic materials are presented as an application of the Green's function and its derivatives.

In Chapter 3, three different explicit expressions of the Green's function and its first and second derivatives for the generally anisotropic linear elastic materials are presented. Besides, the numerical integration method to calculate the Green's function and its derivatives are also presented. All the four methods are coded into FORTRAN programs and compared with each other through numerical examples in details.

In Chapter 4, based on the comparison between the numerical evaluations of the different expressions in Chapter 3, the explicit expressions by using the residue calculus method and the Stroh formalism method are extended to the anisotropic linear piezoelectric materials. The two methods are verified by the analytical solutions and compared with each other with respect to their efficiency and accuracy.

In Chapter 5, the explicit expressions of the Green's function and its derivatives by the Stroh formalism method are further extended to the anisotropic linear magnetoelectroelastic materials, since they have advantages in the accuracy and efficiency compared with the expressions by the residue calculus method.

In Chapter 6, the unified explicit expressions for anisotropic linear elastic materials are implemented into a BEM program, since they seem to be most accurate and efficient. The BEM program is tested by some examples.

The last chapter summarizes the thesis with some concluding remarks and an outlook on future research works.

# Chapter 2

# Mathematical preliminaries

This chapter is about some basic aspects related to the study of the Green's function for the anisotropic materials in the three-dimensional infinite space. The basic equations for the elastic, piezoelectric and magnetoelectroelastic materials are introduced in Secotins 2.1, 2.2 and 2.3, respectively. In Section 2.4, the Stroh formalism, which is very useful in solving the problems with anisotropic materials, is presented briefly with an emphasis on the Stroh eigenvalue problem for an oblique plane, which will be used in the following chapters. In Section 2.5, the role of the Green's function in a general differential equation and the basic knowledge of the Green's function for multifield materials are discussed. Finally, the application of the Green's function and its derivatives in the boundary integral equations are shown in the last section.

## 2.1 Basic equations of anisotropic linear elasticity

For a 3D linear and homogeneous elastic solid, when it is distorted the strain tensor $\varepsilon_{ij}$ is related to the derivative of the displacement $u_i$ by

$$\varepsilon_{ij} = (u_{i,j} + u_{j,i})/2, \tag{2.1}$$

where the comma $()_{,i}$ denotes the spatial derivative. The components of the strain tensor $\varepsilon_{ij}$ are to be distinguished from the usual engineering strains which are equal to $\varepsilon_{ij}$ for $i = j$, but twice the value for $i \neq j$.

The general linear relation between the stress $\sigma_{ij}$ and the strain $\varepsilon_{ij}$ is usually given by Hooke's law

$$\sigma_{ij} = c_{ijkl}\varepsilon_{kl}, \tag{2.2}$$

where the fourth-order tensor $c_{ijkl}$ is the elastic stiffness tensor or the elasticity tensor. It possesses full symmetry

$$c_{ijkl} = c_{jikl} = c_{ijlk} = c_{klij} \tag{2.3}$$

and is positive definite in the sense that

$$c_{ijkl}\varepsilon_{ij}\varepsilon_{kl} > 0 \tag{2.4}$$

for any non-zero strain tensor $\varepsilon_{ij}$.

Considering the body force $f_i$, the static equilibrium equation is given by

$$\sigma_{ij,i} + f_j = 0, \tag{2.5}$$

The governing equation in terms of the displacement $u_i$ for the elasticity problems can be obtained by substituting the Eqs. (2.1) and (2.2) into Eq. (2.5), i.e.,

$$c_{ijkl}u_{k,li} + f_j = 0. \tag{2.6}$$

## 2.2 Basic equations of linear piezoelectricity

We consider a linear and homogeneous piezoelectric solid in a 3D Cartesian coordinate system. The static equilibrium equation and the electrostatic equation are given by

$$\begin{aligned} \sigma_{ij,i} + f_j &= 0, \\ D_{i,i} - f^e &= 0, \end{aligned} \tag{2.7}$$

where $D_i$ and $f^e$ are the electric displacement vector and the electric charge density, respectively. The relation between the electric field $E_i$ and the electric potential $\phi$ is defined by the equation

$$E_i = -\phi_{,i}. \tag{2.8}$$

The linear constitutive relations between $\sigma_{ij}$, $D_i$, $\varepsilon_{ij}$ and $E_i$ are

$$\begin{aligned} \sigma_{ij} &= c_{ijmn}\varepsilon_{mn} - e_{nij}E_n, \\ D_i &= e_{imn}\varepsilon_{mn} + \kappa_{in}E_n, \end{aligned} \tag{2.9}$$

where $e_{imn}$ and $\kappa_{in}$ are the piezoelectricity tensor and the dielectricity tensor, respectively. They have the following symmetry relations

$$e_{imn} = e_{inm}, \quad \kappa_{in} = \kappa_{ni}. \tag{2.10}$$

Moreover the dielectricity tensor $\kappa_{ij}$ is positive definite, i.e.,

$$\kappa_{ij}E_iE_j > 0, \tag{2.11}$$

for any non-zero electric field vector $E_i$.

The basic equations (2.7)-(2.9) can be written into a compact form by introducing the generalized stress and strain tensors and the generalized displacement vector as (Barnett and Lothe, 1975)

$$\sigma_{iJ} = \begin{cases} \sigma_{ij}, & J = j \le 3, \\ D_i, & J = 4, \end{cases} \tag{2.12a}$$

$$\varepsilon_{Mn} = \begin{cases} \varepsilon_{mn}, & M = m \le 3, \\ -E_n, & M = 4, \end{cases} \tag{2.12b}$$

$$u_I = \begin{cases} u_i, & I = i \le 3, \\ \phi, & I = 4. \end{cases} \tag{2.12c}$$

With Eq. (2.12), Eq. (2.7) becomes

$$\sigma_{iJ,i} + f_J = 0, \tag{2.13}$$

where

$$f_J = \begin{cases} f_j, & J = j \le 3, \\ -f^e, & J = 4, \end{cases} \tag{2.14}$$

and Eq. (2.9) becomes

$$\sigma_{iJ} = c_{iJMn}\varepsilon_{Mn} = c_{iJMn}u_{M,n}, \tag{2.15}$$

where

$$c_{iJMn} = \begin{cases} c_{ijmn}, & J = j \le 3, \ M = m \le 3, \\ e_{nij}, & J = j \le 3, \ M = 4, \\ e_{imn}, & J = 4, \ M = m \le 3, \\ -\kappa_{in}, & J = 4, \ M = 4, \end{cases} \tag{2.16}$$

with the symmetry relation

$$c_{iJMn} = c_{nMJi}. \tag{2.17}$$

Substituting Eq. (2.15) into Eq. (2.13), we have the governing equations in terms of the generalized displacement

$$c_{iJMn}u_{M,ni} + f_J = 0. \tag{2.18}$$

## 2.3 Basic equations of linear magnetoelectroelasticity

Let us consider a magnetoelectroelastic solid in a fixed 3D Cartesian coordinate system $x_i$ $(i = 1, 2, 3)$. The equilibrium equations and the Gauss equations are given by

$$\begin{aligned} \sigma_{ij,i} + f_j &= 0, \\ D_{i,i} - f^e &= 0, \\ B_{i,i} - f^m &= 0, \end{aligned} \tag{2.19}$$

where $B_i$ and $f^m$ are the magnetic induction vector and the magnetic charge density, respectively.

It should be remarked here that according to Maxwell's equations for magnetism, the magnetic charge density $f^m$ is always zero, because there are no magnetic monopoles observed (Fitzpatrick, 2008). However, the magnetic charge density $f^m$ is taken into account in this study as in many other references in literature, just for the mathematical convenience.

The gradient equation representing magnetic field-potential relation is determined by

$$H_i = -\psi_{,i}, \tag{2.20}$$

where $H_i$ and $\psi$ are the magnetic field vector and the magnetic potential, respectively.

The constitutive equations are given by

$$\begin{aligned} \sigma_{ij} &= c_{ijkl}\varepsilon_{kl} - e_{lij}E_l - h_{lij}H_l, \\ D_i &= e_{ikl}\varepsilon_{kl} + \kappa_{il}E_l + \alpha_{il}H_l, \\ B_i &= h_{ikl}\varepsilon_{kl} + \alpha_{il}E_l + \mu_{il}H_l, \end{aligned} \tag{2.21}$$

where $\mu_{il}$, $h_{ikl}$ and $\alpha_{il}$ are the magnetic permeability, the piezomagnetic and the magnetoelectric coefficients, respectively. The material property tensors $\mu_{il}$, $h_{ikl}$ and $\alpha_{il}$ have the following symmetry relations

$$\mu_{il} = \mu_{li}, \quad h_{ikl} = h_{ilk}, \quad \alpha_{lk} = \alpha_{li}. \tag{2.22}$$

Moreover the magnetic permeability coefficients are positive definite in the sense that

$$\mu_{ij} H_i H_j > 0, \tag{2.23}$$

for any non-zero magnetic field vector $H_i$.

Following the notation proposed by Barnett and Lothe (1975), the basic equations can be written into a contract form. Introducing the generalized stress and body force as

$$\sigma_{iJ} = \begin{cases} \sigma_{ij} & J \le 3, \\ D_i & J = 4, \\ B_i & J = 5, \end{cases} \quad \text{and } f_J = \begin{cases} f_j & J \le 3, \\ -f^e & J = 4, \\ -f^m & J = 5, \end{cases} \tag{2.24}$$

the equilibrium and Gauss equations (2.19) become

$$\sigma_{iJ,i} + f_J = 0. \tag{2.25}$$

Introducing the generalized strain tensor, elasticity tensor and displacement vector as

$$\varepsilon_{Kl} = \begin{cases} \varepsilon_{kl} & K \le 3, \\ -E_l & K = 4, \\ -H_l & K = 5, \end{cases}$$

$$c_{iJKl} = \begin{cases} c_{ijkl} & J, K \le 3, \\ e_{lij} & J \le 3, K = 4, \\ e_{ikl} & J = 4, K \le 3, \\ q_{lij} & J \le 3, K = 5, \\ q_{ikl} & J = 5, K \le 3, \\ -\alpha_{il} & J = 4, K = 5 \text{ or } J = 5, K = 4, \\ -\kappa_{il} & J, K = 4, \\ -\mu_{il} & J, K = 5, \end{cases} \tag{2.26}$$

$$u_I = \begin{cases} u_i & I \le 3, \\ \phi & I = 4, \\ \psi & I = 5, \end{cases}$$

the constitutive equations (2.21) become

$$\sigma_{iJ} = c_{iJKl} \varepsilon_{Kl} = c_{iJKl} u_{K,l}. \tag{2.27}$$

Here the repeated capital subscript denotes the summation from 1 to 5, and $c_{iJKl}$ has the following symmetry

$$c_{iJKl} = c_{lKJi}. \tag{2.28}$$

8

Substituting Eq. (2.27) into Eq. (2.25), we have the following governing equations in terms of the generalized displacement components,

$$c_{iJMn}u_{M,ni} + f_J = 0. \tag{2.29}$$

The governing equations for the elastic, piezoelectric and magnetoelectroelastic materials, i.e., Eq. (2.6), Eq. (2.18) and Eq. (2.29), are very similar to each other except the range of some indices.

In engineering it is more convenient to give a coefficient tensor in a matrix notation. The contracted form of the coefficient tensor can be recast into a matrix by utilizing the following mapping of indices ($iJ$ or $Mn \to P$)

$$
\begin{array}{cccccc}
11 \to 1, & 22 \to 2, & 33 \to 3, & 23 \to 4, & 31 \to 5, & 12 \to 6, \\
41 \to 7, & 42 \to 8, & 43 \to 9, & 51 \to 10, & 52 \to 11, & 53 \to 12.
\end{array} \tag{2.30}
$$

The sizes of the matrix for elastic, piezoelectric and magnetoelectroelastic materials are $6 \times 6$, $9 \times 9$ and $12 \times 12$, respectively.

## 2.4 Stroh formalism

The classic Stroh formalism is widely used in the analysis of the two-dimensional deformation for linear anisotropic materials. Here the two-dimensional deformation means that the deformation is independent of one of the three coordinates. The first literature on the two-dimensional deformation may be given by Eshelby et al. (1953). Not all results for this well-known formalism are due to Stroh (1958, 1962). It was named after Stroh because he laid the foundations for researchers who followed him. Most of the contents presented in this section are excerpted from Ting (1996) and Hwu (2010).

Since the Stroh formalism for piezoelectric and magnetoelectroelastic materials can be easily extended from the Stroh formalism for the elastic materials, in this section only the elasticity case is considered.

### 2.4.1 A general solution in anisotropic linear elasticity

With absence of the body force and consideration of the symmetries $c_{ijkl} = c_{jikl}$ and $()_{,ij} = ()_{,ji}$, the governing equation (2.6) for the elastic materials becomes

$$c_{ijkl}u_{k,jl} = 0. \tag{2.31}$$

For a three-dimensional elastic state in which the deformation is independent of one (say $x_3$) of the three Cartesian coordinates, Eshelby et al. (1953) gave a general solution of the displacement

$$u_i = \sum_{\alpha=1}^{3} a_{i\alpha}f_\alpha(z_\alpha), \tag{2.32}$$

where $z_\alpha = x_1 + p_\alpha x_2$, $f_\alpha(z)$ is an arbitrary function, $p_\alpha$ is a root with positive imaginary part of a sextic equation

$$|c_{i1k1} + p(c_{i1k2} + c_{i2k1}) + p^2 c_{i2k2}| = 0, \tag{2.33}$$

9

and $a_{i\alpha}$, associated with $p_\alpha$, satisfies

$$\{c_{i1k1} + p(c_{i1k2} + c_{i2k1}) + p^2 c_{i2k2}\}a_i = 0, \tag{2.34}$$

in which $a_{i\alpha}$ and $p_\alpha$ are denoted as $a_i$ and $p$ for simplify. Introducing a vector $\phi_i$ defined by

$$\phi_{i,1} = \sigma_{i2} \quad \phi_{i,2} = -\sigma_{i1}, \tag{2.35}$$

the general solution of the vector $\phi_i$ is

$$\phi_i = \sum_{\alpha=1}^{3} b_{i\alpha} f_\alpha(z_\alpha), \tag{2.36}$$

where $b_i = (c_{i2k1} + pc_{i2k2})a_i$ in which $b_{i\alpha}$ is simplified as $b_i$.

$p$ and $a_i$, as well as $b_i$, can be obtained by solving Eqs. (2.33) and (2.34), or by solving a standard eigenvalue problem which is given in the vector and matrix notation by

$$\mathbf{N}\boldsymbol{\xi} = p\boldsymbol{\xi}, \tag{2.37}$$

$$\mathbf{N} = \begin{pmatrix} \mathbf{N}_1 & \mathbf{N}_2 \\ \mathbf{N}_3 & \mathbf{N}_1^T \end{pmatrix}, \quad \boldsymbol{\xi} = \begin{Bmatrix} \boldsymbol{a} \\ \boldsymbol{b} \end{Bmatrix}, \tag{2.38}$$

$$\mathbf{N}_1 = -\mathbf{T}^{-1}\mathbf{R}^T, \quad \mathbf{N}_2 = \mathbf{T}^{-1} = \mathbf{N}_2^T, \quad \mathbf{N}_3 = \mathbf{R}\mathbf{T}^{-1}\mathbf{R}^T - \mathbf{Q}, \tag{2.39}$$

$$Q_{ik} = c_{i1k1}, \quad R_{ik} = c_{i1k2}, \quad T_{ik} = c_{i2k2}. \tag{2.40}$$

Note the eigenvalues of the standard eigenvalue problem Eq. (2.37), so called Stroh eigen-relation, are three pairs of complex conjugates.

Introducing two matrices

$$\mathbf{A} = [\boldsymbol{a}_1, \boldsymbol{a}_2, \boldsymbol{a}_3], \quad \mathbf{B} = [\boldsymbol{b}_1, \boldsymbol{b}_2, \boldsymbol{b}_3], \tag{2.41}$$

and the orthonormal relation

$$\boldsymbol{b}_\alpha^T \boldsymbol{a}_\beta + \boldsymbol{a}_\alpha^T \boldsymbol{b}_\beta = \delta_{\alpha\beta}, \tag{2.42}$$

where $\delta_{\alpha\beta}$ is the Kronecker delta, there are three useful real matrices $\mathbf{S}$, $\mathbf{H}$ and $\mathbf{L}$ defined by

$$\mathbf{S} = i(2\mathbf{A}\mathbf{B}^T - \mathbf{I}), \quad \mathbf{H} = 2i\mathbf{A}\mathbf{A}^T, \quad \mathbf{L} = -2i\mathbf{B}\mathbf{B}^T. \tag{2.43}$$

The three matrices, known as Barnett-Lothe matrices often appear in the final solutions of the two-dimensional anisotropic elasticity problems in which the deformation is independent of one of the three Cartesian coordinates.

## 2.4.2 Stroh eigenvalue problem for an oblique plane

The standard Stroh eigenvalue problem is assumed to be associated with the plane perpendicular to the $x_3$-axis. However it can be generalized to be associated with the plane perpendicular to any position vector $\boldsymbol{x}$. The form of the Stroh eigenvalue problem, as well as the three matrices $\mathbf{S}$, $\mathbf{H}$ and $\mathbf{L}$, for an oblique plane keeps the same as Eqs. (2.37)-(2.39), but the definitions of matrices $\mathbf{Q}$, $\mathbf{R}$ and $\mathbf{T}$ are changed to be

$$Q_{ij} = c_{kijl}n_k n_l, \quad R_{ij} = c_{kijl}n_k m_l, \quad T_{ij} = c_{kijl}m_k m_l, \tag{2.44}$$

10

where $\boldsymbol{n}$ and $\boldsymbol{m}$ are any two orthogonal unit vectors on the oblique plane perpendicular to $\boldsymbol{x}$.

The Stroh eigenvalue problem and the Barnett-Lothe matrices for an oblique plane are very useful in the three-dimensional anisotropy problems. Particularly, the matrix $\mathbf{H}$ for an oblique plane is very important in the evaluation of the Green's function in infinite three-dimensional space which will be shown in the following chapters.

## 2.5   Fundamentals of the Green's function

### 2.5.1   Green's function in boundary value problems

Many physical and engineering problems can be modeled as boundary value problems with second-order linear differential equations. To show the importance of the Green's function in solving these boundary value problems, let us first consider a simple boundary value problem:

$$Lu(x) = -f(x), \tag{2.45}$$

$$u(a) = \alpha, \quad u(b) = \beta, \tag{2.46}$$

where $L$ is a linear second-order differential operator, $u(x)$ is the unknown function, $f(x)$ is known, $a$ and $b$ are the boundary of the problem, and $\alpha$ and $\beta$ are two prescribed constants on the boundary.

It is well known that the general solution of the linear differential equation Eq. (2.45) is

$$u(x) = u_p(x) + u_c(x), \tag{2.47}$$

where $u_p(x)$ is a particular solution of Eq. (2.45) and $u_c(x)$ is a general solution of the homogeneous counterpart of Eq. (2.45). Then it is convenient to recast the boundary value problem Eqs. (2.45) and (2.46) into two separate boundary value problems

$$Lu_p(x) = -f(x), \quad u_p(a) = u_p(b) = 0 \tag{2.48}$$

and

$$Lu_c(x) = 0, \quad u_c(a) = \alpha, \quad u_c(b) = \beta. \tag{2.49}$$

Since $L$ is a second-order linear differential operator, the general solution $u_c(x)$ is of the form

$$u_c(x) = c_1 u_1(x) + c_2 u_2(x), \tag{2.50}$$

where $u_1(x)$ and $u_2(x)$ are two linear independent solutions of Eq. $(2.49)_1$, and $c_1$ and $c_2$ are determined by $\alpha$ and $\beta$.

To determine the particular solution $u_p(x)$, we introduce the Dirac delta function $\delta(x)$ who has the property

$$f(x) = \int_{-\infty}^{+\infty} f(y)\delta(x-y)dy, \tag{2.51}$$

and suppose

$$u_p(x) = \int_{-\infty}^{+\infty} G(x,y)f(y)dy, \tag{2.52}$$

11

where $G(x, y)$ is unknown and to be determined. Substitution of Eqs. (2.51) and (2.52), with the assumption on the commutativity of the differential operator $L$ with integration, into Eq. (2.48)$_1$ leads to

$$LG(x, y) = -\delta(x - y). \tag{2.53}$$

Substitution of Eq. (2.52) to Eq. (2.48)$_{2,3}$ leads to

$$G(a, y) = G(b, y) = 0. \tag{2.54}$$

If $G(x, y)$ is determined by Eqs. (2.53) and (2.54), the particular solution $u_p(x)$ is determined and further the general solution $u(x)$ of the original boundary value problem Eqs. (2.45) and (2.46). Therefore $G(x, y)$ is called the Green's function of the original boundary value problem.

It is shown by Eqs. (2.53) and (2.54) that the Green's function is dependent on the differential operator and the boundary of the problem. However, the Green's function in the infinite space is more fundamental, since the Green's function in a finite space can be constructed from it. For example, if the Green's function in the infinite space is $G^\infty(x, y)$ satisfying Eq. (2.53), then we suppose the Green's function in a finite space $G(x, y) = G^\infty(x, y) + cx + d$ which also satisfying Eq. (2.53). The coefficients $c$ and $d$ can be determined by the boundary condition Eq. (2.54). Therefore, $G(x, y)$ is the right answer due to the uniqueness of the boundary value problems.

So far, the importance of the Green's function in solving the boundary value problems, as well as the procedure to the solutions, has been shown.

### 2.5.2 Green's function for multifield coupled media

Generally speaking, the Green's function represents the response of a point source. In the framework of magnetoelectroelasticity which can be reduced to piezoelectricity or elasticity, the Green's function $G_{IJ}(\boldsymbol{x})$ ($I, J = 1, 2, \ldots, 5$) denotes the elastic displacement components at $\boldsymbol{x}$ in the $x_I$-direction ($I \leq 3$), the electric potential ($I = 4$) or the magnet potential ($I = 5$) when a unit point force ($J \leq 3$), a unit electric charge ($J = 4$), or a unit magnetic charge ($J = 5$) is prescribed at the origin of the Cartesian coordinates.

Mathematically speaking, the Green's function for the multifield materials is the fundamental solution of the governing equation, e.g., Eq. (2.6), Eq. (2.18) or Eq. (2.29). Since the governing equations are highly similar in the form, the Green's functions for different materials can be written uniformly and thus satisfy the following differential equations

$$c_{iJMn}G_{MR,ni}(\boldsymbol{x}) + \delta_{JR}\delta(\boldsymbol{x}) = 0, \tag{2.55}$$

where $\delta_{JR}$ is the Kronecker delta and $\delta(\boldsymbol{x})$ is the Dirac delta function centered at the origin of the Cartesian coordinates. The ranges of the capital letters in Eq. (2.55) are $(1, 2, 3)$, $(1, 2, \ldots, 4)$ and $(1, 2, \ldots, 5)$ for the elastic, piezoelectric and magnetoelectroelastic materials, respectively.

## 2.6 Boundary integral equations

Green's function and its derivatives are the basic stones of the boundary integral equations. For simplicity, we consider the boundary integral equations for a 3D anisotropic and linear

elastic solid with the volume $\Omega$ bounded by the surface $S = \partial\Omega$. The corresponding equations for the piezoelectric and magnetoelectroelastic materials can be easily obtained based on the following equations. By using the Betti reciprocal theorem, the displacement components at an arbitrary internal point of the domain can be obtained by using the following representation formula

$$u_i(\boldsymbol{x}) = \int_S u_{ij}^G(\boldsymbol{x}, \boldsymbol{y}) t_j(\boldsymbol{y}) dS - \int_S t_{ij}^G(\boldsymbol{x}, \boldsymbol{y}) u_j(\boldsymbol{y}) dS, \quad \boldsymbol{x} \in \Omega, \tag{2.56}$$

where $u_{ij}^G(\boldsymbol{x}, \boldsymbol{y})$ denotes the displacement fundamental solution or Green's function whose source is located at $\boldsymbol{y}$ instead of the origin, in other words when $\boldsymbol{y} = 0$ we have

$$u_{ij}^G(\boldsymbol{x}, 0) = G_{ij}(\boldsymbol{x}), \tag{2.57}$$

$t_{ij}^G(\boldsymbol{x}, \boldsymbol{y}) = \sigma_{ikj}^G(\boldsymbol{x}, \boldsymbol{y}) n_k(\boldsymbol{y})$ represents the traction fundamental solution with $\sigma_{ikj}^G(\boldsymbol{x}, \boldsymbol{y})$ being the stress fundamental solution and $n_k(\boldsymbol{y})$ the outward unit normal vector on the boundary $S$, $t_j = \sigma_{jk} n_k$ stands for the traction vector, $\boldsymbol{x}$ is the position vector of the observation point, and $\boldsymbol{y}$ is the position vector of the source point, respectively. By taking the limit process $\boldsymbol{x} \to S$ one obtains the following displacement boundary integral equations

$$c_{ij}(\boldsymbol{x}) u_j(\boldsymbol{x}) = \int_S u_{ij}^G(\boldsymbol{x}, \boldsymbol{y}) t_j(\boldsymbol{y}) dS - \int_S t_{ij}^G(\boldsymbol{x}, \boldsymbol{y}) u_j(\boldsymbol{y}) dS, \quad \boldsymbol{x} \in S, \tag{2.58}$$

where the free-term coefficients $c_{ij}$ depend on the smoothness of the surface at $\boldsymbol{x}$.

Once the unknown boundary values have been obtained by solving the above boundary integral equations, the displacement field in the interior domain of interest can be computed by using the displacement representation formula (2.56). The corresponding stress components at an arbitrary internal point of the domain can be obtained by substituting the displacement representation formula (2.56) into Hooke's law $\sigma_{ij} = C_{ijkl}\varepsilon_{kl} = C_{ijkl}u_{k,l}$, which results in the following representation formula for the stress components

$$\sigma_{kl}(\boldsymbol{x}) = -\int_S \sigma_{klj}^G(\boldsymbol{x}, \boldsymbol{y}) t_j(\boldsymbol{y}) dS - \int_S s_{klj}^G(\boldsymbol{x}, \boldsymbol{y}) u_j(\boldsymbol{y}) dS, \quad \boldsymbol{x} \in \Omega, \tag{2.59}$$

where the stress fundamental solution $\sigma_{klj}^G(\boldsymbol{x}, \boldsymbol{y})$ and the higher-order stress fundamental solution are given by

$$
\begin{aligned}
\sigma_{klj}^G &= C_{klim} \frac{\partial u_{ij}^G}{\partial y_m} = -C_{klim} \frac{\partial u_{ij}^G}{\partial x_m}, \\
s_{klj}^G &= C_{klim} \frac{\partial t_{ij}^G}{\partial x_m} = C_{klim} n_p(\boldsymbol{y}) \frac{\partial \sigma_{ipj}^G}{\partial x_m} = -C_{klim} n_p(\boldsymbol{y}) \frac{\partial \sigma_{ipj}^G}{\partial y_m} \\
&= -C_{klim} C_{ipnq} n_p(\boldsymbol{y}) \frac{\partial^2 u_{nj}^G}{\partial y_q \partial y_m}.
\end{aligned}
\tag{2.60}
$$

It should be noted here that the relation $\partial(\cdot)/\partial x_i = -\partial(\cdot)/\partial y_i$ has been used in deriving Eq. (2.60). By letting $\boldsymbol{x}$ to $S$, the corresponding stress or traction boundary integral equations can be derived, which are of special interests in crack analysis.

From Eq. (2.60) it can be seen that the stress or traction fundamental solutions involve the first derivative of the displacement fundamental solution or the Green's function, while the higher-order stress fundamental solution contain the second derivative of the displacement fundamental solution or the Green's function.

# Chapter 3

# Green's function in anisotropic linear elasticity

## 3.1 Problem statement

For isotropic and linear elastic materials in the three-dimensional (3D) space, a simple and closed-form elastostatic Green's function is available. In contrast, the corresponding 3D Green's function for anisotropic materials is much more complicated, and it has closed-form analytical expression only in some special cases such as for transversely isotropic materials (Lifshitz and Rozenzweig, 1947; Pan and Chou, 1976; Willis, 1965). Instead of an analytical expression, the 3D anisotropic Green's function can be reduced to a line or contour integral expression (Fredholm, 1900; Lifshitz and Rozenzweig, 1947; Synge, 1957).

Since the analytical expression of the Green's function was invalid, there were many approximate solutions proposed to evaluate the Green's function and its derivatives. The works of Lifshitz and Rozenzweig (1947), Dederichs and Liebfried (1969), Gray et al. (1996), Lie and Koehler (1968), Mura and Kinoshita (1971), Barnett (1972), Gundersen and Lothe (1987), Pan and Yuan (2000) and Shiah et al. (2012) should be cited among others.

In order to find an accurate and efficient evaluation of the Green's function and its derivatives for generally anisotropic elastic materials, the explicit expressions had been investigated by many researchers. There are many different explicit expressions, but they can be generally classified to three categories: 1) explicit expressions in terms of the roots of a polynomial equation which are also called Stroh eigenvalues, 2) explicit expressions in terms of the solutions of the Stroh eigenvalue problem, 3) unified explicit expressions in terms of the Stroh eigenvalues and valid for all cases.

The expressions in the first category arrive after the residue calculus on the line integrals. They have been well studied by Sales and Gray (1998), Lee (2003, 2009), Phan et al. (2004, 2005), Shiah et al. (2010) and Buroni et al. (2011) among others. These explicit expressions can be applicable in degenerate and non-degenerate cases. But care should be taken in the nearly degenerate cases where significant numerical error may arise (Buroni et al., 2011).

The explicit expressions in the second category are constructed from the solutions of an eigenvalue problem. The Green's function was investigated by Malén (1971) and Nakamura and Tanuma (1997). The expressions of the derivatives could be found in the PhD thesis written by Lavagnino (1995). Nakamura and Tanuma (1997) argued their

expressions were valid no matter the Stroh eigenvalues are distinct or identical. While the expressions of the derivatives were applicable only when the Stroh eigenvalues were distinct.

The unified explicit expression of the Green's function for generally anisotropic materials was firstly proposed by Ting and Lee (1997). Very recently, Buroni and Sáez (2013) pointed out a way to get the unified explicit expressions of the derivatives of the Green's function. Although fully explicit expressions were not presented in the paper, they did give the numerical results. The most important feature of the unified explicit expressions is that they are valid in all cases including the nearly degenerate cases.

In this chapter, four different expressions of the Green's function and its derivatives for three-dimensional anisotropic elastic materials are presented. Firstly, the conventional line integral expressions are re-investigated, resulting from alternative line integral expressions, among which the expression of the second derivative of the Green's function are *new*. Secondly, application of the residue calculus to the novel line integrals leads to explicit expressions, among which the Green's function and its first derivative are in some sense similar with existing ones, but the second derivative is *new*. Thirdly, since the Green's function can be constructed from the solutions of the Stroh eigenvalue problem, *a new way* to construct the first and second derivatives of the Green's function in terms of the derivatives of the eigenvalues and eigenvectors is presented. All the above explicit expressions are only applicable when it is in non-degenerate cases. Finally, in order to overcome this difficulty, the novel line integrals are further expressed in terms of two elementary line integrals, which are evaluated by the simple pole residue calculus and then a proper rewritten. The resulting expressions remain applicable in degenerate, nearly-degenerate and non-degenerate cases. These explicit expressions and the methodology are presented *for the first time*. All these expressions are coded into FORTRAN and compared with each other to have a direct comparison of the accuracy and the efficiency.

These contributions have been published or submitted in:

- **L. Xie**, C. Zhang, C. Hwu, J. Sladek, V. Sladek, A Comparison of Three Evaluation Methods for Green's Function and Its Derivatives for 3D General Anisotropic Solids. *European Journal of Computational Mechanics*, accepted on Apr 11, 2016.

- **L. Xie**, C. Hwu, C. Zhang, Advanced Methods for Calculating Green's Function and Its Derivatives for Three-Dimensional Anisotropic Elastic Solids, *International Journal of Solids and Structures*, 80:261-273, 2016.

- **L. Xie**, C. Zhang, J. Sladek, V. Sladek, Unified analytical expressions of the three-dimensional fundamental solutions and their derivatives for linear elastic anisotropic materials, *Proceedings of the Royal Society of London A: Mathematical, Physical and Engineering Sciences*, 472:20150272, 2016.

## 3.2 Line integral Green's function and its derivatives

By applying either Fourier transforms (Fredholm, 1900) or Radon transforms (Wang, 1997) to the Eq. (2.55) in the elasticity case followed by some elementary manipulations, the Green's function in terms of a double integral is

$$G_{ij}(\boldsymbol{x}) = \frac{1}{8\pi^2} \int_{S^2} \delta(\boldsymbol{\xi} \cdot \boldsymbol{x}) K_{ij}^{-1}(\boldsymbol{\xi}) dS(\boldsymbol{\xi}), \tag{3.1}$$

where $\boldsymbol{\xi}$ is a parameter vector, $S^2$ is a unit sphere whose center is the origin, $x$ is the displacement from $\boldsymbol{x}$ to the origin, and $K_{ij}(\boldsymbol{\xi}) = c_{ikjl}\xi_k\xi_l$ has the symmetry relation $K_{ij}(\boldsymbol{\xi}) = K_{ji}(\boldsymbol{\xi})$. Straightforwardly, the derivatives of the Green's function are

$$G_{IJ,k}(\boldsymbol{x}) = \frac{1}{8\pi^2} \int_{S^2} \delta'(\boldsymbol{\xi} \cdot \boldsymbol{x})\xi_k K_{IJ}^{-1}(\boldsymbol{\xi})dS(\boldsymbol{\xi}), \tag{3.2}$$

$$G_{IJ,kl}(\boldsymbol{x}) = \frac{1}{8\pi^2} \int_{S^2} \delta''(\boldsymbol{\xi} \cdot \boldsymbol{x})\xi_k\xi_l K_{IJ}^{-1}(\boldsymbol{\xi})dS(\boldsymbol{\xi}), \tag{3.3}$$

where the superscript prime $'$ denotes the differential with respect to the argument, i.e., $\boldsymbol{\xi} \cdot \boldsymbol{x}$. Further, Mura (1987) presented the Green's function and its derivatives in terms of line integrals over a unit circle

$$G_{ij}(\boldsymbol{x}) = \frac{1}{8\pi^2 r} \oint_{S^1} K_{ij}^{-1}(\boldsymbol{\xi})d\psi, \tag{3.4}$$

$$\begin{aligned} G_{ij,k}(\boldsymbol{x}) = \frac{1}{8\pi^2 r^2} \oint_{S^1} & \left[ -\bar{x}_k K_{ij}^{-1}(\boldsymbol{\xi}) \right. \\ & \left. + \xi_k c_{lpmq}(\bar{x}_p\xi_q + \xi_p\bar{x}_q)K_{li}^{-1}(\boldsymbol{\xi})K_{mj}^{-1}(\boldsymbol{\xi}) \right] d\psi, \end{aligned} \tag{3.5}$$

$$\begin{aligned} G_{ij,kl}(\boldsymbol{x}) = \frac{1}{8\pi^2 r^3} \oint_{S^1} & \left\{ 2\bar{x}_k\bar{x}_l K_{ij}^{-1}(\boldsymbol{\xi}) - 2[(\bar{x}_k\xi_l + \xi_k\bar{x}_l)(\bar{x}_p\xi_q + \xi_p\bar{x}_q) + \xi_k\xi_l\bar{x}_p\bar{x}_q] \right. \\ & \times c_{hpmq}K_{ih}^{-1}(\boldsymbol{\xi})K_{jm}^{-1}(\boldsymbol{\xi}) + \xi_k\xi_l c_{hpmq}(\bar{x}_p\xi_q + \xi_p\bar{x}_q)c_{satb}(\bar{x}_a\xi_b + \xi_a\bar{x}_b) \\ & \left. \times [K_{jm}^{-1}(\boldsymbol{\xi})K_{is}^{-1}(\boldsymbol{\xi})K_{ht}^{-1}(\boldsymbol{\xi}) + K_{ih}^{-1}(\boldsymbol{\xi})K_{js}^{-1}(\boldsymbol{\xi})K_{mt}^{-1}(\boldsymbol{\xi})] \right\} d\psi, \end{aligned} \tag{3.6}$$

where $r = |\boldsymbol{x}|$, $\bar{\boldsymbol{x}} = \boldsymbol{x}/r$, $S^1$ is the unit circle on the oblique plane perpendicular to $\boldsymbol{x}$, and $\psi$ is a parameter along the circle. Note that $\boldsymbol{\xi}$ in Eqs. (3.1)-(3.3) is a little different from $\boldsymbol{\xi}$ in Eqs. (3.4)-(3.6): the former represents a vector in the unit sphere $S^2$ on the $\boldsymbol{\xi}$-space, but the later represents a vector on the unit circle $S^1$ in the oblique plane perpendicular to $\boldsymbol{x}$. The relations between $S^1$, $S^2$ and other parameters are illustrated in Fig. 3.1.

Fredholm (1900) firstly presented the line integral expression of the Green's function by using Fourier transformations. Vogel and Rizzo (1973) presented the same line integral expression with help of the decomposition of the delta function into plane wave functions, similar with Radon transforms (Wang, 1997). The line integral expressions of the derivatives of the Green's function were firstly investigated by Barnett (1972). Based on Barnett's work, Mura (1987) presented Eqs. (3.4)-(3.6), and Lee (2003) presented reformulations of the Green's function and its derivatives in terms of three line integrals. However, the line integral expressions of the derivatives of the Green's function presented by Lee (2003) involved high order tensors, e.g. 10th-order, causing trouble in the programming and reducing the efficiency of the program.

In the following, we present alternative reformulations of the Green's function and its derivatives based on Eqs. (3.4)-(3.6). The main target of the reformulations is to avoid high order tensors in the expressions.

By choosing any two mutually orthogonal unit vectors $\boldsymbol{n}$ and $\boldsymbol{m}$ in the oblique plane perpendicular to $\boldsymbol{x}$, the vector $\boldsymbol{\xi}$ on the unit circle $S^1$ can be written as

$$\boldsymbol{\xi} = \boldsymbol{n}\cos\psi + \boldsymbol{m}\sin\psi, \tag{3.7}$$

where $\psi$ is the angle between $\boldsymbol{n}$ and $\boldsymbol{\xi}$. After substitution of Eq. (3.7) into Eqs. (3.4)-(3.6), the line integrals over the unit circle are transformed to line integrals over $(-\frac{\pi}{2}, \frac{\pi}{2})$,
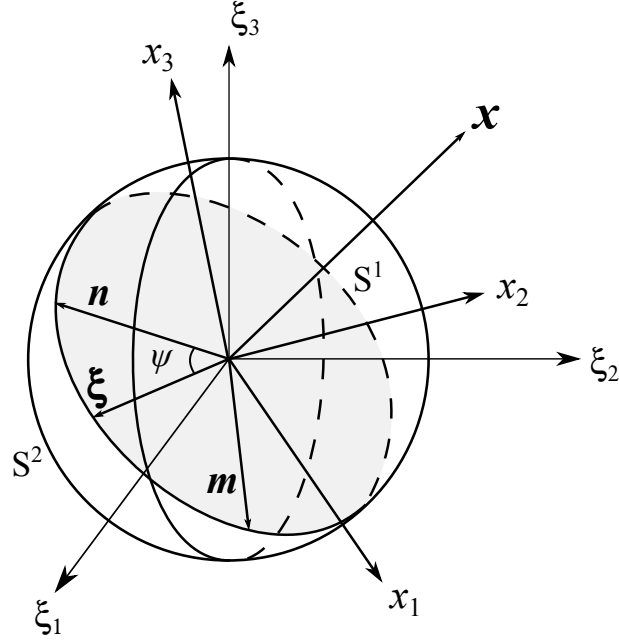
Figure 3.1: An illustration on the unit sphere $S^2$, the oblique plane perpendicular to $\boldsymbol{x}$, the unit circle $S^1$, $\boldsymbol{\xi}$ in $S^1$, $\boldsymbol{n}$, $\boldsymbol{m}$ and $\psi$.

or $(0, \pi)$ if necessary, because the periods of the integrands in Eqs. (3.4)-(3.6) after the substitution are $\pi$. The three newly introduced line integrals are

$$A_{ij}(\bar{\boldsymbol{x}}) = \frac{1}{4\pi} \oint_{S^1} N_{ij}(\boldsymbol{\xi}) D^{-1}(\boldsymbol{\xi}) d\psi = \frac{1}{2\pi} \int_{-\pi/2}^{\pi/2} N_{ij}(\psi) D^{-1}(\psi) d\psi, \tag{3.8}$$

$$P_{ijk}(\bar{\boldsymbol{x}}) = \frac{1}{4\pi} \oint_{S^1} \xi_k H_{ij}(\boldsymbol{\xi}) D^{-2}(\boldsymbol{\xi}) d\psi = \frac{1}{2\pi} \int_{-\pi/2}^{\pi/2} \xi_k H_{ij}(\psi) D^{-2}(\psi) d\psi, \tag{3.9}$$

$$Q_{ijkl}(\bar{\boldsymbol{x}}) = \frac{1}{4\pi} \oint_{S^1} \xi_k \xi_l M_{ij}(\boldsymbol{\xi}) D^{-3}(\boldsymbol{\xi}) d\psi = \frac{1}{2\pi} \int_{-\pi/2}^{\pi/2} \xi_k \xi_l M_{ij}(\psi) D^{-3}(\psi) d\psi, \tag{3.10}$$

where $N_{ij}$ and $D$ are respectively cofactors and determinant of the matrix $K_{ij}$, and $H_{ij}$ and $M_{ij}$ are defined as

$$H_{ij} = F_{im} N_{jm}, \quad M_{ij} = L_{ij} - R_{ij} D, \tag{3.11}$$

with

$$\begin{aligned} F_{im} &= E_{hm} N_{ih}, & E_{hm} &= c_{phmq}(\bar{x}_p \xi_q + \bar{x}_q \xi_p), \\ L_{ij} &= F_{jh} H_{ih}, & R_{ij} &= \bar{x}_p \bar{x}_q c_{phmq} N_{ih} N_{jm}. \end{aligned} \tag{3.12}$$

Note that the arguments in Eqs. (3.11) and (3.12) could be $\boldsymbol{\xi}$ or $\psi$, or even $p$ introduced in the following. Then the reformulated line integral expressions of the Green's function and its derivatives are given by

$$G_{ij}(\boldsymbol{x}) = \frac{1}{2\pi r} A_{ij}(\bar{\boldsymbol{x}}), \tag{3.13}$$

$$G_{ij,k}(\boldsymbol{x}) = \frac{1}{2\pi r^2} \left[ -\bar{x}_k A_{ij}(\bar{\boldsymbol{x}}) + P_{ijk}(\bar{\boldsymbol{x}}) \right], \tag{3.14}$$

18

$$G_{ij,kl}(\boldsymbol{x}) = \frac{1}{\pi r^3} \left\{ A_{ij}(\bar{\boldsymbol{x}})\bar{x}_k\bar{x}_l - [P_{ijk}(\bar{\boldsymbol{x}})\bar{x}_l + P_{ijl}(\bar{\boldsymbol{x}})\bar{x}_k] + Q_{ijkl}(\bar{\boldsymbol{x}}) \right\}. \tag{3.15}$$

These line integral expressions are a little different but equivalent to those proposed by Barnett (1972) and Mura (1987). It should be mentioned that the symmetry of $c_{ijkl}$ and $K_{ij}$ is used to deduce Eqs. (3.14) and (3.15) from Eqs. (3.5) and (3.6).

Quadrature rules such as the standard Gaussian quadrature can be applied on Eqs. (3.8)-(3.12) to calculate the Green's function and its derivatives by Eqs. (3.13)-(3.15). The numerical implementation of these reformulated line integral expressions of the Green's function and its derivatives associated with other methods is discussed in Section 3.5.

## 3.3 Explicit Green's function and its derivatives

In this section, we investigate the explicit expressions of the Green's function and its derivatives in terms of distinct Stroh eigenvalues and/or eigenvectors. Here, *explicit expressions* have mainly two meanings: firstly, they have no integrals; and secondly, they become algebraically analytical as long as the Stroh eigenvalues and/or eigenvectors are algebraically analytical.

### 3.3.1 Residue calculus method

For the easy use of the residue calculus, the intervals of the line integrals in Eqs.(3.8)-(3.10) are further transformed from $(-\pi/2, +\pi/2)$ to $(-\infty, +\infty)$. To illustrate the procedure, we take $A_{ij}(\bar{\boldsymbol{x}})$ as an example.

By setting $p = \tan\psi$, we have

$$\boldsymbol{\xi} = \cos\psi(\boldsymbol{n} + p\boldsymbol{m}), \quad dp = \frac{1}{\cos^2\psi}d\psi. \tag{3.16}$$

Note that due to the definition of $K_{ij}(\boldsymbol{\xi})$ we have

$$N_{ij}(\boldsymbol{\xi}) = \cos^4\psi N_{ij}(\boldsymbol{n} + p\boldsymbol{m}), \quad D(\boldsymbol{\xi}) = \cos^6\psi D(\boldsymbol{n} + p\boldsymbol{m}). \tag{3.17}$$

Then we can obtain

$$N_{ij}(\psi)D^{-1}(\psi) = N_{ij}(\boldsymbol{\xi})D^{-1}(\boldsymbol{\xi}) = \frac{1}{\cos^2\psi}N_{ij}(p)D^{-1}(p), \tag{3.18}$$

where $\boldsymbol{n}$ and $\boldsymbol{m}$ are omitted in the last term for simplicity, and $N_{ij}(p)$ and $D(p)$ are cofactors and determinant of the matrix $K_{ij}(p) = c_{ikjl}\xi_k^*\xi_l^*$, where $\boldsymbol{\xi}^* = \boldsymbol{n} + p\boldsymbol{m}$. Substitution of Eq. (3.16)$_2$ and Eq. (3.18) into Eq. (3.8) leads to

$$A_{ij}(\bar{\boldsymbol{x}}) = \frac{1}{2\pi}\int_{-\infty}^{+\infty} N_{ij}(p)D^{-1}(p)dp. \tag{3.19}$$

Similarly, $P_{ijk}(\bar{\boldsymbol{x}})$ and $Q_{ijkl}(\bar{\boldsymbol{x}})$ become

$$P_{ijk}(\bar{\boldsymbol{x}}) = \frac{1}{2\pi}\int_{-\infty}^{+\infty} \xi_k^* H_{ij}(p)D^{-2}(p)dp, \tag{3.20}$$

$$Q_{ijkl}(\bar{\boldsymbol{x}}) = \frac{1}{2\pi}\int_{-\infty}^{+\infty} \xi_k^*\xi_l^* M_{ij}(p)D^{-3}(p)dp, \tag{3.21}$$

19

where $H_{ij}(p)$ and $M_{ij}(p)$ are determined by Eqs. (3.11) and (3.12), in which $\boldsymbol{\xi}$ is replaced by $\boldsymbol{\xi}^*$. All $\boldsymbol{\xi}^*$, $N_{ij}(p)$, $H_{ij}(p)$ and $M_{ij}(p)$ are polynomials in $p$.

Suppose $f(p)$ is a rational polynomial function of the following form

$$f(p) = \frac{P(p)}{Q(p)}, \tag{3.22}$$

where $P(p)$ and $Q(p)$ are polynomials in $p$, and the order of $Q(p)$ is higher than the order of $P(p)$. Then by using the Cauchy residue theorem, it is easy to conclude that if there are $n$ different poles $p_k$, $k = 1, 2, \ldots, n$ with $\text{Im}(p_k) > 0$ among the poles of $f(x)$, then

$$\int_{-\infty}^{+\infty} f(p)dp = 2\pi i \sum_{k=1}^{n} \text{Res}(p_k). \tag{3.23}$$

If $p_k$ is a pole of $m$th order, then

$$\text{Res}(p_k) = \frac{1}{(m-1)!} \lim_{p \to p_k} \frac{d^{m-1}}{dp^{m-1}} [(p - p_k)^m f(p)]. \tag{3.24}$$

For detailed derivation, readers refer to the Appendix A.

Under the assumption that the Stroh eigenvalues, which are zeros of the polynomial $D(p)$ with positive imaginary parts, are distinct, $A_{ij}(\bar{\boldsymbol{x}})$, $P_{ijk}(\bar{\boldsymbol{x}})$ and $Q_{ijkl}(\bar{\boldsymbol{x}})$ have the same 3 poles. The orders of the 3 poles are the same in $A_{ij}(\bar{\boldsymbol{x}})$, $P_{ijk}(\bar{\boldsymbol{x}})$ or $Q_{ijkl}(\bar{\boldsymbol{x}})$, but orders of each $p_k$ in $A_{ij}(\bar{\boldsymbol{x}})$, $P_{ijk}(\bar{\boldsymbol{x}})$ and $Q_{ijkl}(\bar{\boldsymbol{x}})$ are respectively 1, 2 and 3. In virtue of Eqs. (3.23) and (3.24), Eqs. (3.19)-(3.21) become

$$A_{ij}(\bar{\boldsymbol{x}}) = -\text{Im} \sum_{n=1}^{3} \frac{N_{ij}(p_n)}{D'(p_n)}, \tag{3.25}$$

$$P_{ijk}(\bar{\boldsymbol{x}}) = -\text{Im} \sum_{n=1}^{3} \frac{D'(p_n)\hat{H}'_{ijk}(p_n) - D''(p_n)\hat{H}_{ijk}(p_n)}{D'^3(p_n)}, \tag{3.26}$$

$$Q_{ijkl}(\bar{\boldsymbol{x}}) = -\text{Im} \sum_{n=1}^{3} \frac{1}{2D'^5(p_n)} \left\{ D'^2(p_n)\hat{M}''_{ijkl}(p_n) - 3D'(p_n)D''(p_n)\hat{M}'_{ijkl}(p_n) \right.$$
$$\left. + \left[ 3D''^2(p_n) - D'''(p_n)D'(p_n) \right] \hat{M}_{ijkl}(p_n) \right\}, \tag{3.27}$$

where

$$\hat{H}_{ijk}(p) = \xi_k^* H_{ij}(p), \quad \hat{M}_{ijkl}(p) = \xi_k^* \xi_l^* M_{ij}(p), \tag{3.28}$$

in which $\hat{H}_{ijk}(p)$ and $\hat{M}_{ijkl}(p)$ are polynomials of 10th-order and 16th-order, respectively.

Substitution of Eq. (3.25) into Eq. (3.13) yields the following explicit Green's function

$$G_{ij}(\boldsymbol{x}) = -\frac{1}{2\pi r} \text{Im} \sum_{n=1}^{3} \frac{N_{ij}(p_n)}{D'(p_n)}, \tag{3.29}$$

which was known as Fredholm's formula in the early literature (Dederichs and Liebfried, 1969). Sales and Gray (1998) firstly gave explicit expressions of the derivatives of the Green's function in terms of the Stroh eigenvalues. The starting point of Sales and Gray (1998) was a modulation function, like $A_{ij}(\bar{\boldsymbol{x}})$ in Eq. (3.19). The explicit expressions of the derivatives of the Green's function were obtained after the differentiation of the

modulation function with respect to two angles, namely polar angle and azimuthal angle in the spherical coordinate system, which determined the orientation of $\boldsymbol{x}$. Based on another three integrals, Lee (2003) presented the explicit expressions of the derivatives of the Green's function with respect to the Cartesian coordinates. Note that the Fredholm's formula, explicit expressions by Sales and Gray (1998) and Lee (2003), and Eqs. (3.25)-(3.27) are only applicable when the Stroh eigenvalues are distinct. For a general evaluation, a small perturbation on the material constants is suggested to keep the Stroh eigenvalues distinct. Using multiple pole residue calculus, Phan et al. (2004, 2005) extended the work of Sales and Gray (1998) by giving explicit expressions of the Green's function and its derivatives for repeated Stroh eigenvalues. Buroni et al. (2011) extended the work of Lee (2003). The explicit expressions by Sales and Gray (1998) and Lee (2003) were either with respect to spherical coordinates or contained tensors of the orders higher than 4. Our newly proposed explicit derivatives of the Green's function are given in the Cartesian coordinate system with low order tensors.

### 3.3.2   Stroh formalism method

In three-dimensional theory of linear elasticity, the equation for the 6-dimensional Stroh eigenvalue problem on the oblique plane perpendicular to $\boldsymbol{x}$ is given by Eqs. (2.37)-(2.39) and (2.44) (Hwu, 2010; Ting, 1996).

Since the fundamental elasticity matrix $\mathbf{N}$ is not symmetric, $\boldsymbol{\xi}$ in Eq. (2.37) is a right eigenvector. The left eigenvector denoted by $\boldsymbol{\eta}$ satisfies

$$\boldsymbol{\eta}^T \mathbf{N} = p \boldsymbol{\eta}^T. \tag{3.30}$$

Ting (1996) had proved that

$$\boldsymbol{\eta} = \begin{Bmatrix} \boldsymbol{b} \\ \boldsymbol{a} \end{Bmatrix}. \tag{3.31}$$

As long as the elasticity tensor $c_{kijl}$ is positive definite, in the sense that $c_{kijl}e_{ki}e_{jl} > 0$ for any non-zero $e_{ij}$, the eigenvalues of Eq. (2.37) are three pairs of complex conjugates. It is assumed that $\text{Im}(p_k) > 0$, $p_{k+3} = \bar{p}_k$, $k = 1, 2, 3$ and $p_k$ are distinct which causes all the eigenvectors being independent of each other.

By defining

$$\mathbf{A} = [\boldsymbol{a}_1, \boldsymbol{a}_2, \boldsymbol{a}_3], \ \mathbf{B} = [\boldsymbol{b}_1, \boldsymbol{b}_2, \boldsymbol{b}_3], \tag{3.32}$$

and with the normalized orthogonality relations between eigenvectors

$$\boldsymbol{\eta}_\alpha^T \boldsymbol{\xi}_\beta = \delta_{\alpha\beta}, \ \alpha, \beta = 1, 2, \dots, 6, \tag{3.33}$$

where $\delta_{\alpha\beta}$ was the Kronecker delta, Ting (1996) showed that the Green's function could be written as

$$\mathbf{G}(\boldsymbol{x}) = \frac{1}{4\pi r} \mathbf{H}(\bar{\boldsymbol{x}}), \quad \mathbf{H} = 2i\mathbf{A}\mathbf{A}^T, \tag{3.34}$$

in which $\mathbf{H}$ was one of the three Barnett-Lothe tensors in the oblique plane perpendicular to $\boldsymbol{x}$.

Suppose $\boldsymbol{\xi}^*$ is an arbitrary eigenvector of the fundamental elasticity matrix $\mathbf{N}$, and

$$\boldsymbol{\xi}^* = \begin{Bmatrix} \boldsymbol{a}^* \\ \boldsymbol{b}^* \end{Bmatrix}. \tag{3.35}$$

In order to find the right eigenvector satisfying Eq. (3.33), we suppose

$$\boldsymbol{\xi} = \gamma \boldsymbol{\xi}^*, \tag{3.36}$$

where $\gamma$ is a nonzero constant to be determined. Substitution of Eq. (3.36) into Eq. (3.33) yields

$$\gamma = \frac{1}{\sqrt{2\boldsymbol{a}^* \cdot \boldsymbol{b}^*}}. \tag{3.37}$$

Therefore, the right eigenvector $\boldsymbol{\xi}$ required by the Green's function can be determined by Eqs. (3.35)-(3.37).

By using now called the Stroh formalism, Malén (1971) constructed the explicit expression of the Green's function from the solutions of the Stroh eigenvalue problem with the distinctness assumption of the eigenvalues, while Nakamura and Tanuma (1997) without the distinctness assumption. Hwu (2010) gave explicit components of $\mathbf{A}$ in terms of the Stroh eigenvalues. For the derivatives of the Green's function, Malén (1971) obtained the explicit expression of the first derivative in terms of Stroh eigenvalues and eigenvectors. Xie et al. (2015a) presented the expressions of the first and second derivatives by differentiating the explicit components of $\mathbf{A}$.

In the following, we present new explicit expressions of the first and second derivatives of the Green's function in terms of the Stroh eigenvalues and eigenvectors. Instead of using the spherical coordinate system (Malén, 1971), the Cartesian coordinate system is used directly.

The derivatives of the Green's function become straightforward by differentiating Eq. (3.34) with respect to $x_i$ and further to $x_j$, i.e.,

$$\mathbf{G}_{,i}(\boldsymbol{x}) = \frac{1}{4\pi r^2} \left( -\frac{x_i}{r} \mathbf{H} + r \mathbf{H}_{,i} \right), \tag{3.38}$$

$$\mathbf{G}_{,ij}(\boldsymbol{x}) = \frac{1}{4\pi r^3} \left( \left( \frac{3x_i x_j}{r^2} - \delta_{ij} \right) \mathbf{H} - \left( x_i \mathbf{H}_{,j} + x_j \mathbf{H}_{,i} \right) + r^2 \mathbf{H}_{,ij} \right), \tag{3.39}$$

where

$$\mathbf{H}_{,i} = 2i \left( \mathbf{A}_{,i} \mathbf{A}^T + \left[ \mathbf{A}_{,i} \mathbf{A}^T \right]^T \right), \tag{3.40}$$

$$\mathbf{H}_{,ij} = 2i \left( \mathbf{A}_{,ij} \mathbf{A}^T + \mathbf{A}_{,i} \mathbf{A}_{,j}^T + \left[ \mathbf{A}_{,ij} \mathbf{A}^T + \mathbf{A}_{,i} \mathbf{A}_{,j}^T \right]^T \right). \tag{3.41}$$

According to the above equations, the derivatives of $\mathbf{A}$ are required to calculate the derivatives of the Green's function $\mathbf{G}(\boldsymbol{x})$. The differentiation of Eq. (2.37), which is associated with the eigenvalue $p_\alpha$ and the corresponding right eigenvector $\boldsymbol{\xi}_\alpha$, with respect to $x_i$ leads to

$$(\mathbf{N} - p_\alpha \mathbf{I}) \boldsymbol{\xi}_{\alpha,i} = -(\mathbf{N}_{,i} - p_{\alpha,i} \mathbf{I}) \boldsymbol{\xi}_\alpha. \tag{3.42}$$

*Note that the repeated Greek letter in the above equation does not imply summation, neither does in the following.* Since the derivative of an eigenvector is a 6-dimensional vector, it is a linear combination of the six independent eigenvectors, i.e.,

$$\boldsymbol{\xi}_{\alpha,i} = \sum_{\beta=1}^{6} c_{\alpha\beta}^{(i)} \boldsymbol{\xi}_\beta. \tag{3.43a}$$

and

$$\boldsymbol{\eta}_{\alpha,i} = \sum_{\beta=1}^{6} c_{\alpha\beta}^{(i)} \boldsymbol{\eta}_{\beta}. \tag{3.43b}$$

In Eq. (3.43), the coefficients $c_{\alpha\beta}^{(i)}$ are constants. In virtue of Eqs. (2.37), (3.30) and (3.33), the substitution of Eq. (3.43a) into Eq. (3.42) followed by the premultiplication by $\boldsymbol{\eta}_{\beta}^{T}$ yields

$$c_{\alpha\beta}^{(i)}(p_{\beta} - p_{\alpha}) = -\boldsymbol{\eta}_{\beta}^{T}(\mathbf{N}_{,i} - p_{\alpha,i}\mathbf{I})\boldsymbol{\xi}_{\alpha}. \tag{3.44}$$

When $\beta = \alpha$, the derivative of the eigenvalue $p_{\alpha}$ is given from Eq. (3.44) as

$$p_{\alpha,i} = \boldsymbol{\eta}_{\alpha}^{T}\mathbf{N}_{,i}\boldsymbol{\xi}_{\alpha}. \tag{3.45}$$

If $\beta \neq \alpha$ the coefficients $c_{\alpha\beta}^{(i)}$ in the expressions of the derivatives of eigenvectors $\boldsymbol{\xi}_{\alpha,i}$ are

$$c_{\alpha\beta}^{(i)} = \frac{\boldsymbol{\eta}_{\beta}^{T}\mathbf{N}_{,i}\boldsymbol{\xi}_{\alpha}}{p_{\alpha} - p_{\beta}}. \tag{3.46}$$

Substitution of Eqs. (3.33) and (3.43) into the first derivative of Eq. (3.33) leads to

$$c_{\alpha\beta}^{(i)} + c_{\beta\alpha}^{(i)} = 0. \tag{3.47}$$

When $\beta = \alpha$, we have

$$c_{\alpha\alpha}^{(i)} = 0. \tag{3.48}$$

So far, all the coefficients $c_{\alpha\beta}^{(i)}$ are determined. The 1st derivative of eigenvector can be expressed in terms of all eigenvectors by Eq. (3.43). And further easily arrives $\mathbf{A}_{,i}$ by differentiating Eq. (3.32).

In order to get the 2nd derivative of $\mathbf{A}$, the 2nd derivatives of the right eigenvectors $\boldsymbol{\xi}_{\alpha,ij}$ are required. In the same way, $\boldsymbol{\xi}_{\alpha,ij}$ is a linear combination of the six independent right eigenvectors:

$$\boldsymbol{\xi}_{\alpha,ij} = \sum_{\beta=1}^{6} d_{\alpha\beta}^{(ij)} \boldsymbol{\xi}_{\beta}. \tag{3.49}$$

Taking derivative of Eq. (3.42) with respect to $x_j$ followed by the premultiplication by $\boldsymbol{\eta}_{\beta}^{T}$, and with the substitution of Eq. (3.49) yields

$$d_{\alpha\beta}^{(ij)}(p_{\beta} - p_{\alpha}) = -\boldsymbol{\eta}_{\beta}^{T}(\mathbf{N}_{,ij} - p_{\alpha,ij}\mathbf{I})\boldsymbol{\xi}_{\alpha} - \boldsymbol{\eta}_{\beta}^{T}(\mathbf{N}_{,i} - p_{\alpha,i}\mathbf{I})\boldsymbol{\xi}_{\alpha,j} - \boldsymbol{\eta}_{\beta}^{T}(\mathbf{N}_{,j} - p_{\alpha,j}\mathbf{I})\boldsymbol{\xi}_{\alpha,i}. \tag{3.50}$$

Using the same approach for the 1st derivative of the eigenvectors, the 2nd derivatives of the eigenvalues $p_{\alpha,ij}$ and the coefficients $d_{\alpha\beta}^{(ij)}$ are

$$p_{\alpha,ij} = \boldsymbol{\eta}_{\alpha}^{T}\mathbf{N}_{,ij}\boldsymbol{\xi}_{\alpha} + \boldsymbol{\eta}_{\alpha}^{T}\mathbf{N}_{,i}\boldsymbol{\xi}_{\alpha,j} + \boldsymbol{\eta}_{\alpha}^{T}\mathbf{N}_{,j}\boldsymbol{\xi}_{\alpha,i}, \tag{3.51}$$

$$d_{\alpha\alpha}^{(ij)} = -(\boldsymbol{\eta}_{\alpha,i}^{T}\boldsymbol{\xi}_{\alpha,j} + \boldsymbol{\eta}_{\alpha,j}^{T}\boldsymbol{\xi}_{\alpha,i})/2, \tag{3.52}$$

$$d_{\alpha\beta}^{(ij)} = \frac{\boldsymbol{\eta}_{\beta}^{T}\mathbf{N}_{,ij}\boldsymbol{\xi}_{\alpha} + \boldsymbol{\eta}_{\beta}^{T}(\mathbf{N}_{,i} - p_{\alpha,i}\mathbf{I})\boldsymbol{\xi}_{\alpha,j} + \boldsymbol{\eta}_{\beta}^{T}(\mathbf{N}_{,j} - p_{\alpha,j}\mathbf{I})\boldsymbol{\xi}_{\alpha,i}}{p_{\alpha} - p_{\beta}}, \beta \neq \alpha. \tag{3.53}$$

$\mathbf{N}_{,i}$ and $\mathbf{N}_{,ij}$ can be given by taking derivatives of Eqs. (2.37) and (2.44). Appendix B presents the explicit expressions of $\mathbf{N}_{,i}$ and $\mathbf{N}_{,ij}$ as well as the proper choise of $\boldsymbol{n}$, $\boldsymbol{m}$ and their derivatives.

## 3.4 Unified explicit Green's function and its derivatives

In Section 3.2, the Green's function and its derivatives are expressed in terms of three integrals, $A_{ij}$, $P_{ijk}$ and $Q_{ijkl}$. In Section 3.3.1, the direct evaluation of the three integrals by Cauchy residue calculus leads to explicit expressions. However, the explicit expressions and the counterpart by the Stroh formalism method (Section 3.3.2), are only applicable when the Stroh eigenvalues are distinct. In this section, we derive unified explicit expressions of the Green's function and its derivatives which remain applicable no matter the Stroh eigenvalues are distinct or not. The word *unified* is used to emphasize the difference from the piecewise explicit expressions derived by the multiple pole residue calculus.

### 3.4.1 Rearrangements of the integrals

The evaluations of the integrals $A_{ij}$, $P_{ijk}$ and $Q_{ijkl}$ are the main tasks in the calculations of the Green's function and its derivatives. In this section, we present the rearrangements of the three integrals.

The determinant $D(p)$ is a 6th order polynomial in $p$. Because the elasticity tensor $c_{ijkl}$ is positive definite, the roots of the determinant $D(p)$ are three pairs of complex conjugates. So $D(p)$ can be written as

$$D(p) = \alpha(p - p_1)(p - p_2)(p - p_3)(p - \bar{p}_1)(p - \bar{p}_2)(p - \bar{p}_3),$$

$$= \alpha \prod_{i=1}^{3} (p - p_i)(p - \bar{p}_i), \tag{3.54}$$

where $\alpha$, the coefficient of $p^6$ in $D(p)$, is equal to the determinant of the matrix $c_{ijkl}m_j m_l$, $p_k$ ($\text{Im}[p_k] > 0, k = 1, 2, 3$) are known as the Stroh eigenvalues, and the overbar denotes the complex conjugate. Since $D(p)$ is the determinant of $K_{ij}(p) = c_{ikjl}\xi_k^* \xi_l^*$, it can be concluded that the Stroh eigenvalues depend on the material constants, the direction of the observation point $\boldsymbol{x}$ and maybe the chosen coordinates in the oblique plane.

Since $N_{ij}(p)$, $\hat{H}_{ijk}(p)$ and $\hat{M}_{ijkl}(p)$ are polynomials with highest orders 4, 10 and 16, respectively, they can be written as

$$N_{ij}(p) = \sum_{n=0}^{4} a_{ij}^n p^n, \tag{3.55}$$

$$\hat{H}_{ijk}(p) = \sum_{n=0}^{10} a_{ijk}^n p^n, \tag{3.56}$$

$$\hat{M}_{ijkl}(p) = \sum_{n=0}^{16} a_{ijkl}^n p^n, \tag{3.57}$$

where $a_{ij}^n$, $a_{ijk}^n$ and $a_{ijkl}^n$ are independent of $p$. Substituting Eqs. (3.54)-(3.57) into Eqs. (3.19)-(3.21), the three integrals become

$$A_{ij}(\bar{\boldsymbol{x}}) = \frac{1}{\alpha} \sum_{n=0}^{4} a_{ij}^n I_3^n, \tag{3.58}$$

$$P_{ijk}(\bar{\boldsymbol{x}}) = \frac{1}{\alpha^2} \sum_{n=0}^{10} a_{ijk}^n I_6^n, \tag{3.59}$$

$$Q_{ijkl}(\bar{\boldsymbol{x}}) = \frac{1}{\alpha^3} \sum_{n=0}^{16} a_{ijkl}^n I_9^n, \tag{3.60}$$

where

$$I_3^n = \int_{-\infty}^{+\infty} \frac{p^n}{f(p)} dp, \quad 0 \le n \le 4, \tag{3.61}$$

$$I_6^n = \int_{-\infty}^{+\infty} \frac{p^n}{f^2(p)} dp, \quad 0 \le n \le 10, \tag{3.62}$$

$$I_9^n = \int_{-\infty}^{+\infty} \frac{p^n}{f^3(p)} dp, \quad 0 \le n \le 16, \tag{3.63}$$

in which

$$f(p) = \prod_{i=1}^{3} (p - p_i)(p - \bar{p}_i). \tag{3.64}$$

Although the coefficients $a_{ij}^n$, $a_{ijk}^n$ and $a_{ijkl}^n$ are too complicated to be explicit, they can be obtained nearly exactly in a program by using the polynomial algorithms (Press, 2007). Besides it is not difficult to find that both the coefficients and the integrals $I_3^n$, $I_6^n$ and $I_9^n$ are real-valued.

If the three Stroh eigenvalues $p_1$, $p_2$ and $p_3$ are distinct, the orders of poles in Eqs. (3.62) and (3.63) are, respectively, 2 and 3, which increases the difficulty to obtain the explicit expressions by using the residue calculus. Therefore, instead of Eqs. (3.62) and (3.63) we consider

$$I_6^n = \int_{-\infty}^{+\infty} \frac{p^n}{\prod_{i=1}^{6}(p - p_i)(p - \bar{p}_i)} dp, \quad 0 \le n \le 10, \tag{3.65}$$

$$I_9^n = \int_{-\infty}^{+\infty} \frac{p^n}{\prod_{i=1}^{9}(p - p_i)(p - \bar{p}_i)} dp, \quad 0 \le n \le 16, \tag{3.66}$$

which are identical to Eqs. (3.62) and (3.63) when $p_4$ and $p_7$, $p_5$ and $p_8$, $p_6$ and $p_9$ are respectively set to be $p_1$, $p_2$ and $p_3$.

Further, $I_3^n$, $I_6^n$ and $I_9^n$ can be expressed in terms of two elementary integrals, which are

$$I_m^0 = \int_{-\infty}^{+\infty} \frac{1}{\prod_{i=1}^{m}(p - p_i)(p - \bar{p}_i)} dp, \tag{3.67}$$

$$I_m^1 = \int_{-\infty}^{+\infty} \frac{p}{\prod_{i=1}^{m}(p - p_i)(p - \bar{p}_i)} dp. \tag{3.68}$$

The expressions of $I_3^n$ in terms of $I_m^0$ ($m = 1, 2, 3$) and $I_m^1$ ($m = 2, 3$) are given by

$$\begin{aligned}
I_3^2 =& I_2^0 + 2\operatorname{Re}(p_3) I_3^1 - |p_3|^2 I_3^0, \\
I_3^3 =& I_2^1 + 2\operatorname{Re}(p_3) I_3^2 - |p_3|^2 I_3^1, \\
I_3^4 =& I_1^0 + 2\operatorname{Re}(p_2 + p_3) I_3^3 - \left[|p_2|^2 + |p_3|^2 + 4\operatorname{Re}(p_2)\operatorname{Re}(p_3)\right] I_3^2 \\
& + 2\left[\operatorname{Re}(p_2)|p_3|^2 + \operatorname{Re}(p_3)|p_2|^2\right] I_3^1 - |p_2|^2 |p_3|^2 I_3^0.
\end{aligned} \tag{3.69}$$

The expressions of $I_6^n$ in terms of $I_m^0$ ($m = 1, 2, \ldots, 6$) and $I_m^1$ ($m = 2, 3, \ldots, 6$) are given by

$$I_6^2 = I_5^0 - \sum_{i=1}^{2} (-1)^i E_i^{(66)} I_6^{2-i}, \qquad\qquad I_6^3 = I_5^1 - \sum_{i=1}^{2} (-1)^i E_i^{(66)} I_6^{3-i},$$

$$I_6^4 = I_4^0 - \sum_{i=1}^{4} (-1)^i E_i^{(65)} I_6^{4-i}, \qquad I_6^5 = I_4^1 - \sum_{i=1}^{4} (-1)^i E_i^{(65)} I_6^{5-i},$$

$$I_6^6 = I_3^0 - \sum_{i=1}^{6} (-1)^i E_i^{(64)} I_6^{6-i}, \qquad I_6^7 = I_3^1 - \sum_{i=1}^{6} (-1)^i E_i^{(64)} I_6^{7-i},$$

$$I_6^8 = I_2^0 - \sum_{i=1}^{8} (-1)^i E_i^{(63)} I_6^{8-i}, \qquad I_6^9 = I_2^1 - \sum_{i=1}^{8} (-1)^i E_i^{(63)} I_6^{9-i},$$

$$I_6^{10} = I_1^0 - \sum_{i=1}^{10} (-1)^i E_i^{(62)} I_6^{10-i}, \tag{3.70}$$

in which

$$E_i^{(kl)} = \begin{cases} e_i(p_k, \bar{p}_k, \ldots, p_l, \bar{p}_l), & l < k, \\ e_i(p_k, \bar{p}_k), & l = k, \end{cases} \tag{3.71}$$

where $e_i(x_1, \ldots, x_n)$ is the elementary symmetric polynomial, the sum of all products of $i$ distinct variables out of $x_1, \ldots, x_n$. That is

$$e_1(x_1, \ldots, x_n) = \sum_{i=1}^{n} x_i,$$

$$e_2(x_1, \ldots, x_n) = \sum_{1 \le i_1 < i_2 \le n} x_{i_1} x_{i_2},$$

$$\vdots$$

$$e_m(x_1, \ldots, x_n) = \sum_{1 \le i_1 < \cdots < i_m \le n} x_{i_1} \ldots x_{i_m},$$

$$\vdots$$

$$e_n(x_1, \ldots, x_n) = x_1 x_2 \ldots x_n. \tag{3.72}$$

Finally, the expressions of $I_9^n$ in terms of $I_m^0$ $(m = 1, 2, \ldots, 9)$ and $I_m^1$ $(m = 2, 3, \ldots, 9)$ are given by

$$I_9^2 = I_8^0 - \sum_{i=1}^{2} (-1)^i E_i^{(99)} I_9^{2-i}, \qquad I_9^3 = I_8^1 - \sum_{i=1}^{2} (-1)^i E_i^{(99)} I_9^{3-i},$$

$$I_9^4 = I_7^0 - \sum_{i=1}^{4} (-1)^i E_i^{(98)} I_9^{4-i}, \qquad I_9^5 = I_7^1 - \sum_{i=1}^{4} (-1)^i E_i^{(98)} I_9^{5-i},$$

$$I_9^6 = I_6^0 - \sum_{i=1}^{6} (-1)^i E_i^{(97)} I_9^{6-i}, \qquad I_9^7 = I_6^1 - \sum_{i=1}^{6} (-1)^i E_i^{(97)} I_9^{7-i},$$

$$I_9^8 = I_5^0 - \sum_{i=1}^{8} (-1)^i E_i^{(96)} I_9^{8-i}, \qquad I_9^9 = I_5^1 - \sum_{i=1}^{8} (-1)^i E_i^{(96)} I_9^{9-i},$$

$$\vdots \qquad\qquad\qquad\qquad \vdots$$

$$I_9^{14} = I_2^0 - \sum_{i=1}^{14} (-1)^i E_i^{(93)} I_9^{14-i}, \qquad I_9^{15} = I_2^1 - \sum_{i=1}^{14} (-1)^i E_i^{(93)} I_9^{15-i},$$

$$I_9^{16} = I_1^0 - \sum_{i=1}^{16} (-1)^i E_i^{(92)} I_9^{16-i}. \tag{3.73}$$

By now, the Green's function and its derivatives are expressed in terms of $I_m^0$ ($m = 1, 2, \ldots, 9$) and $I_m^1$ ($m = 2, 3, \ldots, 9$) . These expressions keep the same no matter Stroh eigenvalues are distinct or not.

Besides, we mention an implicit recursive relation which may be helpful in programming. We define

$$I_m^n = \int_{-\infty}^{+\infty} \frac{p^n}{\prod_{i=1}^m (p - p_i)(p - \bar{p}_i)} dp, \quad 0 \leq n \leq 2m - 2. \tag{3.74}$$

then $I_3^n$, $I_6^n$ and $I_9^n$ are subsets of $I_m^n$. Eqs. (3.69), (3.70) and (3.73) have a recursive relation, i.e.,

$$I_m^{n+2} - 2 \operatorname{Re}(p_m) I_m^{n+1} + |p_m|^2 I_m^n = I_{m-1}^n. \tag{3.75}$$

Eqs. (3.69), (3.70), (3.73) and (3.75) show that $I_m^0 (1 \leq m \leq 3)$ and $I_m^1 (2 \leq m \leq 3)$ are required for the calculation of $I_3^n$ which is needed by the Green's function; $I_m^0 (4 \leq m \leq 6)$ and $I_m^1 (4 \leq m \leq 6)$ are required for the calculation of $I_6^n$ which is needed by the first derivative of the Green's function; and $I_m^0 (7 \leq m \leq 9)$ and $I_m^1 (7 \leq m \leq 9)$ are required for the calculation of $I_9^n$ which is needed by the second derivative of the Green's function. So unified explicit expressions of $I_m^0 (1 \leq m \leq 9)$ and $I_m^1 (2 \leq m \leq 9)$ are required by the unified explicit expressions of the Green's function and its derivatives.

## 3.4.2   Unified explicit expressions

By applying the Cauchy residue theorem to Eq. (3.74) with the distinctness assumption of $p_i$, $I_m^n$ becomes the following explicit algebraic expression in terms of $p_i$

$$I_m^n = 2\pi i \sum_{i=1}^m \frac{p_i^n}{(p_i - \bar{p}_i) \prod_{1 \leq j \neq i \leq m} (p_i - p_j)(p_i - \bar{p}_j)}. \tag{3.76}$$

However, the denominator in this expression has the factor $p_i - p_j$, which makes the expression invalid and may also cause remarkable errors in the numerical computation when $p_i$ and $p_j$ are very close to each other. To overcome this difficulty, the rearrangement of $I_m^n$ is required by removing the factor $p_i - p_j$ in the denominator.

When $m = 1, 2, 3$, the rearranged $I_m^n (n = 0, 1)$ are

$$I_1^0 = \frac{\pi}{\beta_1},$$

$$I_2^n = -\frac{\pi}{\beta_1 \beta_2} \operatorname{Im} \left( \frac{p_1^n}{p_1 - \bar{p}_2} \right),$$

$$I_3^n = -\frac{\pi}{2\beta_1 \beta_2 \beta_3} \operatorname{Re} \left[ \frac{p_1^n}{(p_1 - \bar{p}_2)(p_1 - \bar{p}_3)} + \frac{p_2^n}{(p_2 - \bar{p}_1)(p_2 - \bar{p}_3)} \right.$$

$$\left. + \frac{p_3^n}{(p_3 - \bar{p}_1)(p_3 - \bar{p}_2)} \right], \tag{3.77}$$

where $\beta_i$ is the imaginary part of $p_i$. Note that $I_m^n$ are real-valued.

The most important advantage of Eq. (3.77) is that the rearranged explicit expressions are applicable not only when $p_i$ are distinct but also when some $p_i$ are equivalent as well as any two $p_i$ are very close to each other. This advantage will be proved in the following numerical evaluation. Besides, the Green's function in terms of unified explicit

$I_m^n (n = 0, 1, m = 1, 2, 3)$ are equivalent to the explicit expressions proposed by Ting and Lee (1997).

The unified explicit expressions of $I_m^n (n = 0, 1, m = 4, 5, 6)$ are required by the first derivative of the Green's function. The rearranged $I_m^n (n = 0, 1, m = 4, 5, 6)$ followed by the substitutions $p_4 = p_1$, $p_5 = p_2$ and $p_6 = p_3$ are

$$
I_4^n = \frac{\pi}{4\beta_1^2 \beta_2 \beta_3} \operatorname{Im} \left[ \frac{-ip_1^n}{\beta_1(p_1 - \bar{p}_2)(p_1 - \bar{p}_3)} + \frac{p_2^n}{(p_2 - \bar{p}_1)^2(p_2 - \bar{p}_3)} \right.
$$
$$
\left. + \frac{p_3^n}{(p_3 - \bar{p}_1)^2(p_3 - \bar{p}_2)} + 2F_0^{(n)}(1, 2, \bar{1}, \bar{3}) + F_0^{(n)}(1, 1, \bar{2}, \bar{3}) \right],
$$

$$
I_5^n = \frac{\pi}{8\beta_1^2 \beta_2^2 \beta_3} \operatorname{Re} \left[ \frac{-p_1^n i}{\beta_1(p_1 - \bar{p}_2)^2(p_1 - \bar{p}_3)} + \frac{-p_2^n i}{\beta_2(p_2 - \bar{p}_1)^2(p_2 - \bar{p}_3)} \right.
$$
$$
+ \frac{p_3^n}{(p_3 - \bar{p}_1)^2(p_3 - \bar{p}_2)^2} + 4F_1^{(n)}(1, 2, \bar{1}, \bar{2}, \bar{3}) + 2F_1^{(n)}(1, 3, \bar{1}, \bar{2}, \bar{2})
$$
$$
\left. + 2F_1^{(n)}(2, 3, \bar{1}, \bar{1}, \bar{2}) + F_1^{(n)}(1, 1, \bar{2}, \bar{2}, \bar{3}) + F_1^{(n)}(2, 2, \bar{1}, \bar{1}, \bar{3}) \right],
$$

$$
I_6^n = \frac{-\pi}{16\beta_1^2 \beta_2^2 \beta_3^2} \operatorname{Im} \left[ \frac{-p_1^n i}{\beta_1(p_1 - \bar{p}_2)^2(p_1 - \bar{p}_3)^2} + \frac{-p_2^n i}{\beta_2(p_2 - \bar{p}_1)^2(p_2 - \bar{p}_3)^2} \right.
$$
$$
+ \frac{-p_3^n i}{\beta_3(p_3 - \bar{p}_1)^2(p_3 - \bar{p}_2)^2} + 4F_2^{(n)}(1, 2, \bar{1}, \bar{2}, \bar{3}, \bar{3}) + 4F_2^{(n)}(1, 3, \bar{1}, \bar{2}, \bar{2}, \bar{3})
$$
$$
+ 4F_2^{(n)}(2, 3, \bar{1}, \bar{1}, \bar{2}, \bar{3}) + F_2^{(n)}(1, 1, \bar{2}, \bar{2}, \bar{3}, \bar{3}) + F_2^{(n)}(2, 2, \bar{1}, \bar{1}, \bar{3}, \bar{3})
$$
$$
+ F_2^{(n)}(3, 3, \bar{1}, \bar{1}, \bar{2}, \bar{2}) + 4F_3^{(n)}(1, 2, 3, \bar{1}, \bar{2}, \bar{3}) + 2F_3^{(n)}(1, 1, 2, \bar{2}, \bar{3}, \bar{3})
$$
$$
\left. + 2F_3^{(n)}(1, 2, 2, \bar{1}, \bar{3}, \bar{3}) + 2F_3^{(n)}(1, 1, 3, \bar{2}, \bar{2}, \bar{3}) \right]. \tag{3.78}
$$

In Eq. (3.78), the abbreviations $p_k = k$ and $\bar{p}_k = \bar{k}$ for the variables of the functions $F_m^{(n)}(...)$ $(n = 0, 1, m = 1, 2, 3)$ are introduced for convenience, and

$$
F_0^{(0)}(x_1, \ldots, x_4) = \left[ \prod_{i=3}^4 (x_1 - x_i)(x_2 - x_i) \right]^{-1} \times (x_1 + x_2 - x_3 - x_4),
$$

$$
F_1^{(0)}(x_1, \ldots, x_5) = \left[ \prod_{i=3}^5 (x_1 - x_i)(x_2 - x_i) \right]^{-1} \times
$$
$$
[(x_1 - x_3)(x_1 - x_4) + (x_1 - x_3)(x_2 - x_5) + (x_2 - x_4)(x_2 - x_5)],
$$

$$
F_2^{(0)}(x_1, \ldots, x_6) = \left[ \prod_{i=3}^6 (x_1 - x_i)(x_2 - x_i) \right]^{-1} \times
$$
$$
[(x_1 - x_3)(x_1 - x_4)(x_1 - x_5) + (x_1 - x_3)(x_1 - x_4)(x_2 - x_6)
$$
$$
+ (x_1 - x_3)(x_2 - x_5)(x_2 - x_6) + (x_2 - x_4)(x_2 - x_5)(x_2 - x_6)],
$$

$$
F_3^{(0)}(x_1, \ldots, x_6) = \left[ \prod_{i=4}^6 (x_1 - x_i)(x_2 - x_i)(x_3 - x_i) \right]^{-1} \times
$$
$$
[y_2^2 - y_1 y_3 + y_3 y_4 + y_2(-y_1 y_4 + y_4^2 - 2y_5)
$$

$$+ (y_1 - y_4)y_6 + y_5(y_1^2 - y_1y_4 + y_5)],$$

$$F_0^{(1)}(x_1, \ldots, x_4) = [(x_1 - x_3)(x_2 - x_3)]^{-1} + x_4 F_0^{(0)}(x_1, \ldots, x_4),$$

$$F_1^{(1)}(x_1, \ldots, x_5) = F_0^{(0)}(x_1, \ldots, x_4) + x_5 F_1^{(0)}(x_1, \ldots, x_5),$$

$$F_2^{(1)}(x_1, \ldots, x_6) = F_1^{(0)}(x_1, \ldots, x_5) + x_6 F_2^{(0)}(x_1, \ldots, x_6),$$

$$F_3^{(1)}(x_1, \ldots, x_6) = F_1^{(0)}(x_4, x_5, x_1, x_2, x_3) + x_6 F_3^{(0)}(x_1, \ldots, x_6). \tag{3.79}$$

In Eq. (3.79), $y_i$ are elementary symmetric polynomials defined by

$$y_i = \begin{cases} e_i(x_1, x_2, x_3), & i = 1, 2, 3, \\ e_{i-3}(x_4, x_5, x_6), & i = 4, 5, 6. \end{cases} \tag{3.80}$$

The unified explicit expressions of $I_m^n (n = 0, 1, m = 7, 8, 9)$ are required by the second derivative of the Green's function. The rearranged $I_m^n (n = 0, 1, m = 7, 8, 9)$ followed by the substitutions $p_7 = p_4 = p_1$, $p_8 = p_5 = p_2$ and $p_9 = p_6 = p_3$ are

$$I_7^n = \frac{-\pi}{32\beta_1^3\beta_2^2\beta_3^2} \operatorname{Re}\left[ \frac{-3p_1^n}{4\beta_1^2(p_1 - \bar{p}_2)^2(p_1 - \bar{p}_3)^2} + \frac{-p_2^n i}{\beta_2(p_2 - \bar{p}_1)^3(p_2 - \bar{p}_3)^2} \right.$$

$$+ \frac{-p_3^n i}{\beta_3(p_3 - \bar{p}_1)^3(p_3 - \bar{p}_2)^2} + 6F_4^{(n)}(1, 2, \bar{1}, \bar{1}, \bar{2}, \bar{3}, \bar{3})$$

$$+ 6F_4^{(n)}(1, 3, \bar{1}, \bar{1}, \bar{2}, \bar{2}, \bar{3}) + 4F_4^{(n)}(2, 3, \bar{1}, \bar{1}, \bar{1}, \bar{2}, \bar{3})$$

$$+ 3F_4^{(n)}(1, 1, \bar{1}, \bar{2}, \bar{2}, \bar{3}, \bar{3}) + F_4^{(n)}(2, 2, \bar{1}, \bar{1}, \bar{1}, \bar{3}, \bar{2})$$

$$+ F_4^{(n)}(3, 3, \bar{1}, \bar{1}, \bar{1}, \bar{2}, \bar{2}) + 12F_5^{(n)}(1, 2, 3, \bar{1}, \bar{1}, \bar{2}, \bar{3})$$

$$+ 6F_5^{(n)}(1, 1, 2, \bar{1}, \bar{2}, \bar{3}, \bar{3}) + 6F_5^{(n)}(1, 1, 3, \bar{1}, \bar{2}, \bar{2}, \bar{3})$$

$$+ 3F_5^{(n)}(1, 2, 2, \bar{1}, \bar{1}, \bar{3}, \bar{3}) + 3F_5^{(n)}(1, 3, 3, \bar{1}, \bar{1}, \bar{2}, \bar{2})$$

$$+ 2F_5^{(n)}(2, 2, 3, \bar{1}, \bar{1}, \bar{1}, \bar{3}) + 2F_5^{(n)}(2, 3, 3, \bar{1}, \bar{1}, \bar{1}, \bar{2})$$

$$\left. + F_5^{(n)}(1, 1, 1, \bar{2}, \bar{2}, \bar{3}, \bar{3}) \right], \tag{3.81a}$$

$$I_8^n = \frac{\pi}{64\beta_1^3\beta_2^3\beta_3^2} \operatorname{Im}\left[ \frac{-3p_1^n}{4\beta_1^2(p_1 - \bar{p}_2)^3(p_1 - \bar{p}_3)^2} + \frac{-3p_2^n}{4\beta_2^2(p_2 - \bar{p}_1)^3(p_2 - \bar{p}_3)^2} \right.$$

$$+ \frac{-p_3^n i}{\beta_3(p_3 - \bar{p}_1)^3(p_3 - \bar{p}_2)^3} + 9F_6^{(n)}(1, 2, \bar{1}, \bar{1}, \bar{2}, \bar{2}, \bar{3}, \bar{3})$$

$$+ 6F_6^{(n)}(1, 3, \bar{1}, \bar{1}, \bar{2}, \bar{2}, \bar{2}, \bar{3}) + 6F_6^{(n)}(2, 3, \bar{1}, \bar{1}, \bar{1}, \bar{2}, \bar{2}, \bar{3})$$

$$+ 3F_6^{(n)}(1, 1, \bar{1}, \bar{2}, \bar{2}, \bar{2}, \bar{3}, \bar{3}) + 3F_6^{(n)}(2, 2, \bar{1}, \bar{1}, \bar{1}, \bar{2}, \bar{3}, \bar{3})$$

$$+ F_6^{(n)}(3, 3, \bar{1}, \bar{1}, \bar{1}, \bar{2}, \bar{2}, \bar{2}) + 18F_7^{(n)}(1, 2, 3, \bar{1}, \bar{1}, \bar{2}, \bar{2}, \bar{3})$$

$$+ 9F_7^{(n)}(1, 1, 2, \bar{1}, \bar{2}, \bar{2}, \bar{3}, \bar{3}) + 9F_7^{(n)}(1, 2, 2, \bar{1}, \bar{1}, \bar{2}, \bar{3}, \bar{3})$$

$$+ 6F_7^{(n)}(1, 1, 3, \bar{1}, \bar{2}, \bar{2}, \bar{2}, \bar{3}) + 6F_7^{(n)}(2, 2, 3, \bar{1}, \bar{1}, \bar{1}, \bar{2}, \bar{3})$$

$$+ 3F_7^{(n)}(2, 3, 3, \bar{1}, \bar{1}, \bar{1}, \bar{2}, \bar{2}) + 3F_7^{(n)}(1, 3, 3, \bar{1}, \bar{1}, \bar{2}, \bar{2}, \bar{3})$$

$$+ F_7^{(n)}(1, 1, 1, \bar{2}, \bar{2}, \bar{2}, \bar{3}, \bar{3}) + F_7^{(n)}(2, 2, 2, \bar{1}, \bar{1}, \bar{1}, \bar{3}, \bar{3})$$

$$+ 18F_8^{(n)}(1,1,2,3,\bar{1},\bar{2},\bar{2},\bar{3}) + 9F_8^{(n)}(1,1,2,2,\bar{1},\bar{2},\bar{3},\bar{3})$$
$$+ 3F_8^{(n)}(1,1,3,3,\bar{1},\bar{2},\bar{2},\bar{2}) + 3F_8^{(n)}(1,1,1,2,\bar{2},\bar{2},\bar{3},\bar{3})$$
$$+ 2F_8^{(n)}(1,1,1,3,\bar{2},\bar{2},\bar{2},\bar{3})\Big]\,, \tag{3.81b}$$

$$I_9^n = \frac{\pi}{128\beta_1^3\beta_2^3\beta_3^3}\,\mathrm{Re}\left[\frac{-3p_1^n}{4\beta_1^2(p_1-\bar{p}_2)^3(p_1-\bar{p}_3)^3} + \frac{-3p_2^n}{4\beta_2^2(p_2-\bar{p}_1)^3(p_2-\bar{p}_3)^3}\right.$$
$$\frac{-3p_3^n}{4\beta_3^2(p_3-\bar{p}_1)^3(p_3-\bar{p}_2)^3} + 9F_9^{(n)}(1,2,\bar{1},\bar{1},\bar{2},\bar{2},\bar{3},\bar{3},\bar{3})$$
$$+ 9F_9^{(n)}(1,3,\bar{1},\bar{1},\bar{2},\bar{2},\bar{2},\bar{3},\bar{3}) + 9F_9^{(n)}(2,3,\bar{1},\bar{1},\bar{1},\bar{2},\bar{2},\bar{3},\bar{3})$$
$$+ 3F_9^{(n)}(1,1,\bar{1},\bar{2},\bar{2},\bar{2},\bar{3},\bar{3},\bar{3}) + 3F_9^{(n)}(2,2,\bar{1},\bar{1},\bar{1},\bar{2},\bar{3},\bar{3},\bar{3})$$
$$+ 3F_9^{(n)}(3,3,\bar{1},\bar{1},\bar{1},\bar{2},\bar{2},\bar{2},\bar{3}) + 27F_{10}^{(n)}(1,2,3,\bar{1},\bar{1},\bar{2},\bar{2},\bar{3},\bar{3})$$
$$+ 9F_{10}^{(n)}(1,1,2,\bar{1},\bar{2},\bar{2},\bar{3},\bar{3},\bar{3}) + 9F_{10}^{(n)}(1,2,2,\bar{1},\bar{1},\bar{2},\bar{3},\bar{3},\bar{3})$$
$$+ 9F_{10}^{(n)}(1,1,3,\bar{1},\bar{2},\bar{2},\bar{2},\bar{3},\bar{3}) + 9F_{10}^{(n)}(2,2,3,\bar{1},\bar{1},\bar{1},\bar{2},\bar{3},\bar{3})$$
$$+ 9F_{10}^{(n)}(2,3,3,\bar{1},\bar{1},\bar{1},\bar{2},\bar{2},\bar{3}) + 9F_{10}^{(n)}(1,3,3,\bar{1},\bar{1},\bar{2},\bar{2},\bar{2},\bar{3})$$
$$+ F_{10}^{(n)}(1,1,1,\bar{2},\bar{2},\bar{2},\bar{3},\bar{3},\bar{3}) + F_{10}^{(n)}(2,2,2,\bar{1},\bar{1},\bar{1},\bar{3},\bar{3},\bar{3})$$
$$+ F_{10}^{(n)}(3,3,3,\bar{1},\bar{1},\bar{1},\bar{2},\bar{2},\bar{2}) + 27F_{11}^{(n)}(1,1,2,3,\bar{1},\bar{2},\bar{2},\bar{3},\bar{3})$$
$$+ 27F_{11}^{(n)}(1,2,2,3,\bar{1},\bar{1},\bar{2},\bar{3},\bar{3}) + 27F_{11}^{(n)}(1,2,3,3,\bar{1},\bar{1},\bar{2},\bar{2},\bar{3})$$
$$+ 9F_{11}^{(n)}(1,1,2,2,\bar{1},\bar{2},\bar{3},\bar{3},\bar{3}) + 9F_{11}^{(n)}(1,1,3,3,\bar{1},\bar{2},\bar{2},\bar{2},\bar{3})$$
$$+ 9F_{11}^{(n)}(2,2,3,3,\bar{1},\bar{1},\bar{1},\bar{2},\bar{3}) + 3F_{11}^{(n)}(1,1,1,2,\bar{2},\bar{2},\bar{3},\bar{3},\bar{3})$$
$$+ 3F_{11}^{(n)}(1,1,1,3,\bar{2},\bar{2},\bar{2},\bar{3},\bar{3}) + 3F_{11}^{(n)}(1,2,2,2,\bar{1},\bar{1},\bar{3},\bar{3},\bar{3})$$
$$+ 3F_{11}^{(n)}(1,3,3,3,\bar{1},\bar{1},\bar{2},\bar{2},\bar{2}) + 3F_{11}^{(n)}(2,2,2,3,\bar{1},\bar{1},\bar{1},\bar{3},\bar{3})$$
$$+ 3F_{11}^{(n)}(2,3,3,3,\bar{1},\bar{1},\bar{1},\bar{2},\bar{2})\Big]\,, \tag{3.81c}$$

The explicit expressions for the functions $F_m^{(n)}(\cdots)$ $(n=0,1, m=4,\ldots,11)$ are quite lengthy and thus they are given in Appendix C.

In conclusion, substitution of Eq. (3.77) into Eq. (3.69) and then into Eqs. (3.58) yields the explicit expression of $A_{ij}(\bar{\boldsymbol{x}})$; substitution of Eqs. (3.77) and (3.78) into Eq. (3.70) and then into Eq. (3.59) yields the explicit expression of $P_{ijk}(\bar{\boldsymbol{x}})$; substitution of Eqs. (3.77), (3.78) and (3.81) into Eq. (3.73) and then into Eq. (3.60) yields the explicit expression of $Q_{ijkl}(\bar{\boldsymbol{x}})$. Further, the Green's function and its derivatives are determined by Eqs. (3.13)-(3.15) with the unified explicit expressions of $A_{ij}(\bar{\boldsymbol{x}})$, $P_{ijk}(\bar{\boldsymbol{x}})$ and $Q_{ijkl}(\bar{\boldsymbol{x}})$.

## 3.5 Verifications and comparison of the different methods

In the previous sections, we presented four formulae to calculate the 3D Green's function and its derivatives for generally anisotropic elastic materials. In this section, we focus on the numerical evaluation. For convenience, the methods based on the four different formulae are named as the numerical integration method (NIM), the residue calculus

method (RCM), the Stroh formalism method (SFM) and the unified explicit expression method (UEEM), respectively.

The NIM is relatively simple. It requires only a certain numerical integration of the line integrals in Eqs. (3.8)-(3.10) and the substitution of the results into Eqs. (3.13)-(3.15). The numerical integration can be the standard Gaussian quadrature. Different from the other three methods, the NIM doesn't need to know the Stroh eigenvalues.

The RCM is an alternative of the NIM. It applies the residue calculus to the line integrals in Eqs. (3.8)-(3.10) instead of the numerical integration. Resulting from the substitutions of Eqs. (3.25)-(3.27) into Eqs. (3.13)-(3.15), the expressions of the Green's function and its derivatives are explicit, but valid only when the Stroh eigenvalues are distinct. The explicit expressions are analytical if the Stroh eigenvalues are analytical. However, the Stroh eigenvalues are analytical only for special cases, for example when the material is isotropic or transversely isotropic. Generally, a numerical subroutine is needed to find the Stroh eigenvalues. In our program, the Stroh eigenvalues are calculated as the eigenvalues of the fundamental elasticity matrix $\mathbf{N}$ on an oblique plane to have a better accuracy.

The SFM is different from the other methods. It is based on the fact that the Green's function can be constructed from the solutions of an Stroh eigenvalue problem. Therefore, the explicit expressions of the Green's function and its derivatives in the SFM are in terms of the eigenvalues and the eigenvectors of the Stroh eigenvalue problem, not only the Stroh eigenvalues like in the RCM. For the convenience of the readers, the relations between the equations in the SFM are illustrated in Fig. 3.2. In the numerical calculation, the Stroh eigenvalue problem is solved by using the subroutine ZGEEV in the LAPACK library (Anderson et al., 1999).

$$
\begin{array}{ccccccc}
\boldsymbol{m},\boldsymbol{n},\boldsymbol{x},C_{ijkl} & \longrightarrow & \mathbf{N} & \longrightarrow & \text{Normalized } \boldsymbol{\xi}_\alpha \ (3.33) & \xrightarrow{p_\alpha} & \mathbf{A} \ (3.32) \longrightarrow \mathbf{G} \ (3.34) \\
\text{(B.6) or (B.10)} & & (2.37) & & \boldsymbol{\eta}_\alpha \ (3.30) & & \\
\downarrow & & \downarrow & & & & \\
\boldsymbol{n}_{,i},\boldsymbol{m}_{,i} & \longrightarrow & \mathbf{N}_{,i} & \longrightarrow & c^{(i)}_{\alpha\beta} & \xrightarrow{\ \ } & p_{\alpha,i}\ (3.45) \\
\text{(B.9) or (B.11)} & & & & (3.46) \ \& \ (3.48) & & \boldsymbol{\xi}_{\alpha,i}\ (3.43a) \longrightarrow \mathbf{A}_{,i} \longrightarrow \mathbf{G}_{,i}\ (3.38) \\
& & & & & & \boldsymbol{\eta}_{\alpha,i}(3.43b) \\
\downarrow & & \downarrow & & & & \\
\boldsymbol{n}_{,ij},\boldsymbol{m}_{,ij} & \longrightarrow & \mathbf{N}_{,ij} & \longrightarrow & d^{(ij)}_{\alpha\beta} & \xrightarrow{\ \ } & \boldsymbol{\xi}_{\alpha,ij}\ (3.49) \longrightarrow \mathbf{A}_{,ij} \longrightarrow \mathbf{G}_{,ij}\ (3.39) \\
\text{(B.9) or (B.11)} & & & & (3.52) \ \& \ (3.53) & & \\
\end{array}
$$
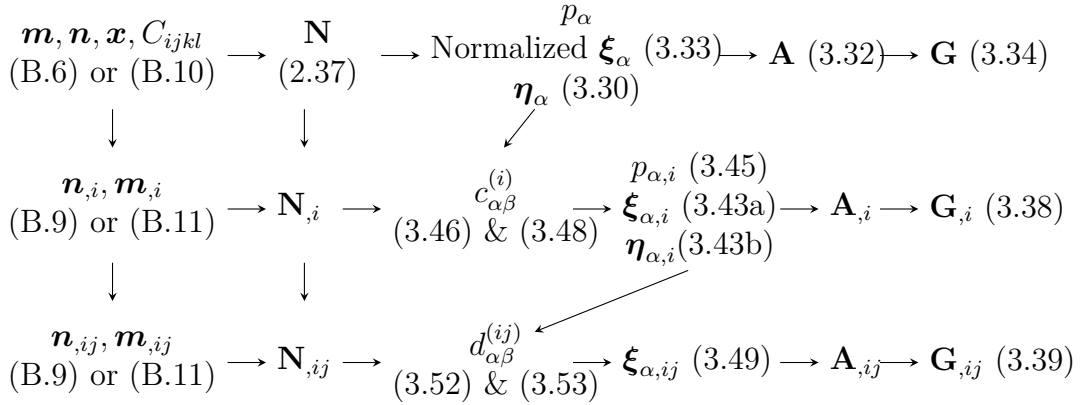
Figure 3.2: Diagram of the Stroh formalism method.

The UEEM is an improvement of the RCM. It results in unified explicit expressions of the Green's function and its derivatives, i.e., the explicit expressions remain valid when the Stroh eigenvalues repeat. For the Green's function, the unified explicit expression is a straightforward rewritten of the explicit expression in RCM when the Stroh eigenvalues are distinct. The feature, the explicit expression in the RCM when the Stroh eigenvalues are distinct can be recast into a unified explicit one, was firstly found by Ting and Lee (1997). But the use of this feature in the derivatives of the Green's function was not yet fully explored. In Section 3.4, the feature in the derivatives of the Green's function is found by presenting the unified explicit expressions of the derivatives of the Green's function after

reformulations of the three integrals. The procedure is thus not as simple as that in the RCM. For the convenience of readers, Fig. 3.3 is a diagram of the procedure of the UEEM with the known Stroh eigenvalues. In the numerical calculation, the Stroh eigenvalues are evaluated as the eigenvalues of the fundamental elasticity matrix $\mathbf{N}$ associated with the oblique plane perpendicular to $\boldsymbol{x}$.

$$
\begin{array}{ccccc}
I_m^n\ (3.77) & & I_3^n\ (3.69) & & \\
(n=0,1,m=1,2,3) & \to & (n=0,1,\ldots,4) & \to A_{ij}(\bar{\boldsymbol{x}})\ (3.58) \to & G_{ij}(\boldsymbol{x})\ (3.13) \\[2ex]
I_m^n\ (3.78) & & I_6^n\ (3.70) & & \\
(n=0,1,m=4,5,6) & \to & (n=0,1,\ldots,10) & \to P_{ijk}(\bar{\boldsymbol{x}})\ (3.59) \to & G_{ij,k}(\boldsymbol{x})\ (3.14) \\[2ex]
I_m^n\ (3.81) & & I_9^n\ (3.73) & & \\
(n=0,1,m=7,8,9) & \to & (n=0,1,\ldots,16) & \to Q_{ijkl}(\bar{\boldsymbol{x}})\ (3.60) \to & G_{ij,kl}(\boldsymbol{x})\ (3.15)
\end{array}
$$
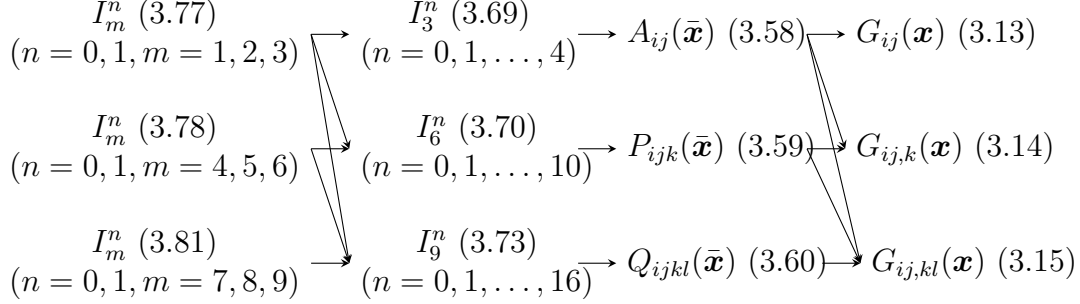
Figure 3.3: Diagram of the unified explicit expression method with known Stroh eigenvalues.

In the following, firstly, we verify the four different methods by the comparison with the analytical Green's function for transversely isotropic materials (Pan and Chou, 1976) which is evaluated by using the algebra algorithm software MATHEMATICA, as well as its derivatives. Secondly, the abilities of the different methods to deal with the nearly degenerate cases are investigated by the numerical evaluations near a fully degenerate point in a transversely isotropic material. Then the CPU times for calculating the Green's function and its derivatives of different methods are obtained to give a direct comparison on the efficiencies of the four methods. Finally, a general evaluation of the Green's function and its derivatives on a unit sphere by the UEEM is presented.

### 3.5.1   Verification of the numerical integration method

The numerical integration method (NIM) avoids the need of solving a polynomial equation or the Stroh eigenvalue problem, but requires the numerical integration. The standard Gaussian quadrature is adopted for the numerical evaluation of the three integrals, i.e., Eqs. (3.8)-(3.10). Since transversely isotropic materials have analytical Green's function (Pan and Chou, 1976), we use the transversely isotropic materials Mg and C as examples to verify the NIM, and investigate the effect of the number of the Gaussian points on the accuracy. Choosing the symmetry axis of the transversely isotropic material as the $x_3$ coordinate axis, the nonzero elastic constants $C_{ij}$ of Mg and C are, respectively,

$$
\begin{aligned}
C_{11} = C_{22} = 59.7\text{GPa}, \quad & C_{33} = 61.7\text{GPa}, \quad C_{13} = C_{23} = 21.7\text{GPa}, \\
C_{12} = 26.2\text{GPa}, \quad & C_{44} = C_{55} = 16.4\text{GPa}, \quad C_{66} = 16.75\text{GPa},
\end{aligned} \tag{3.82}
$$

and

$$
\begin{aligned}
C_{11} = C_{22} = 1160\text{GPa}, \quad & C_{33} = 46.6\text{GPa}, \quad C_{13} = C_{23} = 109\text{GPa}, \\
C_{12} = 290\text{GPa}, \quad & C_{44} = C_{55} = 2.3\text{GPa}, \quad C_{66} = 435\text{GPa}.
\end{aligned} \tag{3.83}
$$

Here the capital $C$ represents the elastic constant matrix, i.e., the elasticity tensor $c_{ijkl}$ in Voigt notation.

| | NIM | Pan and Chou (1976) | Unit |
|---|---|---|---|
| $G_{11}$ | $8.3782981337130575 \times 10^{-4}$ | $8.3782981337130640 \times 10^{-4}$ | |
| $G_{12}$ | $6.0007221557104541 \times 10^{-5}$ | $6.0007221557104690 \times 10^{-5}$ | |
| $G_{13}$ | $8.0163881274800664 \times 10^{-5}$ | $8.0163881274800705 \times 10^{-5}$ | $10^{-9}m$ |
| $G_{22}$ | $9.2784064570696238 \times 10^{-4}$ | $9.2784064570696325 \times 10^{-4}$ | |
| $G_{23}$ | $1.6032776254960144 \times 10^{-4}$ | $1.6032776254960141 \times 10^{-4}$ | |
| $G_{33}$ | $1.0578889644135979 \times 10^{-3}$ | $1.0578889644135983 \times 10^{-3}$ | |
| $G_{11,1}$ | $-5.9117971638181820 \times 10^{-6}$ | $-5.9117971638178034 \times 10^{-6}$ | |
| $G_{12,1}$ | $4.7768458294984388 \times 10^{-5}$ | $4.7768458294984570 \times 10^{-5}$ | |
| $G_{13,1}$ | $6.1775349906881231 \times 10^{-5}$ | $6.1775349906880784 \times 10^{-5}$ | $1$ |
| $G_{22,1}$ | $-8.4277163614102321 \times 10^{-5}$ | $-8.4277163614102660 \times 10^{-5}$ | |
| $G_{23,1}$ | $-3.6777062735840222 \times 10^{-5}$ | $-3.6777062735839842 \times 10^{-5}$ | |
| $G_{33,1}$ | $-1.2597090883943352 \times 10^{-4}$ | $-1.2597090883943393 \times 10^{-4}$ | |
| $G_{11,11}$ | $-1.5317520185559242 \times 10^{-5}$ | $-1.5317520185560475 \times 10^{-5}$ | |
| $G_{12,11}$ | $-3.2300147619148905 \times 10^{-5}$ | $-3.2300147619146344 \times 10^{-5}$ | |
| $G_{13,11}$ | $-4.7740579505162444 \times 10^{-5}$ | $-4.7740579505166856 \times 10^{-5}$ | $10^{9}m^{-1}$ |
| $G_{22,11}$ | $-6.2581146860783276 \times 10^{-5}$ | $-6.2581146860784102 \times 10^{-5}$ | |
| $G_{23,11}$ | $-2.1927033538652794 \times 10^{-5}$ | $-2.1927033538654044 \times 10^{-5}$ | |
| $G_{33,11}$ | $-8.3977103691749630 \times 10^{-5}$ | $-8.3977103691742474 \times 10^{-5}$ | |

Table 3.1: Components of the Green's function and its derivatives by the numerical integration method with 25 Gaussian points and analytical solutions for transversely isotropic material Mg at the point $(1, 2, 3)$.

| | NIM | Pan and Chou (1976) | Unit |
|---|---|---|---|
| $G_{11}$ | $4.3827891652552302 \times 10^{-5}$ | $4.3827896221260168 \times 10^{-5}$ | |
| $G_{12}$ | $4.6263482483389481 \times 10^{-7}$ | $4.6263223755486290 \times 10^{-7}$ | |
| $G_{13}$ | $2.8820782772483946 \times 10^{-5}$ | $2.8820815639128441 \times 10^{-5}$ | $10^{-9}m$ |
| $G_{22}$ | $4.4521843889803126 \times 10^{-5}$ | $4.4521844577592456 \times 10^{-5}$ | |
| $G_{23}$ | $5.7641565544967844 \times 10^{-5}$ | $5.7641631278256881 \times 10^{-5}$ | |
| $G_{33}$ | $3.7072713618185576 \times 10^{-3}$ | $3.7072624469392692 \times 10^{-3}$ | |
| $G_{11,1}$ | $5.5705998231869374 \times 10^{-7}$ | $5.5707948825936928 \times 10^{-7}$ | |
| $G_{12,1}$ | $2.6022193925293714 \times 10^{-7}$ | $2.6022823188120547 \times 10^{-7}$ | |
| $G_{13,1}$ | $1.9733666048006437 \times 10^{-5}$ | $1.9731677292333889 \times 10^{-5}$ | $1$ |
| $G_{22,1}$ | $-2.0914680362270449 \times 10^{-7}$ | $-2.0915875780597971 \times 10^{-7}$ | |
| $G_{23,1}$ | $-1.8179372682933386 \times 10^{-5}$ | $-1.8178276693589096 \times 10^{-5}$ | |
| $G_{33,1}$ | $-6.6489143291522670 \times 10^{-4}$ | $-6.6490424049481050 \times 10^{-4}$ | |
| $G_{11,11}$ | $1.3079233547358874 \times 10^{-7}$ | $1.3037961156879091 \times 10^{-7}$ | |
| $G_{12,11}$ | $-4.4897325479577848 \times 10^{-7}$ | $-4.4871709609986970 \times 10^{-6}$ | |
| $G_{13,11}$ | $-2.1307363510067809 \times 10^{-5}$ | $-2.1314882684275725 \times 10^{-5}$ | $10^{9}m^{-1}$ |
| $G_{22,11}$ | $6.8035444137838627 \times 10^{-9}$ | $6.6917582324103661 \times 10^{-9}$ | |
| $G_{23,11}$ | $-6.2707614770661805 \times 10^{-6}$ | $-6.273211981373254 9\times 10^{-6}$ | |
| $G_{33,11}$ | $-3.0808030564059499 \times 10^{-4}$ | $-3.0719075049198089 \times 10^{-4}$ | |

Table 3.2: Components of the Green's function and its derivatives by the numerical integration method with 25 Gaussian points and analytical solutions for transversely isotropic material C at the point $(1, 2, 3)$.

Tables 3.1 and 3.2 are respectively the numerical results for the transversely isotropic materials Mg and C by the NIM, as well as the analytical ones. The numerical results by the NIM in Table 3.1 agree well with the analytical results. Compared with the numerical results for the material Mg, the results by the NIM for the material C in Table 3.2 have less accuracy, but are of practical interest. The less accuracy of the NIM for the material C may be due to the larger difference between the material constants of the material C. Therefore it can be concluded that the larger difference between the material constants, the more Gaussian points are needed to ensure the same accuracy.

To investigate the effect of the number of the Gaussian points on the accuracy, the relative error is defined as

$$e = |(b - a)/a|, \tag{3.84}$$

where $a$ is the analytical result and $b$ is the numerical result by the NIM. For simplicity, we choose 3 maximum relative errors in the components of $G_{ij}$, $G_{ij,1}$ and $G_{ij,11}$, respectively. Fig. 3.4 shows the relation between the 3 maximum relative errors and the number of Gaussian points. For both materials, the maximum relative errors decrease with the increment of the number of the Gaussian points until the number reach a certain value. Thereafter, the maximum relative errors become unstable around a certain value. This may be due to the use of the double precision real numbers. Therefore, we suggest that the number of Gaussian points should be less than 25 for the material Mg, and 60 for the material C. But for practical interest where the efficiency is very important, the number of the Gaussian points could be 10 for the material Mg, and 30 for the material C.
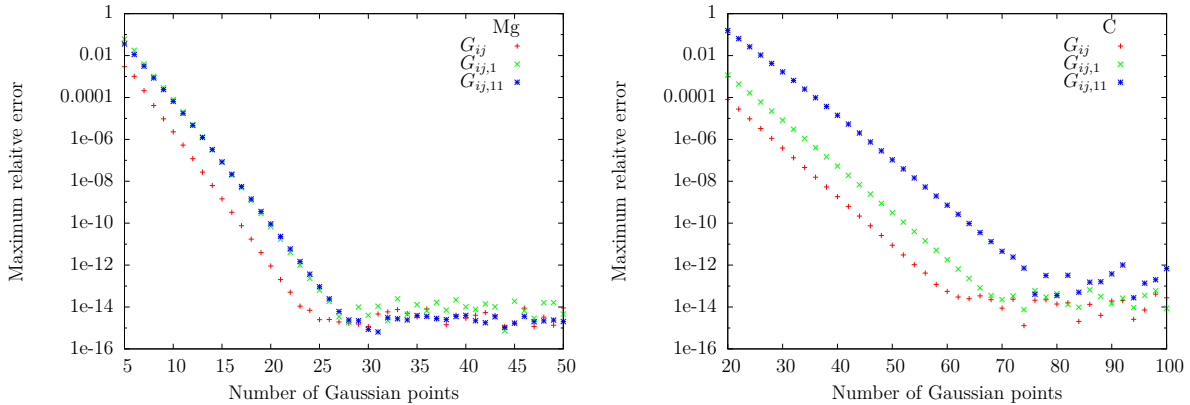


Figure 3.4: The maximum relative errors in $G_{ij}$, $G_{ij,1}$ and $G_{ij,11}$ versus the number of Gaussian points for the transversely isotropic materials Mg and C at point $(1, 2, 3)$.

### 3.5.2  Verification of the residue calculus method

Instead of the numerical integration of the line integrals in Eqs. (3.8)-(3.10), the residue calculus method (RCM) applies Cauchy residue theorem to the line integrals in Eqs. (3.19)-(3.21). Eqs. (3.25)-(3.27) are the resulting explicit expressions for the three line integrals when the Stroh eigenvalues, the poles of the integrands, are distinct. The explicit expressions when the Stroh eigenvalues repeat could be derived in the same way, but would be rather complicated. For simplicity, this section focuses on the simple explicit expressions.

When the Stroh eigenvalues repeat, the numerical evaluation of the Green's function and its derivatives based on the RCM is discussed in Section 3.6.1.

The Stroh eigenvalues are essential in the numerical implementation of the RCM. As described in Section 3.3, there are two ways to find the Stroh eigenvalues. One way is to find the zeros of the polynomial $D(p)$, the other way is to solve the Stroh eigenvalue problem Eq. (2.37). In practice, the Jenkins and Traub algorithm (Jenkins and Traub, 1970) known as the subroutine RPOLY (Jenkins, 1975) is used to find the zeros of the polynomial $D(p)$, and the subroutine ZGEEV in the LAPACK library (Anderson et al., 1999) is used to solve the Stroh eigenvalue problem. The author finds that the later gives more accurate results.

Table 3.3 is the numerical results of the RCM with the Stroh eigenvalues solved by the subroutine ZGEEV for transversely materials Mg and C. The underlined digits are exactly the same as the analytical results. Like the NIM, numerical results by the RCM for the material Mg are more accurate than those for the material C.

| | RCM (Mg) | RCM (C) | Unit |
|---|---|---|---|
| $G_{11}$ | $8.3782981337141092 \times 10^{-4}$ | $4.3824896404691421 \times 10^{-5}$ | |
| $G_{12}$ | $6.0007221556859634 \times 10^{-5}$ | $4.6241642169880919 \times 10^{-7}$ | |
| $G_{13}$ | $8.0163881274806153 \times 10^{-5}$ | $2.8817891209387289 \times 10^{-5}$ | $10^{-9}m$ |
| $G_{22}$ | $9.2784064570683217 \times 10^{-4}$ | $4.4491366507167915 \times 10^{-5}$ | |
| $G_{23}$ | $1.6032776254963158 \times 10^{-4}$ | $5.7578050333220220 \times 10^{-5}$ | |
| $G_{33}$ | $1.0578889644135944 \times 10^{-3}$ | $3.7070971754411272 \times 10^{-3}$ | |
| $G_{11,1}$ | $-5.9117971643756500 \times 10^{-6}$ | $5.5694078578199283 \times 10^{-7}$ | |
| $G_{12,1}$ | $4.7768458294935781 \times 10^{-5}$ | $2.6005858060506650 \times 10^{-7}$ | |
| $G_{13,1}$ | $6.1775349906918487 \times 10^{-5}$ | $1.9730968193245177 \times 10^{-5}$ | $1$ |
| $G_{22,1}$ | $-8.4277163613431945 \times 10^{-5}$ | $-2.0872808972732553 \times 10^{-7}$ | |
| $G_{23,1}$ | $-3.6777062735798426 \times 10^{-5}$ | $-1.8168694111521020 \times 10^{-5}$ | |
| $G_{33,1}$ | $-1.2597090883938349 \times 10^{-4}$ | $-6.6489947207387407 \times 10^{-4}$ | |
| $G_{11,11}$ | $-1.5317520228453641 \times 10^{-5}$ | $1.3037528193975853 \times 10^{-7}$ | |
| $G_{12,11}$ | $-3.2300147602260451 \times 10^{-5}$ | $-4.4853020715143876 \times 10^{-7}$ | |
| $G_{13,11}$ | $-4.7740579727232704 \times 10^{-5}$ | $-2.1308729164912853 \times 10^{-5}$ | $10^{9}m^{-1}$ |
| $G_{22,11}$ | $-6.2581147470664643 \times 10^{-5}$ | $6.8659218966670354 \times 10^{-9}$ | |
| $G_{23,11}$ | $-2.1927033545174070 \times 10^{-5}$ | $-6.2606845775305411 \times 10^{-6}$ | |
| $G_{33,11}$ | $-8.3977104326935273 \times 10^{-5}$ | $-3.0717839128942558 \times 10^{-4}$ | |

Table 3.3: Components of the Green's function and its derivatives by the residue calculus method for transversely isotropic materials Mg and C at the point $(1, 2, 3)$.

### 3.5.3 Verification of the Stroh formalism method

The SFM is an alternative of the RCM resulting in the explicit expressions of the Green's function and its derivatives. It constructs the Green's function with the help of the solutions of the Stroh eigenvalue problem Eq. (2.37), which means, in some sense, the governing equation Eq. (2.55) in elasticity case can be replaced by the Stroh eigenvalue problem Eq. (2.37). Therefore, the Green's function and its derivatives can be solved in the theory of the eigenvalue problems.

Like the RCM, the explicit expressions in the SFM are only applicable when the Stroh eigenvalues are distinct. The numerical evaluation when the Stroh eigenvalues repeat is discussed in Section 3.6.1 together with the RCM.

In the FORTRAN program, the Stroh eigenvalue problem is solved by the subroutine ZGEEV in the LAPACK library. Table 3.4 contains the corresponding numerical results of the Green's function and its derivatives for the materials Mg and C. The underlined digits are exactly the same as the analytical solutions. The numerical results for the material C are less accurate than those for the material Mg. However, compared with the results by the NIM and the RCM, the numerical results by the SFM for the material C are more accurate. So the SFM are better at evaluating the Green's function and its derivatives for strongly anisotropic materials like C than the NIM and the RCM.

| | SFM (Mg) | SFM (C) | Unit |
|---|---|---|---|
| $G_{11}$ | $\underline{8.378298133713}4370 \times 10^{-4}$ | $\underline{4.3827896251658}357 \times 10^{-5}$ | |
| $G_{12}$ | $\underline{6.0007221557027}949 \times 10^{-5}$ | $\underline{4.6263216287962}473 \times 10^{-7}$ | |
| $G_{13}$ | $\underline{8.0163881274}811818 \times 10^{-5}$ | $\underline{2.8820815639}255452 \times 10^{-5}$ | $10^{-9}m$ |
| $G_{22}$ | $\underline{9.2784064570692}107 \times 10^{-4}$ | $\underline{4.4521844547125}352 \times 10^{-5}$ | |
| $G_{23}$ | $\underline{1.6032776254961}957 \times 10^{-4}$ | $\underline{5.7641631278404}827 \times 10^{-5}$ | |
| $G_{33}$ | $\underline{1.0578889644135}981 \times 10^{-3}$ | $\underline{3.7072624469392}723 \times 10^{-3}$ | |
| $G_{11,1}$ | $-\underline{5.911797163805}4452 \times 10^{-6}$ | $\underline{5.5707858596426}121 \times 10^{-7}$ | |
| $G_{12,1}$ | $\underline{4.7768458294993}996 \times 10^{-5}$ | $\underline{2.6022661806317}575 \times 10^{-7}$ | |
| $G_{13,1}$ | $\underline{6.1775349906884}700 \times 10^{-5}$ | $\underline{1.9731677300777}066 \times 10^{-5}$ | 1 |
| $G_{22,1}$ | $-\underline{8.4277163614110}222 \times 10^{-5}$ | $-\underline{2.0915785653823}394 \times 10^{-7}$ | |
| $G_{23,1}$ | $-\underline{3.6777062735840}134 \times 10^{-5}$ | $-\underline{1.8178276707770}339 \times 10^{-5}$ | |
| $G_{33,1}$ | $-\underline{1.2597090883943}480 \times 10^{-4}$ | $-\underline{6.6490424049476}117 \times 10^{-4}$ | |
| $G_{11,11}$ | $-\underline{1.5317520185524}825 \times 10^{-5}$ | $\underline{1.3033886315670}495 \times 10^{-7}$ | |
| $G_{12,11}$ | $-\underline{3.230014761914}5314 \times 10^{-5}$ | $-\underline{4.4956207299378}750 \times 10^{-7}$ | |
| $G_{13,11}$ | $-\underline{4.7740579505173}436 \times 10^{-5}$ | $-\underline{2.1314880907310}438 \times 10^{-5}$ | $10^{9}m^{-1}$ |
| $G_{22,11}$ | $-\underline{6.2581146860816}642 \times 10^{-5}$ | $\underline{6.7320118850785}253 \times 10^{-9}$ | |
| $G_{23,11}$ | $-\underline{2.1927033538643}924 \times 10^{-5}$ | $-\underline{6.2732112011148}431 \times 10^{-6}$ | |
| $G_{33,11}$ | $-\underline{8.3977103691742}081 \times 10^{-5}$ | $-\underline{3.0719075049768}016 \times 10^{-4}$ | |

Table 3.4: Components of the Green's function and its derivatives by the Stroh formalism method for transversely isotropic materials Mg and C at the point $(1, 2, 3)$.

### 3.5.4 Verification of the unified explicit expressions

The UEEM is based on the RCM. The explicit expressions by the UEEM are in terms of the Stroh eigenvalues. Although the expressions by the UEEM are more complicated than those by the RCM, they are applicable not only when the Stroh eigenvalues are distinct but also when they repeat.

For the Green's function, the explicit expressions in the UEEM is a straightforward reformulation of those in the RCM. Ting and Lee (1997) presented the unified explicit expression of the Green's function for the first time. It is easy to find out that our new explicit expression of the Green's function is equivalent to that proposed by Ting and Lee (1997). Very recently, Buroni and Sáez (2013) presented unified or unique explicit expressions for the derivatives of Green's function by taking the derivatives of the expression of Green's function by Ting and Lee (1997).

In the FORTRAN program, the Stroh eigenvalues are obtained by solving the Stroh eigenvalue problem Eq. (4.1). Table 3.5 contains the numerical results of the Green's

function and its derivatives by the UEEM for materials Mg and C. The underlined digits agree well with the analytical solutions. In the Table 3.5, the number of underlined digits for the material C is almost equal to that for the material Mg, where the number of underlined digits for material C is significantly less than that for material Mg. This implies that compared with the NIM, the RCM and the SFM, the UEEM has the most advantage of accuracy in computing the Green's function and its derivatives for strongly anisotropic materials.

| | UEEM (Mg) | UEEM (C) | Unit |
|---|---|---|---|
| $G_{11}$ | $\underline{8.3782981337130}402 \times 10^{-4}$ | $\underline{4.3827896221260}154 \times 10^{-5}$ | |
| $G_{12}$ | $\underline{6.000722155710}4867 \times 10^{-5}$ | $\underline{4.6263223755486}468 \times 10^{-7}$ | |
| $G_{13}$ | $\underline{8.0163881274800}475 \times 10^{-5}$ | $\underline{2.8820815639128}454 \times 10^{-5}$ | $10^{-9}m$ |
| $G_{22}$ | $\underline{9.2784064570696}130 \times 10^{-4}$ | $\underline{4.4521844577592}456 \times 10^{-5}$ | |
| $G_{23}$ | $\underline{1.6032776254960}092 \times 10^{-4}$ | $\underline{5.7641631278256}841 \times 10^{-5}$ | |
| $G_{33}$ | $\underline{1.0578889644135}964 \times 10^{-3}$ | $\underline{3.7072624469392}710 \times 10^{-3}$ | |
| $G_{11,1}$ | $-\underline{5.9117971638177}865 \times 10^{-6}$ | $\underline{5.5707948825936}864 \times 10^{-7}$ | |
| $G_{12,1}$ | $\underline{4.7768458294984}333 \times 10^{-5}$ | $\underline{2.6022823188120}584 \times 10^{-7}$ | |
| $G_{13,1}$ | $\underline{6.1775349906880}689 \times 10^{-5}$ | $\underline{1.9731677292333}828 \times 10^{-5}$ | $1$ |
| $G_{22,1}$ | $-\underline{8.4277163614102}633 \times 10^{-5}$ | $-\underline{2.0915875780597}619 \times 10^{-7}$ | |
| $G_{23,1}$ | $-\underline{3.6777062735839}781 \times 10^{-5}$ | $-\underline{1.8178276693589}039 \times 10^{-5}$ | |
| $G_{33,1}$ | $-\underline{1.2597090883943}341 \times 10^{-4}$ | $-\underline{6.6490424049481}234 \times 10^{-4}$ | |
| $G_{11,11}$ | $-\underline{1.5317520185560}367 \times 10^{-5}$ | $\underline{1.3037961156922}419 \times 10^{-7}$ | |
| $G_{12,11}$ | $-\underline{3.2300147619146}337 \times 10^{-5}$ | $-\underline{4.4871709610018}432 \times 10^{-7}$ | |
| $G_{13,11}$ | $-\underline{4.7740579505166}646 \times 10^{-5}$ | $-\underline{2.1314882684264}957 \times 10^{-5}$ | $10^{9}m^{-1}$ |
| $G_{22,11}$ | $-\underline{6.2581146860783}736 \times 10^{-5}$ | $\underline{6.6917582325344}854 \times 10^{-9}$ | |
| $G_{23,11}$ | $-\underline{2.1927033538653}885 \times 10^{-5}$ | $-\underline{6.2732119813698}278 \times 10^{-6}$ | |
| $G_{33,11}$ | $-\underline{8.3977103691742}231 \times 10^{-5}$ | $-\underline{3.0719075049293}141 \times 10^{-4}$ | |

Table 3.5: Components of the Green's function and its derivatives by the unified explicit expression method for transversely isotropic materials Mg and C at the point $(1, 2, 3)$.

### 3.5.5 Comparison of the efficiency

Before the general evaluations of the Green's function and its derivatives by the four methods, a comparison of the four methods on the efficiency is presented first.

The FORTRAN programs of the four different methods are implemented under the same computing environment. Fig. 3.5 is a comparison of the computing time required by the four methods. The material is Mg, and the evaluation point is $(1, 2, 3)$m. The number of the Gaussian points in the NIM is set to be 25 for a comparable accuracy with the other methods. The bottom box of each method represents the computing time for the Green's function including the time for the Gaussian points and the weights in the NIM, the Stroh eigenvalues in the RCM and the UEEM, and the eigenvalues and eigenvectors of $\mathbf{N}$ in the SFM. The middle box represents the additional computing time for the first derivative of the Green's function excluding the time for the Green's function. The total computing time for the second derivative of the Green's function is represented by the three boxes, i.e., the stacked column. From Fig. 3.5, the explicit methods, namely the RCM, the SFM and the UEEM, have a higher efficiency for computing the Green's function and its first derivative compared to the NIM, but may lose the advantage for computing the second derivative of the Green's function, especially, in the RCM and the SFM. Both the RCM
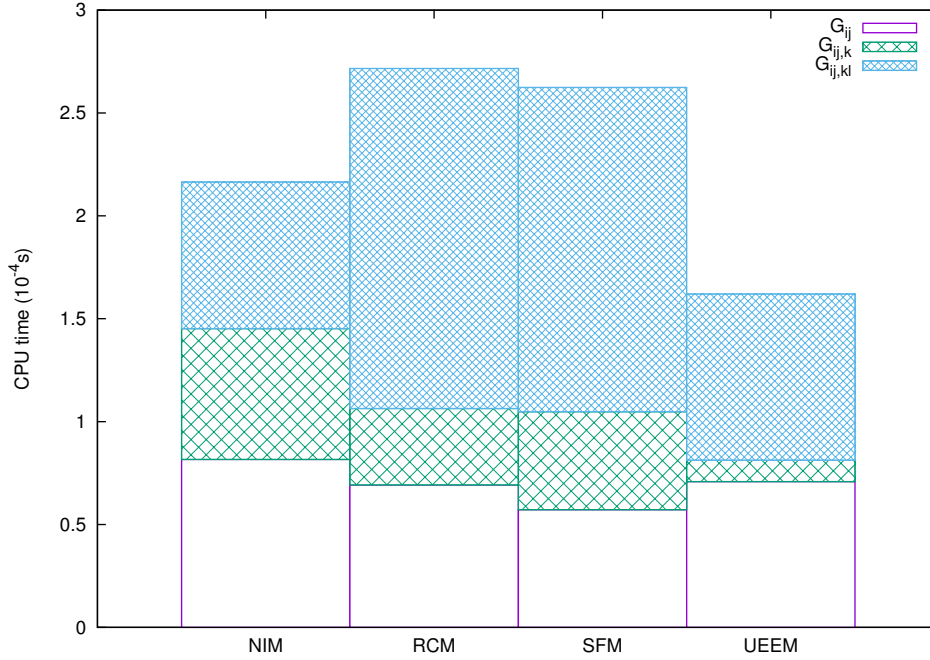
Figure 3.5: The CPU time for calculating the Green's function and its derivatives by the four methods.

and the UEEM need more computing time than the SFM for the Green's function. It is maybe due to the algorithm we have chosen for the Stroh eigenvalues in the RCM and the UEEM. Besides, the UEEM has great advantage in computing the first derivative of the Green's function and is the most efficient one among the four different methods for computing the first and the second derivatives of the Green's function.

## 3.6 Numerical examples

In the last section, the NIM, the RCM, the SFM and the UEEM are numerically evaluated at a specific point for transversely isotropic materials Mg and C. The numerical results agree well with the analytical solutions (Pan and Chou, 1976), which verifies the correctness of the formulae in the four different methods. In this section, the stabilities of different methods in nearly degenerate case are investigated. And then the UEEM is used to evaluation the Green's function and its derivatives on a unit sphere centered at the origin.

### 3.6.1 Numerical results near the degenerated point

The expressions in the NIM are in terms of line integrals, while the expressions in the RCM, the SFM and the UEEM are in terms of the Stroh eigenvalues, which are the zeros of $D(p)$ or the eigenvalues of the fundamental elasticity matrix $\mathbf{N}$.

According to the derivations of the explicit expressions of the Green's function and its derivatives, the expressions in the RCM, the SFM and UEEM are only applicable when the Stroh eigenvalues are distinct. However, like the expression proposed by Ting and

Lee (1997), the explicit expressions in the UEEM are assumed to be applicable when the Stroh eigenvalues repeat which will be proved by the numerical examples.

Since the expressions are dependent on the Stroh eigenvalues, here we give a study on the Stroh eigenvalues for transversely isotropic materials whose symmetry axis is along with the $x_3$-axis. When $\boldsymbol{\xi}$ is defined in Eq. $(3.16)_1$, the zeros of $D(p)$ are equal to those of $D(\boldsymbol{\xi})$. The expression of $D(\boldsymbol{\xi})$ is (Mura, 1987)

$$D(\boldsymbol{\xi}) = \left(\alpha'\eta^2 + \gamma\xi_3^2\right)\left\{\alpha\gamma\eta^4 + \left(\alpha\beta + \gamma^2 - \gamma'^2\right)\eta^2\xi_3^2 + \beta\gamma\xi_3^4\right\}, \qquad (3.85)$$

where

$$\begin{aligned}
\alpha &= C_{11} = C_{22}, & \alpha' &= C_{66} = (C_{11} - C_{12})/2, \\
\beta &= C_{33}, & \gamma' - \gamma &= C_{13} = C_{23}, \\
\gamma &= C_{44} = C_{55}, & \eta^2 &= \xi_1^2 + \xi_2^2.
\end{aligned} \qquad (3.86)$$

Generally, the zeros of Eq. (3.85) are three distinct pairs of complex conjugates, i.e., three distinct Stroh eigenvalues. But the Stroh eigenvalues repeat when $\boldsymbol{x} = (0, 0, a)$, $a \neq 0$. When $\boldsymbol{x} = (0, 0, a)$, $a \neq 0$, the corresponding $\boldsymbol{n}$ and $\boldsymbol{m}$ can be arbitrarily chosen as

$$\boldsymbol{n} = (\cos\theta, \sin\theta, 0), \quad \boldsymbol{m} = (-\sin\theta, \cos\theta, 0), \qquad (3.87)$$

where $\theta$ is a parameter in the plane $x_3 = 0$. Substitution of Eq. (3.87) into Eq. $(3.16)_1$ yields

$$\xi_3 = 0, \quad \eta^2 = \cos^2\psi(1 + p^2). \qquad (3.88)$$

Furthermore, substitution of Eq. (3.88) into Eq. (3.85) leads to the unique zeros $p = \pm i$, which means the three Stroh eigenvalues are identical or fully degenerated when $\boldsymbol{x} = (0, 0, a)$.

To investigate the abilities of the expressions in the NIM, the RCM, the SFM and the UEEM in dealing with the degenerate and nearly degenerate cases, a numerical evaluation of the four methods near the fully degenerated point $(0, 0, 1)$ is performed. For the numerical examples, the material is taken as the transversely isotropic material Mg, and the evaluation points are $\boldsymbol{x} = (0, \sin\theta, \cos\theta)$ near $\theta = 0$.

Fig. 3.6 is the numerical results of a component of the Green's function evaluated by the expressions in the NIM, the RCM, the SFM and the UEEM for the material Mg near the point $\boldsymbol{x} = (0, 0, 1)$. The results evaluated by the NIM, the SFM and the UEEM are almost the same even at the degenerated point (when $\theta = 0$). But the results evaluated by the RCM become unstable near the degenerated point. Therefore, the applicability of the expressions in the SFM and the UEEM for the Green's function in degenerate and nearly degenerate cases is confirmed but not the expression in the RCM. The numerical errors of the explicit expression in the RCM may be due to the items like $(p_i - p_j)$ in denominators, which is close to zero in the nearly degenerate cases.

Fig. 3.7 is the numerical results of $G_{33,2}$ evaluated by the expressions in the four methods for the transversely isotropic matherial Mg near the degenerate point. The results evaluated by the NIM and the UEEM still agree perfectly with each other, even at the degenerate point. In the RCM, significant errors arise when $\theta < 1.5°$, moreover the numerical errors are too large to plot the results in the figure near the area very close to the degenerate point. In the SFM, numerical errors arise when $\theta < 0.1°$. The numerical
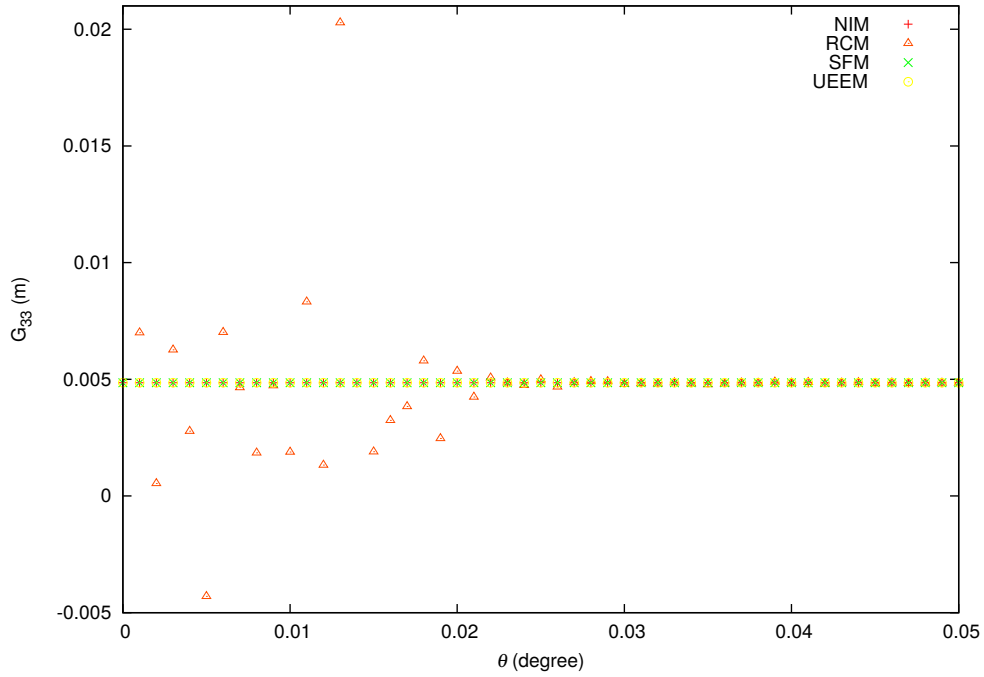
Figure 3.6: Numerical evaluations of the Green's function around the denegerated point for the transversely isotropic material Mg
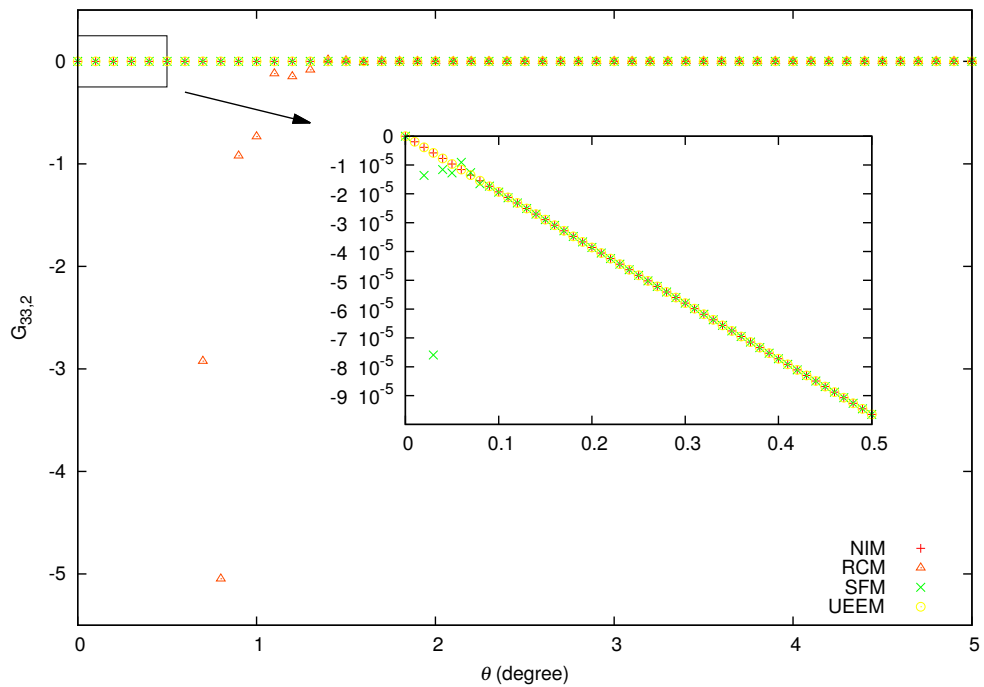


Figure 3.7: Numerical evaluations of the first derivatvie of the Green's function around the denegerated point for the transversely isotropic material Mg

40
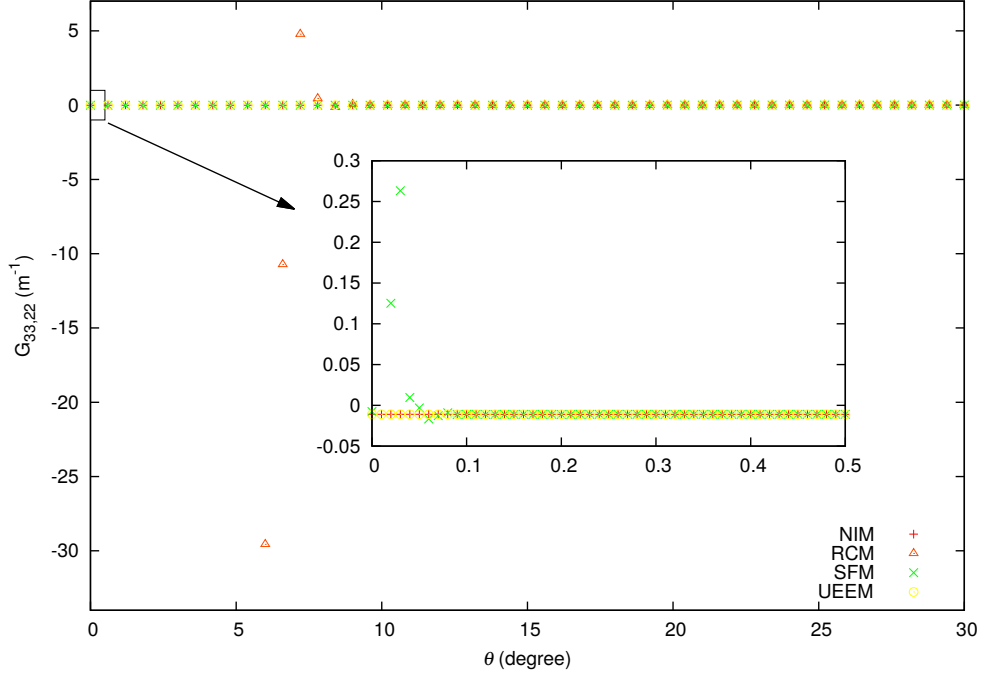
Figure 3.8: Numerical evaluations of the second derivatvie of the Green's function around the denegerated point for the transversely isotropic material Mg

errors in the SFM may also come from the items like $(p_i - p_j)$ in the denominators. But the error area in the SFM is about 6.67% of that in the RCM.

Fig. 3.8 is the numerical results of $G_{33,22}$ evaluated by the expressions in the four methods for the transversely isotropic material Mg near the degenerate point. The results evaluated by the NIM and the UEEM agree perfectly with each other. But the numerical errors arise near the degenerate point in both the RCM and the SFM. The error area in the evaluation of $G_{33,22}$ by the RCM is about $\theta < 8°$ which is about 5.3 times of the error area in the evaluation of $G_{33,2}$ by the RCM. The error area of the second derivative $G_{33,22}$ in the SFM is similar with that of the first derivative $G_{33,2}$ in the SFM, and is about 1.25% of that in the RCM.

Through the above numerical evaluations, it may be concluded on the three explicit methods that

1. The expressions of the Green's function and its derivatives in the UEEM and the expression of the Green's function in the SFM may be applicable no matter the Stroh eigenvalues are distinct or not.

2. The expressions of the Green's function and its derivatives in the RCM and the expression of the derivatives of the Green's function in the SFM are only applicable when the Stroh eigenvalues are distinct (the non-degenerate case). They fail when the Stroh eigenvalues repeat (the degenerate case) and cause significant numerical errors at the area very close to the degenerated point (the nearly degenerate case).

3. The SFM is more stable than the RCM near the fully degenerate cases.

Besides, although the RCM and the SFM are not applicable in the degenerate and nearly-degenerate cases, they are still of practical interest as long as the Stroh eigenvalues

keep distinct by using some numerical techniques, For example, a small perturbation such as $10^{-6}$ on some material constants.

### 3.6.2  Numerical results for an arbitrary point on a unit sphere

As the previous sections reveal, compared to the other three methods, the UEEM has the most advantage in the numerical evaluation of the Green's function and its derivatives for 3D anisotropic materials. In this section, the Green's function and its derivatives on a unit sphere are evaluated by the UEEM. The evaluation points on the upper half sphere are denoted by $(\cos\theta\cos\phi, \cos\theta\sin\phi, \sin\theta)$ with $\phi \in (0, 2\pi)$ and $\theta \in (0, \pi)$. The geometry of the sphere is illustrated by Fig. 3.9. The material is the transversely isotropic material
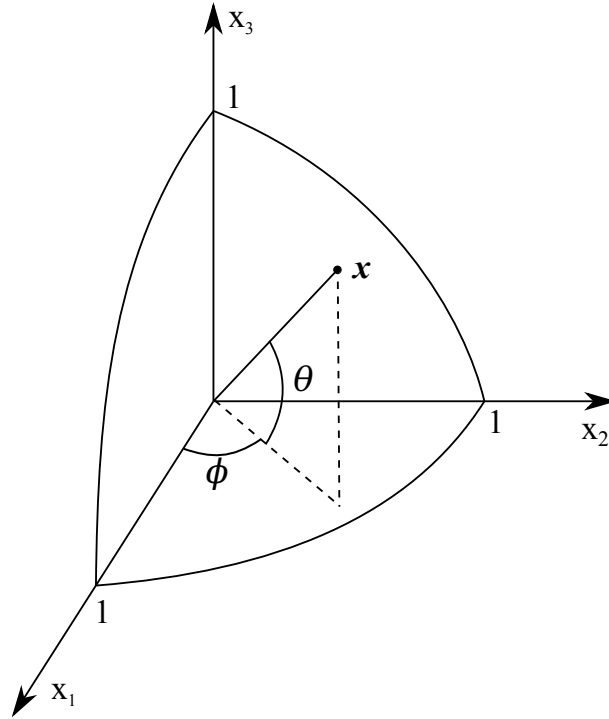


Figure 3.9: Spherical coordinates of the field point $\boldsymbol{x}$

Mg. Figs. 3.10-3.12 are respectively the numerical results of the Green's function, its first derivative and its second derivative on the upper half sphere, and the contours of the Green's function and its derivatives are presented on the base planes of the coordinate systems. It is observed that the periods of the Green's function and its derivatives are $\pi$ in $\theta$, and $2\pi$ in $\phi$, while for some components may be $\pi$ in $\phi$.

Similar figures can be plotted by the NIM. In order to give the similar figures by the RCM and the SFM, a small perturbation of the material constants is required to keep the Stroh's eigenvalues distinct so that the explicit expressions can be used for practical interest.

## 3.7  Concluding remarks

Four different methods for computing the Green's function and its first and second derivatives are presented in this chapter. The Green's function and its derivatives are expressed
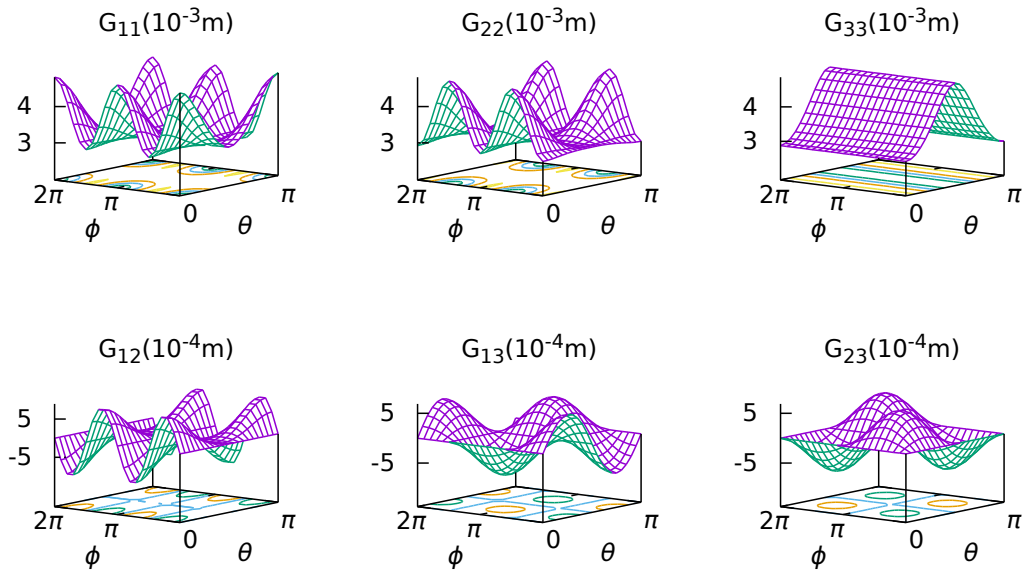
Figure 3.10: General evaluation of the anisotropic elastic Green's function by the UEEM.
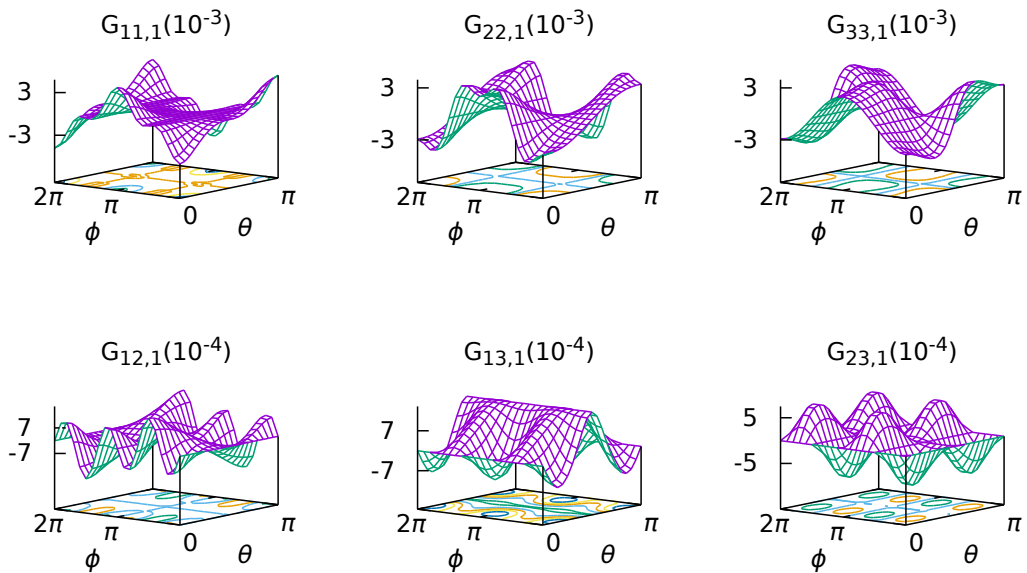


Figure 3.11: General evaluation of the first derivative of the anisotropic elastic Green's function by the UEEM.
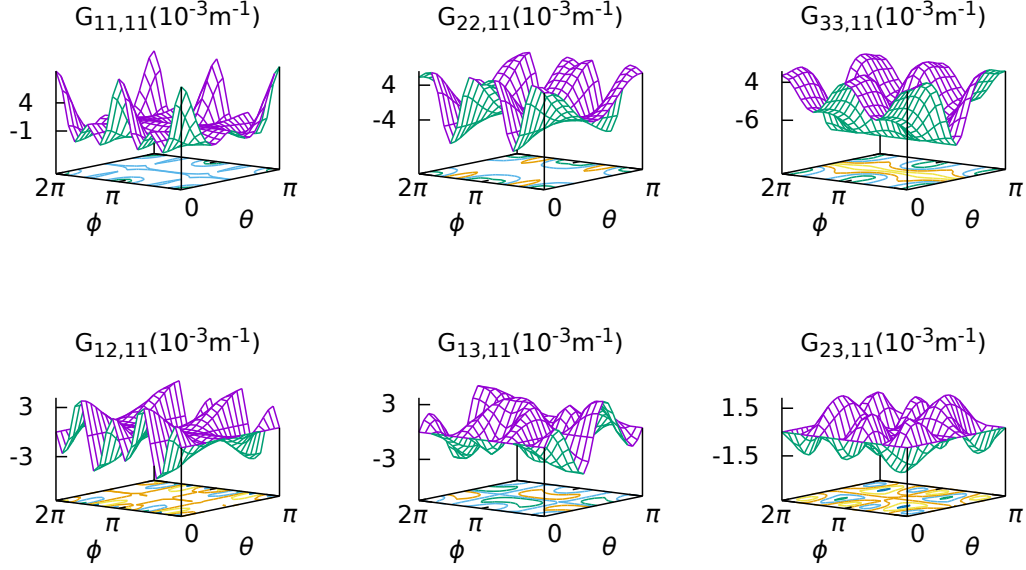
Figure 3.12: General evaluation of the second derivative of the anisotropic elastic Green's function by the UEEM.

in terms of three line integrals. The line integral expressions are a little different from the conventional line integral expressions of the 3D anisotropic Green's function and its derivatives, especially for the second derivative of the Green's function where the symmetry of some tensors is used to simplify it. The first method (NIM) is straightforwardly based on the numerical integration of the line integrals. The second method (RCM) is based on the explicit expressions derived by applying the residue calculus with the distinctness assumption of the Stroh eigenvalues to the line integrals. The integrals in the first and second methods are the same. In the third method (SFM), the Green's function and its derivatives are constructed from the solutions of a six-dimensional formulation of an eigenvalue problem. In the fourth method (UEEM), the line integrals are firstly expressed in terms of two elementary line integrals, and then evaluated by the simple pole residue calculus followed by a rewritten of the resulting explicit expressions. Although the explicit expressions in the UEEM are derived with the distinctness assumption of the Stroh eigenvalues, after the rewritten they are applicable when the Stroh eigenvalues repeat. The correctness of the expressions in the four methods is confirmed by comparing the numerical results of the Green's function and its derivatives for transversely isotropic materials at an arbitrary point with the analytical results. The numerical results of the RCM and the SFM near a degenerate point may become unstable, while the NIM and UEEM remain applicable near and at the degenerate point. According to the CPU times used by the four different methods to calculate the Green's function and its derivatives, the UEEM seems to be the most efficient one.

# Chapter 4

# Green's function in linear piezoelectricity

## 4.1 Problem statement

In linear elasticity, the 3D anisotropic Green's function has been well studied. It was first investigated by Fredholm (1900). There are now many methods to evaluate the Green's function, among which we only mention the numerical integration method, the residue calculus method and the Stroh formalism method (Fredholm, 1900; Malén, 1971). To calculate the derivatives of the 3D anisotropic elastic Green's function, Malén (1971) used the Stroh formalism method, Barnett (1972) used the numerical integration method, and Sales and Gray (1998) used the residue calculus method. The last two methods were based on the line integral expressions. Both the Stroh formalism and the residue calculus methods can lead to explicit expressions of the 3D anisotropic elastic Green's function and its derivatives. The residue calculus method has been further investigated by Ting and Lee (1997), Phan et al. (2004, 2005), Lee (2003, 2009), Buroni and Sáez (2013) and Xie et al. (2013) among others.

However, in contrast to the 3D anisotropic elastic Green's function and its derivatives, relatively few studies can be found in the literature on the 3D anisotropic piezoelectric Green's function and its derivatives. For transversely isotropic piezoelectric materials, Dunn and Wienecke (1996) and Ding et al. (1996) derived the analytical expression of the Green's function, while Soh et al. (2003) presented 3D Green's function for transversely isotropic magnetoelectroelastic solids. In contrast, the 3D Green's function and its derivatives for generally anisotropic piezoelectric materials are very complicated and have no analytical expressions known in literature. Deeg (1980) derived the Green's function in terms of line integrals by using Radon transform. Chen (1993) and Chen and Lin (1993) derived the Green's function and its derivatives as line integrals by Fourier transform and then computed them by numerical integration. Dunn (1994) and Pan and Tonon (2000) obtained the Green's function by applying the residue calculus method to the infinite line integrals. And the later also evaluated the first derivative of the Green's function by a finite difference scheme. By using the Stroh formalism method, Akamatsu and Tanuma (1997) gave an explicit expression for the 3D anisotropic piezoelectric Green's function but not its derivatives. The advantage of the Stroh formalism and the residue calculus methods is that they give rise to explicit expressions instead of integral expressions. Though the residue calculus method was used to derive the Green's function and its first

and second derivatives for magneto-electro-elastic solids by Buroni and Sáez (2010), no numerical results of the second derivative were presented. An excellent monograph on static Green's functions in anisotropic media was recently published by Pan and Chen (2015), and interested readers may find a detailed review, comprehensive references and many new results in this monograph.

In this Chapter, explicit expressions for the Green's function and its first and second derivatives in 3D anisotropic piezoelectricity are derived by both the Stroh formalism method and the residue calculus method. In the Stroh formalism method, the approach to calculate the derivatives of the eigenvectors proposed by Nelson (1976) is used to derive the explicit expressions for the derivatives of the Green's function. In the residue calculus method, line integral expressions of the Green's function and its derivatives are obtained by generalizing the elastic results of Mura (1987), which are subsequently evaluated by using the Cauchy's residue theorem. Different from the expressions given by Lee (2003), the present integral expressions are easy to evaluate, especially for the second derivative of the Green's function, since they do not involve tensors higher than 4th-order. The explicit expressions obtained by both methods are coded into FORTRAN programs. The accuracy and the efficiency of both methods are compared with each other by numerical examples.

The contributions in the chapter have be published in

- **L. Xie**, C. Zhang, C. Hwu, J. Sladek, V. Sladek, On two accurate methods for computing 3D Green's function and its first and second derivatives in piezoelectricity, *Engineering Analysis with Boundary Elements*, 61:183-193, 2015.

## 4.2   Stroh formalism method

The generalized displacement Green's function $G_{IJ}(\boldsymbol{x})$ is governed by the equation (2.55) in piezoelectricity case.

The Green's function $G_{IJ}(\boldsymbol{x})$ ($I, J = 1, 2, \ldots, 4$) denotes the mechanical displacement at $\boldsymbol{x}$ in the $x_I$-direction ($I \leq 3$) or the electric potential ($I = 4$) when a unit point force at the origin in the $x_J$-direction ($J \leq 3$), or a unit point charge at origin ($J = 4$) is applied. Besides, the Green's function and its derivatives vanish when $|\boldsymbol{x}| \to \infty$.

Malén (1971) showed that the Green's function in 3D linear elasticity can be expressed in terms of the solution of an eigensystem, which is known as the Stroh eigen-relation. So the Green's function in piezoelectric solids could be expressed in terms of the solution of the Stroh eigen-relation in piezoelectricity.

### 4.2.1   Representation of the Green's function

The Stroh eigen-relation or the Stroh eigenvalue problem at a point $\boldsymbol{x}$ in a piezoelectric solid with the material constants $c_{kIJl}$ is given by a 8-dimensional eigensystem as (Hwu, 2010)

$$\mathbf{N}\boldsymbol{\xi} = p\boldsymbol{\xi}, \tag{4.1a}$$

in which

$$\mathbf{N} = \begin{pmatrix} \mathbf{N}_1 & \mathbf{N}_2 \\ \mathbf{N}_3 & \mathbf{N}_1^T \end{pmatrix}, \quad \boldsymbol{\xi} = \begin{Bmatrix} \boldsymbol{a} \\ \boldsymbol{b} \end{Bmatrix}, \tag{4.1b}$$

$$\mathbf{N}_1 = -\mathbf{T}^{-1}\mathbf{R}^T, \quad \mathbf{N}_2 = \mathbf{T}^{-1} = \mathbf{N}_2^T, \quad \mathbf{N}_3 = \mathbf{R}\mathbf{T}^{-1}\mathbf{R}^T - \mathbf{Q},$$

and

$$Q_{IJ} = c_{kIJl}n_k n_l, \quad R_{IJ} = c_{kIJl}n_k m_l, \quad T_{IJ} = c_{kIJl}m_k m_l, \tag{4.1c}$$

where $\boldsymbol{n}$ and $\boldsymbol{m}$ are two mutually orthogonal unit vectors on the oblique plane perpendicular to $\boldsymbol{x}$. Since $\mathbf{N}$ is not symmetric, $\boldsymbol{\xi}$ in Eq. (4.1a) is a right eigenvector. The left eigenvector denoted by $\boldsymbol{\eta}$ satisfies

$$\boldsymbol{\eta}^T\mathbf{N} = p\boldsymbol{\eta}^T, \tag{4.2}$$

where Ting (1996) had proved that

$$\boldsymbol{\eta} = \begin{Bmatrix} \boldsymbol{b} \\ \boldsymbol{a} \end{Bmatrix}. \tag{4.3}$$

It can be shown that the eigenvalues of Eq. (4.1a) are four pairs of complex conjugates (Akamatsu and Tanuma, 1997). It is assumed that $\mathrm{Im}(p_k) > 0$, $p_{k+4} = \bar{p}_k$, $k = 1, 2, 3, 4$ and $p_k$ are distinct which causes that all the eigenvectors are independent of each other.

By defining

$$\mathbf{A} = [\boldsymbol{a}_1, \boldsymbol{a}_2, \boldsymbol{a}_3, \boldsymbol{a}_4], \quad \mathbf{B} = [\boldsymbol{b}_1, \boldsymbol{b}_2, \boldsymbol{b}_3, \boldsymbol{b}_4], \tag{4.4}$$

and with the relation between the eigenvectors

$$\boldsymbol{\eta}_\alpha^T\boldsymbol{\xi}_\beta = \delta_{\alpha\beta}, \quad \alpha, \beta = 1, 2, \ldots, 8, \tag{4.5}$$

where $\delta_{\alpha\beta}$ is the Kronecker delta, the Green's function can be expressed as

$$\mathbf{G}(\boldsymbol{x}) = \frac{1}{4\pi r}\mathbf{H}(\bar{\boldsymbol{x}}), \quad \mathbf{H} = 2i\mathbf{A}\mathbf{A}^T, \tag{4.6}$$

in which $r = |\boldsymbol{x}|$, $\bar{\boldsymbol{x}}$ is the unit vector of $\boldsymbol{x}$, and $\mathbf{H}$ is one of the three Barnett-Lothe matrices in linear piezoelectricity. The explicit expression of $\mathbf{A}$ can be found in Hwu (2010), and is listed in Appendix D for the completeness.

## 4.2.2 First derivative of the Green's function

The first derivative of the Green's function becomes straightforward by differentiating Eq. (4.6) with respect to $x_i$, i.e.,

$$\mathbf{G}_{,i}(\boldsymbol{x}) = \frac{1}{4\pi r^2}\left(-\frac{x_i}{r}\mathbf{H} + r\mathbf{H}_{,i}\right), \tag{4.7a}$$

where

$$\mathbf{H}_{,i} = 2i\left(\mathbf{A}_{,i}\mathbf{A}^T + \left[\mathbf{A}_{,i}\mathbf{A}^T\right]^T\right). \tag{4.7b}$$

According to the above equations, the first derivatives of $\mathbf{A}$ is required to calculate the derivative of $\mathbf{G}(\boldsymbol{x})$. All components of $\mathbf{A}$ and its derivatives in 3D linear elasticity can be expressed explicitly in terms of the Stroh eigenvalues (Hwu, 2010), So the derivatives of $\mathbf{A}$ can be obtained by taking the derivatives of all the components. However the

expressions would be too complex. In the following we present an alternative way to get the derivatives of $\mathbf{A}$ for 3D linear piezoelectric materials.

Taking the derivative of Eq. (4.1a), which is associated with the eigenvalue $p_\alpha$ and the corresponding right eigenvector $\boldsymbol{\xi}_\alpha$, with respect to $x_i$ leads to

$$(\mathbf{N} - p_\alpha \mathbf{I})\boldsymbol{\xi}_{\alpha,i} = -(\mathbf{N}_{,i} - p_{\alpha,i}\mathbf{I})\boldsymbol{\xi}_\alpha. \tag{4.8}$$

*Note that the repeated Greek indices in the above equation do not imply summation, neither do in the following.* Since the derivative of an eigenvector is an 8-dimensional vector, it is a linear combination of the 8 independent eigenvectors, i.e.,

$$\boldsymbol{\xi}_{\alpha,i} = \sum_{\beta=1}^{8} c_{\alpha\beta}^{(i)} \boldsymbol{\xi}_\beta, \tag{4.9a}$$

and

$$\boldsymbol{\eta}_{\alpha,i} = \sum_{\beta=1}^{8} c_{\alpha\beta}^{(i)} \boldsymbol{\eta}_\beta. \tag{4.9b}$$

In Eq. (4.9), the coefficients $c_{\alpha\beta}^{(i)}$ are constants. In virtue of Eqs. (4.1a), (4.2) and (4.5), the substitution of Eq. (4.9a) into Eq. (4.8) followed by the premultiplication by $\boldsymbol{\eta}_\beta^T$ gives

$$c_{\alpha\beta}^{(i)}(p_\beta - p_\alpha) = -\boldsymbol{\eta}_\beta^T(\mathbf{N}_{,i} - p_{\alpha,i}\mathbf{I})\boldsymbol{\xi}_\alpha. \tag{4.10}$$

When $\beta = \alpha$, the derivative of the eigenvalue $p_\alpha$ is given from Eq. (4.10) as

$$p_{\alpha,i} = \boldsymbol{\eta}_\alpha^T \mathbf{N}_{,i} \boldsymbol{\xi}_\alpha. \tag{4.11}$$

If $\beta \neq \alpha$ the coefficients $c_{\alpha\beta}^{(i)}$ in the expressions of the derivatives of the eigenvectors $\boldsymbol{\xi}_{\alpha,i}$ are given by

$$c_{\alpha\beta}^{(i)} = \frac{\boldsymbol{\eta}_\beta^T \mathbf{N}_{,i} \boldsymbol{\xi}_\alpha}{p_\alpha - p_\beta}. \tag{4.12}$$

Substitution of Eqs. (4.5) and (4.9) into the first derivative of Eq. (4.5) leads to

$$c_{\alpha\beta}^{(i)} + c_{\beta\alpha}^{(i)} = 0. \tag{4.13}$$

When $\beta = \alpha$, we have

$$c_{\alpha\alpha}^{(i)} = 0. \tag{4.14}$$

So far, all the coefficients $c_{\alpha\beta}^{(i)}$ are determined. The first derivative of the eigenvector can be expressed in terms of all eigenvectors by Eq. (4.9). And one further easily arrives at $\mathbf{A}_{,i}$ by differentiating Eq. (4.4). The explicit expressions of the $\mathbf{N}_{,i}$ are presented in Appendix B. It should be mentioned that different explicit expressions of the derivatives of the anisotropic elastic Green's function were investigated by Lavagnino (1995).

### 4.2.3 Second derivative of the Green's function

The second derivative of the Green's function is obtained by taking derivative of Eq. (4.7) with respect to $x_j$, i.e.,

$$\mathbf{G}_{,ij}(\boldsymbol{x}) = \frac{1}{4\pi r^3}\left[\left(\frac{3x_i x_j}{r^2} - \delta_{ij}\right)\mathbf{H} - (x_i\mathbf{H}_{,j} + x_j\mathbf{H}_{,i}) + r^2\mathbf{H}_{,ij}\right], \tag{4.15a}$$

where

$$\mathbf{H}_{,ij} = 2i\left(\mathbf{A}_{,ij}\mathbf{A}^T + \mathbf{A}_{,i}\mathbf{A}_{,j}^T + \left[\mathbf{A}_{,ij}\mathbf{A}^T + \mathbf{A}_{,i}\mathbf{A}_{,j}^T\right]^T\right). \tag{4.15b}$$

In order to get the second derivative of $\mathbf{A}$, the second derivative of the right eigenvectors $\boldsymbol{\xi}_{\alpha,ij}$ is required. In the same way, $\boldsymbol{\xi}_{\alpha,ij}$ is a linear combination of the 8 independent right eigenvectors as

$$\boldsymbol{\xi}_{\alpha,ij} = \sum_{\beta=1}^{8} d_{\alpha\beta}^{(ij)}\boldsymbol{\xi}_\beta. \tag{4.16}$$

Taking the derivative of Eq. (4.8) with respect to $x_j$ followed by the premultiplication by $\boldsymbol{\eta}_\beta^T$ with the substitution of Eq. (4.16) yields

$$d_{\alpha\beta}^{(ij)}(p_\beta - p_\alpha) = -\boldsymbol{\eta}_\beta^T(\mathbf{N}_{,ij} - p_{\alpha,ij}\mathbf{I})\boldsymbol{\xi}_\alpha - \boldsymbol{\eta}_\beta^T(\mathbf{N}_{,i} - p_{\alpha,i}\mathbf{I})\boldsymbol{\xi}_{\alpha,j} - \boldsymbol{\eta}_\beta^T(\mathbf{N}_{,j} - p_{\alpha,j}\mathbf{I})\boldsymbol{\xi}_{\alpha,i}. \tag{4.17}$$

Using the same approach for the first derivative of the eigenvectors, the second derivative of the eigenvalues $p_{\alpha,ij}$ and the coefficients $d_{\alpha\beta}^{(ij)}$ are

$$p_{\alpha,ij} = \boldsymbol{\eta}_\alpha^T\mathbf{N}_{,ij}\boldsymbol{\xi}_\alpha + \boldsymbol{\eta}_\alpha^T\mathbf{N}_{,i}\boldsymbol{\xi}_{\alpha,j} + \boldsymbol{\eta}_\alpha^T\mathbf{N}_{,j}\boldsymbol{\xi}_{\alpha,i}, \tag{4.18}$$

$$d_{\alpha\alpha}^{(ij)} = -(\boldsymbol{\eta}_{\alpha,i}^T\boldsymbol{\xi}_{\alpha,j} + \boldsymbol{\eta}_{\alpha,j}^T\boldsymbol{\xi}_{\alpha,i})/2, \tag{4.19}$$

$$d_{\alpha\beta}^{(ij)} = \frac{\boldsymbol{\eta}_\beta^T\mathbf{N}_{,ij}\boldsymbol{\xi}_\alpha + \boldsymbol{\eta}_\beta^T(\mathbf{N}_{,i} - p_{\alpha,i}\mathbf{I})\boldsymbol{\xi}_{\alpha,j} + \boldsymbol{\eta}_\beta^T(\mathbf{N}_{,j} - p_{\alpha,j}\mathbf{I})\boldsymbol{\xi}_{\alpha,i}}{p_\alpha - p_\beta}, \quad \beta \neq \alpha. \tag{4.20}$$

In Eqs. (4.18)-(4.20), $\mathbf{N}_{,i}$ and $\mathbf{N}_{,ij}$ can be straightforwardly obtained by taking the derivatives of Eqs. (4.1b) and (4.1c). Appendix B presents the explicit expressions of $\mathbf{N}_{,ij}$ as well as the proper choice of $\boldsymbol{n}$, $\boldsymbol{m}$ and their derivatives.

## 4.3  Residue calculus method

Since the Green's function can be reduced to a line integral, it is straightforward to evaluate the Green's function by using the Cauchy's residue theorem. In this section, we introduce this alternative method.

### 4.3.1  Representation of the Green's function

Eq. (2.55) in piezoelectricity case can be solved by using either Fourier transform or Radon transform (Qin, 2010). The Green's function can be expressed by an area integral as

$$G_{IJ}(\boldsymbol{x}) = \frac{1}{8\pi^2}\int_{S^2}\delta(\boldsymbol{\xi}\cdot\boldsymbol{x})K_{IJ}^{-1}(\boldsymbol{\xi})dS(\boldsymbol{\xi}), \tag{4.21}$$

where $\boldsymbol{\xi}$ is a parameter vector, $S^2$ is the surface of the unit sphere in the $\boldsymbol{\xi}$-space and $K_{IJ}(\boldsymbol{\xi}) = c_{kIJl}\xi_k\xi_l$ with the symmetry relation $K_{IJ} = K_{JI}$.

Further, the area integral can be reduced to be a line integral over a unit circle as

$$G_{IJ}(\boldsymbol{x}) = \frac{1}{8\pi^2 r}\oint_S K_{IJ}^{-1}(\boldsymbol{\xi})d\phi, \tag{4.22}$$

49

where $S$ is the unit circle on the oblique plane perpendicular to $\boldsymbol{x}$ and $\phi$ is a parameter in the oblique plane.

To get the explicit expressions of the Green's function, the line integrals over the unit circle are transformed into improper integrals from $-\infty$ to $+\infty$. By choosing any two mutually orthogonal unit vectors $\mathbf{n}$ and $\mathbf{m}$ on the oblique plane as the bases, $\boldsymbol{\xi}$ can be written as

$$\boldsymbol{\xi} = \boldsymbol{n}\cos\phi + \boldsymbol{m}\sin\phi, \tag{4.23}$$

where $\phi$ is the angle between $\boldsymbol{n}$ and $\boldsymbol{\xi}$. Setting

$$p = \tan\phi, \quad \boldsymbol{\xi}^* = \boldsymbol{n} + p\,\boldsymbol{m}, \tag{4.24}$$

we have

$$\boldsymbol{\xi} = \cos\phi\,\boldsymbol{\xi}^*, \quad d\phi = \cos^2\phi\, dp. \tag{4.25}$$

Substituting Eq. (4.25) into Eqs. (4.22), the Green's function yields

$$G_{IJ}(\boldsymbol{x}) = \frac{1}{2\pi r} A_{IJ}(\bar{\boldsymbol{x}}), \tag{4.26}$$

where

$$A_{IJ}(\bar{\boldsymbol{x}}) = \frac{1}{2\pi} \int_{-\infty}^{+\infty} N_{IJ}(p) D^{-1}(p) dp. \tag{4.27}$$

In Eqs. (4.27), $N_{IJ}(p)$ and $D(p)$ are the cofactors and the determinant of $K_{IJ}(p) = c_{kIJl}\xi_k^*\xi_l^*$, respectively.

$D(p)$ is an 8th-order polynomial, which leads to eight roots with four pairs of complex conjugates. Note that $\boldsymbol{n}$ or $\boldsymbol{m}$ in the Stroh's formalism method and the residue calculus method are not necessarily the same, but if they are chosen the same, the roots of $D(p)$ are equal to the eigenvalues of the Stroh's eigen-relation (4.1).

By now, the Green's function is expressed in terms of an improper line integral, i.e., Eq. (4.27). Since $N_{IJ}(p)$ is a 6th-order polynomial in $p$, the explicit expression of the Green's function can be obtained by applying Cauchy's residue theorem on the improper line integral $A_{IJ}(\bar{\boldsymbol{x}})$.

With distinctness assumption on the four pairs of the complex conjugates, the explicit expression of $A_{IJ}(\bar{\boldsymbol{x}})$ is given by

$$A_{IJ}(\bar{\boldsymbol{x}}) = -\operatorname{Im} \sum_{n=1}^{4} \frac{N_{IJ}(p_n)}{D'(p_n)}, \tag{4.28}$$

where the prime $'$ denotes the derivative with respect to $p$ and $p_n$ are the complex roots of $D(p)$ with positive imaginary parts. For details, the readers refer to Appendix A.

Therefore the explicit expression of the Green's function is obtained by substituting Eq. (4.28) into Eq. (4.26).

## 4.3.2 First derivative of the Green's function

Differentiating Eq. (4.21) with respect to $x_k$ leads to the first derivative of the Green's function as

$$G_{IJ,k}(\boldsymbol{x}) = \frac{1}{8\pi^2} \int_{S^2} \delta'(\boldsymbol{\xi}\cdot\boldsymbol{x})\xi_k K_{IJ}^{-1}(\boldsymbol{\xi}) dS(\boldsymbol{\xi}), \tag{4.29}$$

where the prime $'$ denotes the derivative with respect to the argument, i.e., $\boldsymbol{\xi} \cdot \boldsymbol{x}$.

After some mathematical elementary manipulations, Eq. (4.29) can be recast into the following line integrals over a unit circle as

$$
\begin{aligned}
G_{IJ,k}(\boldsymbol{x}) = \frac{1}{8\pi^2 r^2} \oint_S \Big[ &-\bar{x}_k K_{IJ}^{-1}(\boldsymbol{\xi}) \\
&+ \xi_k c_{pLMq}(\bar{x}_p \xi_q + \xi_p \bar{x}_q) K_{LI}^{-1}(\boldsymbol{\xi}) K_{MJ}^{-1}(\boldsymbol{\xi}) \Big] d\phi.
\end{aligned}
\tag{4.30}
$$

Similar equations as above for the elastic materials with detailed derivations were presented by Mura (1987). For simplify, Eq. (4.30) can be rewritten as the following equation

$$
G_{IJ,k}(\boldsymbol{x}) = \frac{1}{2\pi r^2} \left[ -\bar{x}_k A_{IJ}(\bar{\boldsymbol{x}}) + P_{IJk}(\bar{\boldsymbol{x}}) \right],
\tag{4.31}
$$

in which $A_{IJ}(\bar{\boldsymbol{x}})$ is defined by Eq. (4.27) and

$$
P_{IJk}(\bar{\boldsymbol{x}}) = \frac{1}{2\pi} \int_{-\infty}^{+\infty} \xi_k^* H_{IJ}(p) D^{-2}(p) dp,
\tag{4.32}
$$

where $H_{IJ}(p)$ is given by

$$
H_{IJ}(p) = F_{IM}(p) N_{JM}(p), \quad F_{IM}(p) = E_{HM}(p) N_{IH}(p),
$$
$$
F_{IM}(p) = E_{HM}(p) N_{IH}(p).
\tag{4.33}
$$

In Eq. (4.32) $\xi_i^*$ is a 1st-order polynomial in $p$ and $H_{IJ}(p)$ is a 13th-order polynomial in $p$. Therefore following the derivation in Appendix A, the explicit expression of $P_{IJk}(\bar{\boldsymbol{x}})$ is given by

$$
P_{IJk}(\bar{\boldsymbol{x}}) = -\operatorname{Im} \sum_{n=1}^4 \frac{D'(p_n)\hat{H}'_{IJk}(p_n) - D''(p_n)\hat{H}_{IJk}(p_n)}{D'^3(p_n)},
\tag{4.34}
$$

where

$$
\hat{H}_{IJk}(p) = \xi_k^* H_{IJ}(p).
\tag{4.35}
$$

The first derivative of the Green's function is obtained by substituting Eqs. (4.28) and (4.34) into Eq. (4.31).

### 4.3.3 Second derivative of the Green's function

The second derivative of the Green's function is given by taking the derivative of Eq. (4.29) with respect to $x_j$, i.e.,

$$
G_{IJ,kl}(\boldsymbol{x}) = \frac{1}{8\pi^2} \int_{S^2} \delta''(\boldsymbol{\xi} \cdot \boldsymbol{x}) \xi_k \xi_l K_{IJ}^{-1}(\boldsymbol{\xi}) dS(\boldsymbol{\xi}).
\tag{4.36}
$$

After some manipulations (Mura, 1987), the second derivative of the Green's function becomes

$$
\begin{aligned}
G_{IJ,kl}(\boldsymbol{x}) = \frac{1}{4\pi^2 r^3} \oint_S \Big\{ &\bar{x}_k \bar{x}_l K_{IJ}^{-1}(\boldsymbol{\xi}) - [(\bar{x}_k \xi_l + \xi_k \bar{x}_l)(\bar{x}_p \xi_q + \xi_p \bar{x}_q) + \xi_k \xi_l \bar{x}_p \bar{x}_q] \\
&\times c_{pHMq} K_{IH}^{-1}(\boldsymbol{\xi}) K_{JM}^{-1}(\boldsymbol{\xi}) + \xi_k \xi_l c_{pHMq}(\bar{x}_p \xi_q + \xi_p \bar{x}_q) c_{aSTb}(\bar{x}_a \xi_b + \xi_a \bar{x}_b) \\
&\times K_{JM}^{-1}(\boldsymbol{\xi}) K_{IS}^{-1}(\boldsymbol{\xi}) K_{HT}^{-1}(\boldsymbol{\xi}) \Big\} d\phi,
\end{aligned}
\tag{4.37}
$$

Note that Eq. (4.37) is a little different from the corresponding equation by Mura (1987) for the elastic materials, since the symmetry relations of $c_{iJMn}$ and $K_{IJ}$ are used. Further Eq. (4.37) can be recast into the following equation

$$G_{IJ,kl}(\boldsymbol{x}) = \frac{1}{\pi r^3} \left\{ A_{IJ}(\bar{\boldsymbol{x}})\bar{x}_k\bar{x}_l - [P_{IJk}(\bar{\boldsymbol{x}})\bar{x}_l + P_{IJl}(\bar{\boldsymbol{x}})\bar{x}_k] + Q_{IJkl}(\bar{\boldsymbol{x}}) \right\}, \qquad (4.38)$$

where $A_{IJ}(\bar{\boldsymbol{x}})$ is defined by Eq. (4.27), $P_{IJk}(\bar{\boldsymbol{x}})$ is defined by Eq. (4.32), and $Q_{IJkl}(\bar{\boldsymbol{x}})$ is defined by

$$Q_{IJkl}(\bar{\boldsymbol{x}}) = \frac{1}{2\pi} \int_{-\infty}^{+\infty} \xi_k^* \xi_l^* M_{IJ}(p) D^{-3}(p) dp, \qquad (4.39)$$

in which $M_{IJ}(p)$ is given by

$$M_{IJ}(p) = L_{IJ}(p) - R_{IJ}(p)D(p), \quad L_{IJ}(p) = F_{JH}(p)H_{IH}(p),$$
$$R_{IJ}(p) = \bar{x}_p\bar{x}_q C_{pHMq}N_{IH}(p)N_{JM}(p). \qquad (4.40)$$

Since $M_{IJ}(p)$ is a 20th-order polynomial in $p$, following the derivation in Appendix A, the explicit expression of $Q_{IJkl}(\bar{\boldsymbol{x}})$ is given by

$$Q_{IJkl}(\bar{\boldsymbol{x}}) = -\operatorname{Im} \sum_{n=1}^{4} \frac{1}{2D'^5(p_n)} \left\{ D'^2(p_n)\hat{M}''_{IJkl}(p_n) - 3D'(p_n)D''(p_n)\hat{M}'_{IJkl}(p_n) \right.$$
$$\left. + \left[3D''^2(p_n) - D'''(p_n)D'(p_n)\right] \hat{M}_{IJkl}(p_n) \right\}, \qquad (4.41)$$

where

$$\hat{M}_{IJkl}(p) = \xi_k^* \xi_l^* M_{IJ}(p). \qquad (4.42)$$

Here, $\hat{M}_{IJkl}(p)$ is a polynomial of 22th-order respectively.

Since $D(p)$, $\hat{H}_{IJk}(p)$ and $\hat{M}_{IJkl}(p)$ are polynomials, they and their derivatives can be calculated almost exactly by proper algorithms for polynomials.

Finally, the second derivative of the Green's function is obtained by substituting Eqs. (4.28), (4.34) and (4.41) into Eq. (4.38).

## 4.4 Numerical procedures

The numerical procedure for each of the two methods can be divided into four steps. In the SFM, the four steps are:

i) Determination of $\boldsymbol{n}$, $\boldsymbol{m}$ and their derivatives.
$\boldsymbol{n}$ and $\boldsymbol{m}$ can be any two mutually orthogonal unit vectors on the oblique plane perpendicular to the given position vector $\boldsymbol{x}$. In our analysis $\boldsymbol{n}$ and $\boldsymbol{m}$ are chosen as Eq. (B.6) or Eq. (B.10), and their derivatives are evaluated correspondingly by Eq. (B.9) or Eq. (B.11).

ii) Determination of the Stroh fundamental piezoelectricity matrix $\mathbf{N}$ and its derivatives.
$\mathbf{N}$ is determined by Eq. (4.1). The derivatives of $\mathbf{N}$ can be derived from Eq. (4.1) and the derivatives of $\boldsymbol{n}$ and $\boldsymbol{m}$.

iii) Computation of the eigenvalues $p_\alpha$, the right eigenvectors $\boldsymbol{\xi}_\alpha$ and their derivatives.
In our analysis, the subroutine ZGEEV in LAPACK library (Anderson et al., 1999) is used to calculate $p_\alpha$ and $\boldsymbol{\xi}_\alpha$. Eqs. (4.9a) and (4.11) are used to calculate the first derivatives of $\boldsymbol{\xi}_\alpha$ and $p_\alpha$. Eqs. (4.16) and (4.18) are used to calculate the second derivatives of $\boldsymbol{\xi}_\alpha$ and $p_\alpha$.

iv) Computation of $G_{IJ}(\boldsymbol{x})$, $G_{IJ,k}(\boldsymbol{x})$ and $G_{IJ,kl}(\boldsymbol{x})$.
The Green's function and its derivatives are computed by Eqs. (4.6), (4.7) and (4.15). For this purpose, $\boldsymbol{\xi}_\alpha$ and their derivatives are used to construct $\mathbf{A}$ and its derivatives.

In the RCM, the four steps are:

i) Determination of $\boldsymbol{n}$ and $\boldsymbol{m}$.
There is no need to calculate the derivatives of $\boldsymbol{n}$ and $\boldsymbol{m}$. In our method, $\boldsymbol{n}$ and $\boldsymbol{m}$ are chosen as (B.6) or (B.10).

ii) Computation of the Stroh eigenvalues $p_k$ $(k = 1, 2, 3, 4)$.
The eigenvalues $p_k$ are zeros of the polynomial $D(p)$, which is the determinant of $K_{IJ}(p) = c_{kIJl}\xi_k^*\xi_l^*$ with $\boldsymbol{\xi}^* = \boldsymbol{n} + p\,\boldsymbol{m}$. Many algorithms can be used to find the zeros of $D(p)$. In our method, we use the same algorithm as in the SFM to find $p_k$ $(k = 1, 2, 3, 4)$, since the zeros of the polynomial $D(p)$ are equal to the eigenvalues of $\mathbf{N}$ if $\boldsymbol{n}$ and $\boldsymbol{m}$ are the same.

iii) Evaluation of $N_{IJ}(p)$, $D(p)$, $\hat{H}_{IJk}(p)$, $\hat{M}_{IJkl}(p)$ and their derivatives.
Because $N_{IJ}(p)$, $D(p)$, $\hat{H}_{IJk}(p)$ and $\hat{M}_{IJkl}(p)$ are polynomials, their coefficients can be determined in an accurate way by using the suitable algorithms for polynomials in a computer program.

iv) Computation of $G_{IJ}(\boldsymbol{x})$, $G_{IJ,k}(\boldsymbol{x})$ and $G_{IJ,kl}(\boldsymbol{x})$.
The Green's function and its derivatives can be determined by $A_{IJ}(\bar{\boldsymbol{x}})$, $P_{IJk}(\bar{\boldsymbol{x}})$ and $Q_{IJkl}(\bar{\boldsymbol{x}})$ with Eqs. (4.26), (4.31) and (4.38). The Green's function $G_{IJ}(\boldsymbol{x})$ is determined by $A_{IJ}(\bar{\boldsymbol{x}})$ only. Additionally, $P_{IJk}(\bar{\boldsymbol{x}})$ is required to determine the first derivative of the Green's function $G_{IJ,k}(\boldsymbol{x})$. And the second derivative of the Green's function $G_{IJ,kl}(\boldsymbol{x})$ is determined by $A_{IJ}(\bar{\boldsymbol{x}})$, $P_{IJk}(\bar{\boldsymbol{x}})$ and $Q_{IJkl}(\bar{\boldsymbol{x}})$, which are defined by Eqs. (4.28), (4.34) and (4.41), respectively.

It should be mentioned that the Green's function can be evaluated without assuming the distinctness of the eigenvalues $p_\alpha$ of $\mathbf{N}$, also known as the Stroh eigenvalues (Akamatsu and Tanuma, 1997), but according to Eqs. (4.12) and (4.20) the distinctness assumption is necessary to evaluate the derivatives of the Green's function in the SFM. However, the distinctness of the Stroh eigenvalues is required in the RCM for both the Green's function and its derivatives. Hence, for the cases with repeated Stroh eigenvalues, a small perturbation on the material constants is suggested to avoid repeated or degenerated eigenvalues in the RCM.

## 4.5 Numerical examples and discussions

The transversely isotropic piezoelectric material, Lead Zirconate Titanate (PZT), is used in the numerical examples. Choosing the axis of the material symmetry as the $x_3$-axis,

the non-zero components of the elasticity tensor $C_{ijkl}$ in contracted notation are given by

$$C_{11} = C_{22} = 139, \quad C_{12} = 77.8, \quad C_{13} = C_{23} = 74.3, \tag{4.43}$$

$$C_{33} = 115, \quad C_{44} = C_{55} = 25.6, \quad C_{66} = 30.6, \quad \left(\text{unit: } 10^9 \text{N/m}^2\right)$$

The non-zero components of the piezoelectric constants $e_{nij}$ in contracted notation are

$$e_{31} = e_{32} = -5.1, \quad e_{33} = 15.1, \quad e_{24} = e_{15} = 12.7, \quad (\text{unit: C/m}), \tag{4.44}$$

and the non-zero components of the dielectric constants $\kappa_{in}$ are

$$\kappa_{11} = \kappa_{22} = 6.461, \quad \kappa_{33} = 5.620, \quad \left(\text{unit: } 10^{-9}\text{C/(Vm)}\right). \tag{4.45}$$

The source of the Green's function is located at the origin of the Cartesian coordinate system and the observation point is arbitrarily chosen as $(1, 2, 3)$.

In order to compare the numerical results with the analytical results, the analytical solution for transversely isotropic piezoelectric material presented by Ding et al. (1996) is evaluated by MATHEMATICA to give the exact results of the Green's function and its derivatives. The SFM is implemented in double precision and the RCM is implemented in quadruple precision to have a similar accuracy in the two methods. Tables 4.1, 4.2 and 4.3 present the numerical results of the Green's function, its first derivatives and second derivatives, respectively. The numerical results show that both methods can give highly accurate results.

| $G_{IJ}\,(\times 10^{-4})$ | SFM | RCM | Ding et al. (1996) |
|:---:|:---:|:---:|:---:|
| $G_{11}$ | 4.505586760 | 4.505586760 | 4.505586760 |
| $G_{12}$ | 0.341535419 | 0.341535419 | 0.341535419 |
| $G_{13}$ | 0.442087059 | 0.442087059 | 0.442087059 |
| $G_{14}$ | 0.586632878 | 0.586632878 | 0.586632878 |
| $G_{22}$ | 5.017889889 | 5.017889889 | 5.017889889 |
| $G_{23}$ | 0.884174119 | 0.884174119 | 0.884174119 |
| $G_{24}$ | 1.173265756 | 1.173265756 | 1.173265756 |
| $G_{33}$ | 4.016244535 | 4.016244535 | 4.016244535 |
| $G_{34}$ | 7.703838268 | 7.703838268 | 7.703838268 |
| $G_{44}$ | $-18.56559227$ | $-18.56559227$ | $-18.56559227$ |

Table 4.1: Components of the Green's function $\mathrm{G}_{IJ}$ for PZT at point $(1, 2, 3)$

Table 4.4 shows the CPU time needed in the two methods for evaluating the Green's function and its derivatives. The second column in the table is the computing time for the Green's function including the time for solving the Stroh eigensystem. The third column in the table is the additional time needed to evaluate the first derivatives of the Green's function. The fourth column in the table is the time needed to evaluate the second derivatives of the Green's function apart from the time for the Green's function and its first derivatives. The table shows that the SFM is much more efficient than the RCM, if a similar accuracy should be ensured.

| $G_{IJ,1}$ ($\times 10^{-5}$) | SFM | RCM | Ding et al. (1996) |
|---|---|---|---|
| $G_{11,1}$ | 0.273798678 | 0.273798678 | 0.273798678 |
| $G_{12,1}$ | 2.807551643 | 2.807551643 | 2.807551643 |
| $G_{13,1}$ | 3.670552502 | 3.670552502 | 3.670552502 |
| $G_{14,1}$ | 4.720160351 | 4.720160351 | 4.720160351 |
| $G_{22,1}$ | $-4.053259346$ | $-4.053259345$ | $-4.053259346$ |
| $G_{23,1}$ | $-1.500636194$ | $-1.500636194$ | $-1.500636194$ |
| $G_{24,1}$ | $-2.292336860$ | $-2.292336860$ | $-2.292336860$ |
| $G_{33,1}$ | $-3.586215224$ | $-3.586215224$ | $-3.586215224$ |
| $G_{34,1}$ | $-7.208139532$ | $-7.208139532$ | $-7.208139532$ |
| $G_{44,1}$ | 8.156849750 | 8.156849750 | 8.156849750 |

Table 4.2: Components of the first derivative of the Green's function $G_{IJ,1}$ for PZT at point $(1, 2, 3)$

| $G_{IJ,11}$ ($\times 10^{-5}$) | SFM | RCM | Ding et al. (1996) |
|---|---|---|---|
| $G_{11,11}$ | $-0.292020389$ | $-0.292020390$ | $-0.292020389$ |
| $G_{12,11}$ | $-1.646729346$ | $-1.646729347$ | $-1.646729346$ |
| $G_{13,11}$ | $-2.045111717$ | $-2.045111717$ | $-2.045111717$ |
| $G_{14,11}$ | $-3.074641374$ | $-3.074641373$ | $-3.074641374$ |
| $G_{22,11}$ | $-3.138455843$ | $-3.138455844$ | $-3.138455843$ |
| $G_{23,11}$ | $-1.088951047$ | $-1.088951047$ | $-1.088951047$ |
| $G_{24,11}$ | $-1.564609027$ | $-1.564609026$ | $-1.564609027$ |
| $G_{33,11}$ | $-2.797084793$ | $-2.797084793$ | $-2.797084793$ |
| $G_{34,11}$ | $-5.431632234$ | $-5.431632234$ | $-5.431632234$ |
| $G_{44,11}$ | 7.407256662 | 7.407256662 | 7.407256662 |

Table 4.3: Components of the second derivative of the Green's function $G_{IJ,11}$ for PZT at point $(1, 2, 3)$

| CPU Time [$10^{-4}$s] | $G_{IJ}$ | $G_{IJ,k}$ | $G_{IJ,kl}$ |
|---|---|---|---|
| SFM | 0.91204977 | 1.09204865 | 4.14409828 |
| RCM | 4.16835785 | $8.00323486 \times 10^{-3}$ | 73.1817322 |

Table 4.4: Computing time for the Green's function and its derivatives for PZT at point $(1, 2, 3)$

It should be noted that the explicit expressions in both methods are applicable only when the Stroh eigenvalues are distinct. The explicit expressions are much more complicated when the Stroh eigenvalues are identical. In practical applications, a small perturbation can be applied to the material constants $C_{iJKl}$, to keep the Stroh eigenvalues distinct. In the following, by using the SFM, the Green's function and its derivatives are evaluated at the field point $(\cos\theta\cos\phi, \cos\theta\sin\phi, \sin\theta)$ where $\theta$ and $\phi$ are illustrated in Fig. 3.9. It is observed that considerable numerical error occurs around $\theta = \pi/2$, i.e., $(0, 0, 1)$ with the direct use of the SFM. According to the authors' experience, similar error appears in the explicit expressions of the Green's function and its derivatives for transversely isotropic solids, when the evaluation point is chosen along the symmetry axis of the material, i.e., $x_3$ where the Stroh eigenvalues degenerate. So the numerical error around the point $(0, 0, 1)$ in the SFM for piezoelectric solids may result from the degeneracy of the Stroh eigenvalues. To get rid of the error, the SFM is used with a very small perturbation, say $10^{-6}$, on some material constants of PZT, e.g., $C_{22}$, $C_{55}$ and $\kappa_{22}$. Figs. 4.1 and 4.2 show the components of the Green's function, while Figs. 4.3 and 4.4 present some components of the first and second derivatives of the Green's function, respectively. All figures show that good results for the Green's function and its derivatives for 3D piezoelectric solids can be achieved by using the SFM with a small perturbation on the material constants. By the way, similar results can also be obtained from the RCM with a small perturbation greater than $10^{-4}$ to avoid repeated or degenerated Stroh eigenvalues.
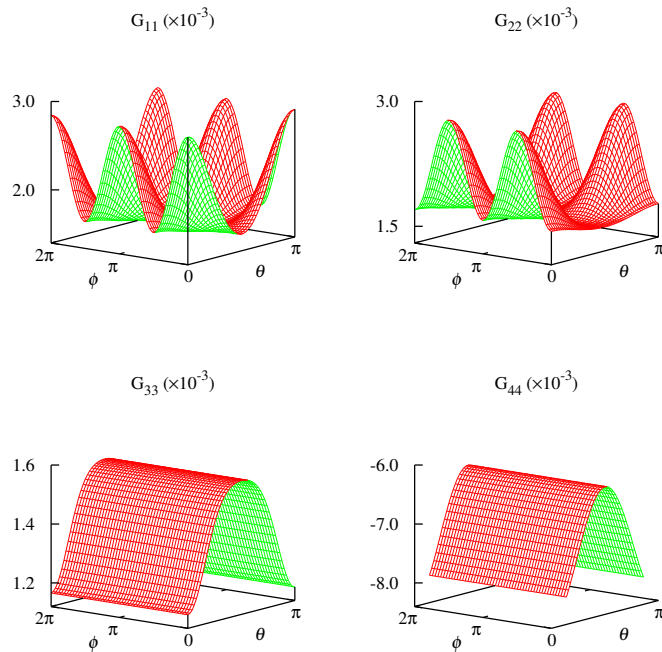


Figure 4.1: Diagonal components of the Green's function for PZT at field points
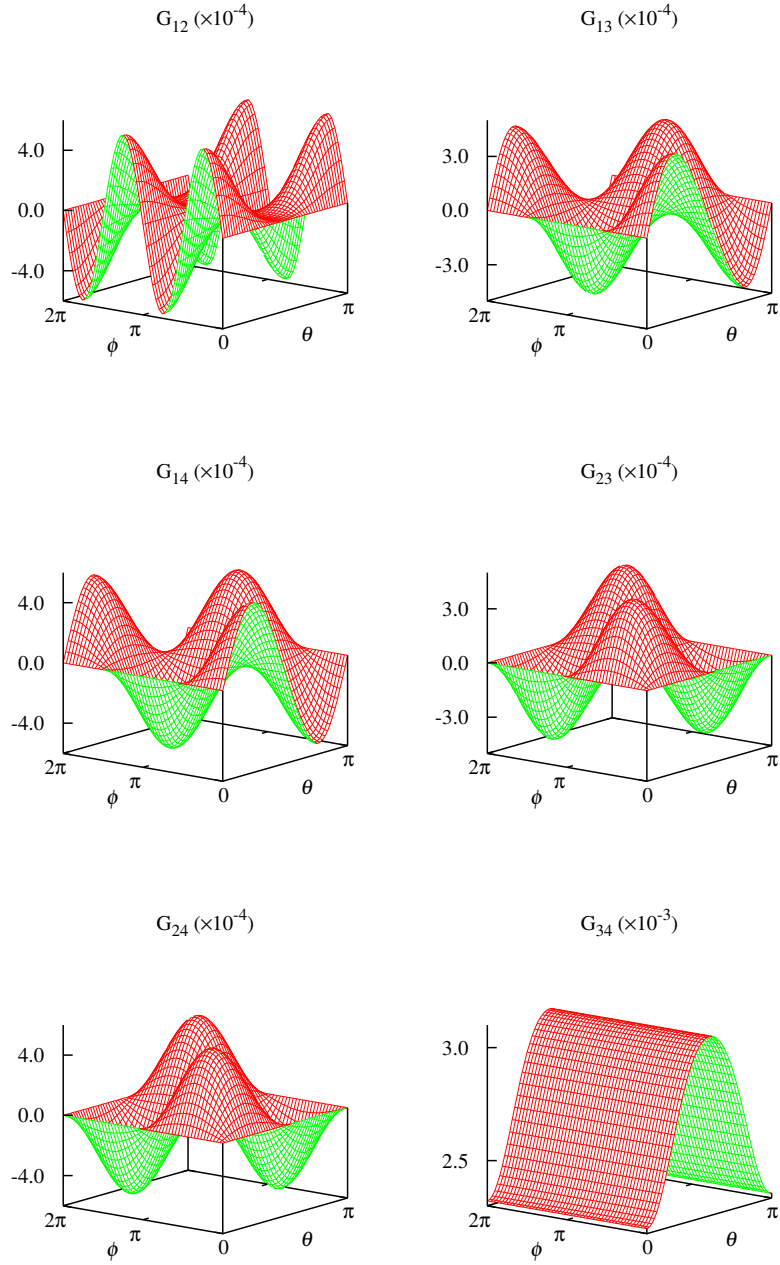
Figure 4.2: Non-diagonal components of the Green's function for PZT at field points

$G_{11,1}$ ($\times 10^{-3}$)  $G_{14,1}$ ($\times 10^{-4}$)

$G_{11,2}$ ($\times 10^{-3}$)  $G_{14,2}$ ($\times 10^{-4}$)

$G_{11,3}$ ($\times 10^{-3}$)  $G_{14,3}$ ($\times 10^{-3}$)

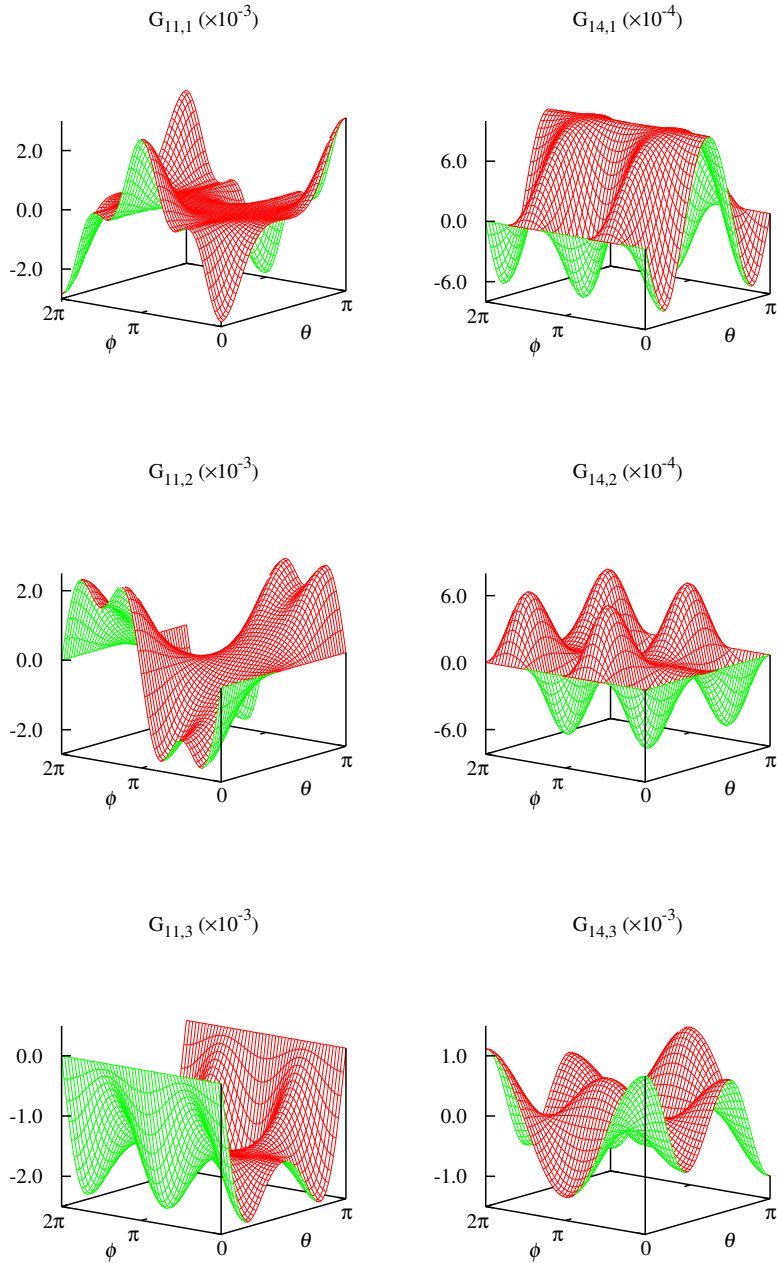Figure 4.3: Some components of the first derivative of the Green's function for PZT at field points
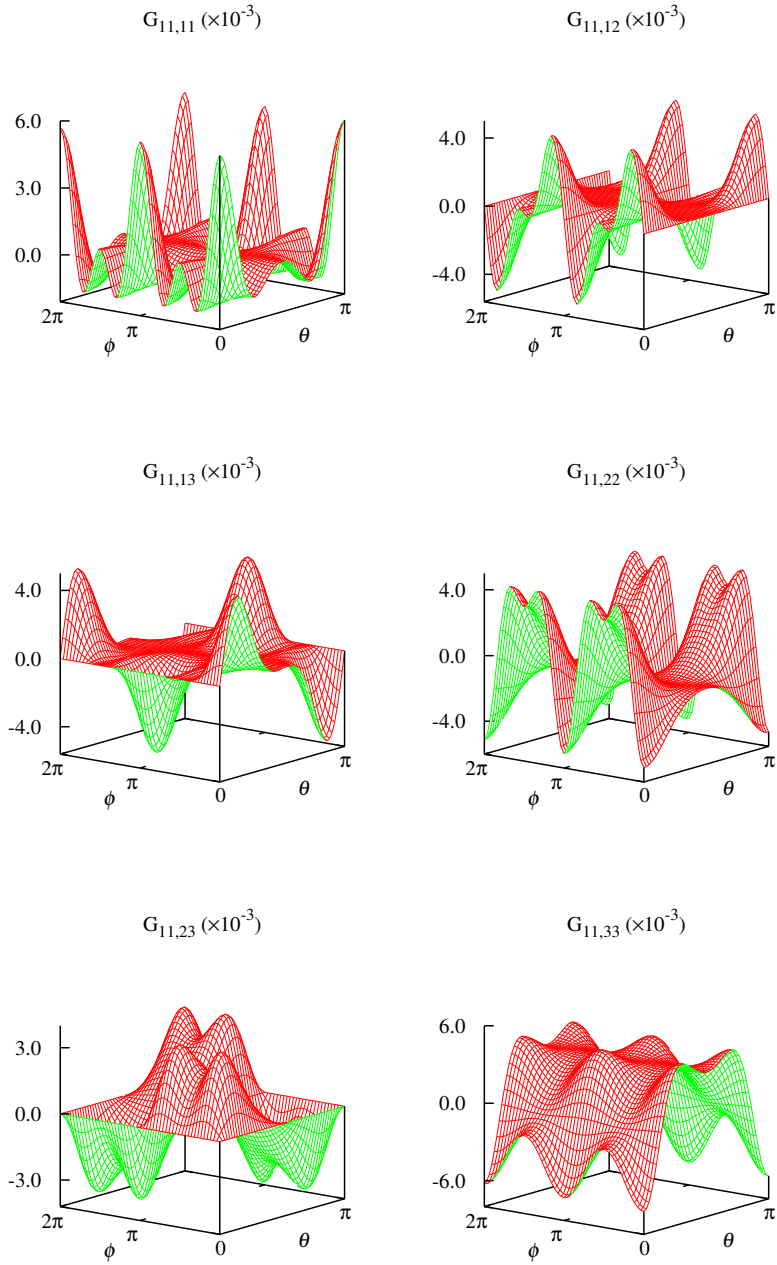
Figure 4.4: Some components of the second derivative of the Green's function for PZT at field points

## 4.6  Concluding remarks

In this chapter, two accurate methods are presented for computing the Green's function and its first and second derivatives for three-dimensional anisotropic piezoelectric solids. The derivatives of the generalized displacement Green's function are needed for computing the generalized stress and higher-order stress Green's functions, which are required by the displacement-based and stress-based BEM or by the integral representation formulae for calculating the generalized displacement and stress at internal points in the analyzed domain. In the first method, the Stroh formalism is applied to derive explicit expressions for the Green's function as well as its first and second derivatives as a linear combination of the Stroh eigenvectors. The coefficients are expressed in terms of the eigenvalues and the eigenvectors. In the second method, the Cauchy residue theorem is applied to the infinite or improper line integrals arising in the Green's function and its derivatives, which can be evaluated analytically. Both methods work well under the assumption that the Stroh eigenvalues are distinct. The obtained new expressions by the two methods are implemented into a FORTRAN code. Good accuracy of both methods is verified by the results from the analytical solutions. If a similar accuracy is required, the expressions obtained by the Stroh formalism method are much more efficient than those by the residue calculus method. Although the new explicit expressions in both methods are only applicable when the Stroh eigenvalues are distinct, a general evaluation of the Green's function and its derivatives can be performed by using these expressions with a small perturbation in the material constants to avoid repeated or identical eigenvalues.

# Chapter 5

# Green's function in linear magnetoelectroelasticity

## 5.1 Problem statement

Magnetoelectroelastic solids and/or multiferroic materials have magneto-electro-mechanical energy conversion capacities. Due to the potential applications in the technologies of smart and adaptive materials and structures such as magnetic/electric transducers, actuators and sensors, the magnetoelectroelastic solids have drawn increasing interest of the scientists and engineers. The natural single-phase multiferroic materials have very weak magnetoelectric coupling at room temperature, while the magnetoelectric composites constituting of piezoelectric and piezomagnetic material phases, reported for example by van Suchtelen (1972), may have a strong magnetoelectric coupling even at room temperature (Eerenstein et al., 2006; Srinivasan, 2010).

Although there is no magnetoelectric coupling in either piezoelectric materials or piezomagnetic materials, the magnetoelectric composites have a magnetoelectric coupling due to the interaction between the electromechanical and magnetomechanical behaviors of the constituent materials. Many investigations can be found in literature on the theoretical modeling of magnetoelectric composites. Alshits et al. (1992) investigated the existence of the surface wave in semi-infinite anisotropic magnetoelectroelastic solids, Benveniste (1995), Huang and Kuo (1997) and Li and Dunn (1998) analyzed the inclusion and inhomogeneity problems of the magnetoelectric composites by treating both the piezoelectric and the piezomagnetic materials as single-phase magnetoelectroelastic materials. These previous works may be considered as some of the pioneer works on the magnetoelectroelastic materials after which numerous theoretical models have been proposed.

The Green's function in the magnetoelectroelastic materials has already been investigated by some researchers. For the transversely isotropic magnetoelectroelastic materials, the Green's function could be obtained analytically by using the potential theory. Wang and Shen (2002) derived the fundamental solution for the dislocation and the Green's function in a half-space magnetoelectroelastic solid. Soh et al. (2003) and Ding and Jiang (2003) derived the Green's function in a full-space magnetoelectroelastic solid and the later authors implemented the Green's function in the BEM. For generally anisotropic materials, the Green's function can be represented explicitly in terms of the Stroh eigenvalues or Stroh eigenvectors. Chung and Ting (1995) presented the two-dimensional (2D) Green's function for anisotropic magnetoelectroelastic materials with an elliptic hole or

rigid inclusion by the Stroh formalism in magnetoelectroelasticity. Liu et al. (2001) presented the 2D Green's function for anisotropic magnetoelectroelastic solids with an elliptical cavity or a crack based on the Stroh formalism combined with the technique of conformal mapping and the Laurent series expansion. Further, Pan (2002) derived the three-dimensional (3D) Green's functions in anisotropic magnetoelectroelastic full-space, half-space, and bimaterials based on the Stroh formalism. Qin (2004) derived the Green's functions with an arbitrarily oriented half-plane or bimaterial interface. Buroni and Sáez (2010) presented the 3D anisotropic magnetoelectroelastic Green's function and its first and second derivatives in terms of the Stroh eigenvalues by the Cauchy residue calculus applied to the line integrals. More details on the anisotropic and multifield coupled Green's function can be found in the textbooks by Qin (2010) and Pan and Chen (2015).

In this Chapter, the explicit expression for the 3D generally anisotropic magnetoelectroelastic Green's function is derived by using the Stroh formalism associated with an oblique plane in the 3D full-space. Since the derivatives of the Green's function are also essential issues in BEM as well as many other applications, the explicit derivatives of the Green's function are also derived based on the Stroh eigen-relation on the oblique plane and the orthonormal or orthogonality relation for the Green's function. The main difference between the novel expressions and those proposed by Buroni and Sáez (2010) are that in the present paper, we utilize the Stroh formalism while the later used Cauchy residue calculus to evaluate the Green's function and its derivatives. Although the numerical results of the second derivative of the Green's function was not presented, Buroni and Sáez (2010) pointed out that it could be obtained by applying the Cauchy residue calculus to the line integral. In this work, not only the explicit expressions for the first derivative but also for the second derivative of the Green's function as well as the corresponding numerical results are presented. Besides, Xie et al. (2015b) demonstrated that the Stroh formalism method may have advantages compared to the residue calculus method for the numerical calculations of the Green's function and its derivatives. The newly proposed expressions for 3D generally anisotropic magnetoelectroelastic solids are verified by the comparison of the present numerical results and those evaluated by the analytical solutions derived by Ding and Jiang (2003) for transversely isotropic magnetoelectroelastic solids at a particular point. The CPU time for the calculation of the Green's function and its derivatives is also given. In addition, for degenerate and nearly degenerate cases the Green's function and its derivatives at arbitrary field points by the present novel explicit expressions with a small perturbation on some material coefficients are also computed and discussed for practical interest.

The contribution in this chapter has been published in:

- **L. Xie**, C. Zhang, C. Hwu, E. Pan, On novel explicit expressions of Green's function and its derivatives for magnetoelectroelastic materials. *European Journal of Mechanics – A/Solids.* submitted.

## 5.2   Stroh formalism method

In Chapters 3 and 4, it is demonstrated that compared to the residue calculus method, the Stroh formalism may have higher accuracy and efficiency in the numerical calculation of the Green's function and its derivatives. So in this section, we extend the Stroh formalism

method proposed in Chapter 3 and 4 to derive the Green's function and its first and second derivatives for linear generally anisotropic magnetoelectroelastic materials.

## 5.2.1  Representation of the Green's function

In linear elastic and piezoelectric solids, the Green's function can be constructed from the solutions of the Stroh eigenvalue problem. Similarly, in linear magnetoelectroelastic solids, the 3D Green's function can also be constructed from the solutions of the Stroh eigenvalue problem in magnetoelectroelasticity. The Stroh eigenvalue problem in the linear magnetoelectroelastic solids in terms of the fundamental magnetoelectroelasticity matrix $\mathbf{N}$ is given by

$$\mathbf{N}\boldsymbol{\xi} = p\boldsymbol{\xi}, \tag{5.1}$$

where

$$\mathbf{N} = \begin{pmatrix} \mathbf{N}_1 & \mathbf{N}_2 \\ \mathbf{N}_3 & \mathbf{N}_1^T \end{pmatrix}, \tag{5.2a}$$

$$\mathbf{N}_1 = -\mathbf{T}^{-1}\mathbf{R}^T, \quad \mathbf{N}_2 = \mathbf{T}^{-1} = \mathbf{N}_2^T, \quad \mathbf{N}_3 = \mathbf{R}\mathbf{T}^{-1}\mathbf{R}^T - \mathbf{Q},$$

in which

$$Q_{IJ} = c_{kIJl}n_k n_l, \quad R_{IJ} = c_{kIJl}n_k m_l, \quad T_{IJ} = c_{kIJl}m_k m_l. \tag{5.2b}$$

Here, $\boldsymbol{n}$ and $\boldsymbol{m}$ are two mutually orthogonal unit vectors on the oblique plane perpendicular to $\boldsymbol{x}$. Since the fundamental magnetoelectroelasticity matrix $\mathbf{N}$ is a non-symmetric 10×10 matrix, the vector $\boldsymbol{\xi}$ is a 10-dimensional right eigenvector of the matrix $\mathbf{N}$. If the right eigenvector $\boldsymbol{\xi}$ is denoted as

$$\boldsymbol{\xi} = \begin{Bmatrix} \boldsymbol{a} \\ \boldsymbol{b} \end{Bmatrix}, \tag{5.3}$$

where $\boldsymbol{a}$ and $\boldsymbol{b}$ are two 5-dimensional vectors, then as proved by Ting (1996) in linear elastic solids, the corresponding left eigenvector $\boldsymbol{\eta}$ of the matrix $\mathbf{N}$ is determined by

$$\boldsymbol{\eta} = \begin{Bmatrix} \boldsymbol{b} \\ \boldsymbol{a} \end{Bmatrix}. \tag{5.4}$$

Similar to the elastic and piezoelectric cases, the eigenvalues of the matrix $\mathbf{N}$ should be 5 pairs of complex conjugates. Among the eigenvalues, we choose $\text{Im}(p_K) > 0$, $K = 1, 2, \ldots, 5$, which are known as Stroh eigenvalues, and $p_{K+5} = \bar{p}_K$. Further, we assume that the Stroh eigenvalues $p_K$ ($K = 1, 2, \ldots, 5$) are distinct, which ensures that the eigenvectors associated with the different Stroh eigenvalues are independent of each other.

By defining

$$\mathbf{A} = [\boldsymbol{a}_1, \boldsymbol{a}_2, \boldsymbol{a}_3, \boldsymbol{a}_4, \boldsymbol{a}_5], \quad \mathbf{B} = [\boldsymbol{b}_1, \boldsymbol{b}_2, \boldsymbol{b}_3, \boldsymbol{b}_4, \boldsymbol{b}_5], \tag{5.5}$$

and with the following orthonormal relation between the left and the right eigenvectors

$$\boldsymbol{\eta}_\alpha^T \boldsymbol{\xi}_\beta = \delta_{\alpha\beta}, \quad \alpha, \beta = 1, 2, \ldots, 10, \tag{5.6}$$

where $\delta_{\alpha\beta}$ is the Kronecker delta, the Green's function can be expressed as

$$\mathbf{G}(\boldsymbol{x}) = \frac{1}{4\pi r}\mathbf{H}(\bar{\boldsymbol{x}}), \quad \mathbf{H} = 2i\mathbf{A}\mathbf{A}^T, \tag{5.7}$$

in which $r = |\boldsymbol{x}|$, $\bar{\boldsymbol{x}}$ is the unit vector of $\boldsymbol{x}$, and $\mathbf{H}$ is one of the three Barnett-Lothe matrices in linear magnetoelectroelasticity.

## 5.2.2 First derivative of the Green's function

Differentiation of Eq. (5.7) with respect to $x_i$ yields the first derivative of the Green's function as

$$\mathbf{G}_{,i}(\boldsymbol{x}) = \frac{1}{4\pi r^2} \left( -\frac{x_i}{r}\mathbf{H} + r\mathbf{H}_{,i} \right), \tag{5.8a}$$

where

$$\mathbf{H}_{,i} = 2i \left( \mathbf{A}_{,i}\mathbf{A}^T + \left[ \mathbf{A}_{,i}\mathbf{A}^T \right]^T \right). \tag{5.8b}$$

The columns of the matrix $\mathbf{A}$ are parts of the eigenvectors satisfying Eq. (5.6). So in order to calculate the first derivative of the Green's function, we need to firstly calculate the first derivatives of the eigenvectors satisfying Eqs. (5.1) and (5.6). In the following, with the distinctness assumption of the eigenvalues, the derivation of the first derivatives of the eigenvectors is presented.

Differentiating Eq. (5.1), associated with the eigenvalue $p_\alpha$ and the corresponding right eigenvector $\boldsymbol{\xi}_\alpha$, with respect to $x_i$ leads to

$$(\mathbf{N} - p_\alpha\mathbf{I})\boldsymbol{\xi}_{\alpha,i} = -(\mathbf{N}_{,i} - p_{\alpha,i}\mathbf{I})\boldsymbol{\xi}_\alpha. \tag{5.9}$$

Note here that the repeated Greek indices do not imply summation. As the 10-dimensional eigenvectors associated with distinct eigenvalues are independent of each other and the derivative of an eigenvector is still a vector in the 10-dimensional space, the first derivative of the right eigenvector $\boldsymbol{\xi}_{\alpha,i}$ is a linear combination of the 10 independent eigenvectors, i.e.,

$$\boldsymbol{\xi}_{\alpha,i} = \sum_{\beta=1}^{10} c_{\alpha\beta}^{(i)}\boldsymbol{\xi}_\beta, \tag{5.10a}$$

and

$$\boldsymbol{\eta}_{\alpha,i} = \sum_{\beta=1}^{10} c_{\alpha\beta}^{(i)}\boldsymbol{\eta}_\beta, \tag{5.10b}$$

where $c_{\alpha\beta}^{(i)}$ are constants to be determined. Substitution of Eq. (5.10a) into Eq. (5.9) followed by the pre-multiplication by $\boldsymbol{\eta}_\beta^T$ yields

$$c_{\alpha\beta}^{(i)}(p_\beta - p_\alpha) = -\boldsymbol{\eta}_\beta^T(\mathbf{N}_{,i} - p_{\alpha,i}\mathbf{I})\boldsymbol{\xi}_\alpha, \tag{5.11}$$

which results from the use of Eqs. (5.1) and (5.6). When $\beta = \alpha$, the derivative of the eigenvalue $p_\alpha$ is obtained by

$$p_{\alpha,i} = \boldsymbol{\eta}_\alpha^T\mathbf{N}_{,i}\boldsymbol{\xi}_\alpha. \tag{5.12}$$

If $\beta \neq \alpha$, the coefficients $c_{\alpha\beta}^{(i)}$ are given by

$$c_{\alpha\beta}^{(i)} = \frac{\boldsymbol{\eta}_\beta^T\mathbf{N}_{,i}\boldsymbol{\xi}_\alpha}{p_\alpha - p_\beta}. \tag{5.13}$$

Substitution of Eqs. (5.6) and (5.10) into the first derivative of Eq. (5.6) leads to

$$c_{\alpha\beta}^{(i)} + c_{\beta\alpha}^{(i)} = 0. \tag{5.14}$$

When $\beta = \alpha$, we have

$$c_{\alpha\alpha}^{(i)} = 0. \tag{5.15}$$

Although similar expressions as Eqs. (5.13) and (5.15) were derived by Malén (1971), Lavagnino (1995) and Pan and Chen (2015), the present expression may be preferred since it is in the Cartesian coordinate system rather than in the spherical coordinate system. In the conventional methods, in order to get the expressions of the derivatives of the Green's function in the Cartesian coordinate system, the corresponding expressions in the spherical coordinate system have to be tranformed into the desired ones in the Cartesian coordinate system. While in the present method, the vectors $\boldsymbol{n}$ and $\boldsymbol{m}$ are expressed directly in terms of the Cartesian coordinates and consequently also the expressions of the derivatives of the Green's function.

So far, since all coefficients $c_{\alpha\beta}^{(i)}$ are determined, the first derivatives of the eigenvectors can be determined explicitly in terms of the eigenvalues and the eigenvectors. The explicit expression of the derivative of the fundamental magnetoelectroelasticity matrix $\mathbf{N}_{,i}$ is presented in Appendix B. Thereafter the first derivatives of the eigenvectors can be used to construct the matrices $\mathbf{A}_{,i}$ as well as the first derivative of the Green's function.

### 5.2.3 Second derivative of the Green's function

Differentiating Eq. (5.8) with respect to $x_j$ yields the second derivative of the Green's function

$$\mathbf{G}_{,ij}(\boldsymbol{x}) = \frac{1}{4\pi r^3} \left[ \left( \frac{3x_i x_j}{r^2} - \delta_{ij} \right) \mathbf{H} - (x_i \mathbf{H}_{,j} + x_j \mathbf{H}_{,i}) + r^2 \mathbf{H}_{,ij} \right], \qquad (5.16a)$$

where

$$\mathbf{H}_{,ij} = 2i \left[ \mathbf{A}_{,ij} \mathbf{A}^T + \mathbf{A}_{,i} \mathbf{A}_{,j}^T + \left( \mathbf{A}_{,ij} \mathbf{A}^T + \mathbf{A}_{,i} \mathbf{A}_{,j}^T \right)^T \right]. \qquad (5.16b)$$

In order to calculate the second derivative of the Green's function, we need to know the second derivative of the matrix $\mathbf{A}$ which is constructed from the second derivatives of the eigenvectors $\boldsymbol{\xi}_{\alpha,ij}$ ($\alpha = 1, 2, \ldots, 5$). Since $\boldsymbol{\xi}_{\alpha,ij}$ is a 10-dimensional vector, it is a linear combination of the 10 independent eigenvectors, i.e.,

$$\boldsymbol{\xi}_{\alpha,ij} = \sum_{\beta=1}^{10} d_{\alpha\beta}^{(ij)} \boldsymbol{\xi}_{\beta}, \qquad (5.17)$$

where $d_{\alpha\beta}^{(ij)}$ are constants to be determined. Following the similar procedure to determine $c_{\alpha\beta}^{(i)}$, the expressions of $d_{\alpha\beta}^{(ij)}$ can be derived by differentiating Eqs. (5.1) and (5.6) with respect to $x_i$ and further to $x_j$. They are

$$d_{\alpha\alpha}^{(ij)} = -(\boldsymbol{\eta}_{\alpha,i}^T \boldsymbol{\xi}_{\alpha,j} + \boldsymbol{\eta}_{\alpha,j}^T \boldsymbol{\xi}_{\alpha,i})/2,$$

$$d_{\alpha\beta}^{(ij)} = \frac{\boldsymbol{\eta}_{\beta}^T \mathbf{N}_{,ij} \boldsymbol{\xi}_{\alpha} + \boldsymbol{\eta}_{\beta}^T (\mathbf{N}_{,i} - p_{\alpha,i} \mathbf{I}) \boldsymbol{\xi}_{\alpha,j} + \boldsymbol{\eta}_{\beta}^T (\mathbf{N}_{,j} - p_{\alpha,j} \mathbf{I}) \boldsymbol{\xi}_{\alpha,i}}{p_{\alpha} - p_{\beta}}, \quad \beta \neq \alpha. \qquad (5.18)$$

The explicit expressions of $\mathbf{N}_{,ij}$ can be found in Appendix B.

## 5.3 Numerical examples and discussions

The verification of the present novel expressions of the Green's function and its derivatives is presented in the following for a virtual transversely isotropic magnetoelectroelastic

solid used by Pan (2002). The nonzero coefficients of the virtual solid in the contracted notations are given by

$$c_{11} = 166, \quad c_{12} = 77, \quad c_{13} = 78, \quad c_{33} = 162, \quad c_{44} = 43, \quad c_{66} = 44.5,$$
$$e_{31} = -4.4, \quad e_{33} = 18.6, \quad e_{15} = 11.6, \quad \kappa_{11} = 11.2, \quad \kappa_{33} = 12.6, \quad (5.19)$$
$$h_{31} = 580.3, \quad h_{33} = 699.7, \quad h_{15} = 550, \quad \mu_{11} = 5, \quad \mu_{33} = 10.$$

The units of the coefficients $c_{ij}$, $e_{ij}$, $\kappa_{ij}$, $h_{ij}$ and $\mu_{ij}$ are $10^9 \text{N/m}^2$, $\text{C/m}^2$, $10^{-9}\text{C/(Vm)}$, $\text{N/(Am)}$ and $10^{-6}\text{Ns}^2/\text{C}^2$, respectively.

In order to validate the derived formulae, they are implemented into FORTRAN code. The Stroh eigen-relation Eq. (5.1) is solved by the subroutine ZGEEV in LAPACK library (Anderson et al., 1999). Note the eigenvectors should be normalized by Eqs. (3.36) and (3.37) to be the right ones for the Green's function and its derivatives. The numerical results are compared with those of the analytical solutions derived by Ding and Jiang (2003) which are obtained by the software MATHEMATICA where the derivatives of the Green's function are evaluated by algebraic algorithm. We point out here that in our Green's function solutions, the only numerical technique involved is the solution of the Stroh eigenequation. However, by controlling the accuracy in the Stroh eigenvalues and eigenvectors, one can obtain the Green's function as accurate as one wishes. For example, Tables 5.1-5.3 are the numerical results from the present method, which are exactly the same as those of the analytical solutions in Ref.(Ding and Jiang, 2003) even after 10 digits. The high accuracy of the numerical results demonstrate that the present novel formulae are correct and accurate for generally anisotropic magnetoelectroelastic materials. It should be noted here that the remaining components of the Green's function and its derivatives, which are not listed in Tables 1-3, can be obtained by using the symmetry property of the Green's function.

| $G_{11}$ | 314.16063654 | $G_{12}$ | 22.361037823 | $G_{24}$ | 71.012378811 |
|---|---|---|---|---|---|
| $G_{22}$ | 347.70219328 | $G_{13}$ | 42.153781088 | $G_{25}$ | -3.3834594255 |
| $G_{33}$ | 97.861922990 | $G_{14}$ | 35.506189405 | $G_{34}$ | 82.045333135 |
| $G_{44}$ | -1788.9486757 | $G_{15}$ | -1.6917297128 | $G_{35}$ | 33.169143465 |
| $G_{55}$ | -4.8033844483 | $G_{23}$ | 84.307562176 | $G_{45}$ | 38.107859915 |

Table 5.1: Numerical results of the Green's function $G_{ij}(\times 10^{-6})$ at the point $(1, 2, 3)$m.

The efficiency of the present novel expressions is revealed by the CPU time for the calculation of the Green's function and its derivatives on the high performance computer cluster of the University of Siegen, Germany. The second column of Table 5.4 is the CPU time for the calculation of the Green's function. The third column is the additional CPU time for the calculation of the first derivative of the Green's function. And the last column is the additional CPU time for the calculation of the second derivative of the Green's function.

The accuracy of the present novel formulae is confirmed by the numerical example evaluated at the point $(1, 2, 3)$m for the transversely isotropic magnetoelectroelastic material. However, strictly speaking, the formulae are inapplicable when some Stroh eigenvalues are identical (degenerate cases), and in the numerical evaluation, significant errors may arise when some Stroh eigenvalues are very close to each other (nearly degenerate cases).

| | | | | | |
|---|---|---|---|---|---|
| $G_{11,1}$ | -28.206176634 | $G_{12,1}$ | 168.20787807 | $G_{24,1}$ | -91.773348299 |
| $G_{22,1}$ | -334.92030509 | $G_{13,1}$ | 352.28107640 | $G_{25,1}$ | -5.2660645067 |
| $G_{33,1}$ | 118.21555830 | $G_{14,1}$ | 309.17521990 | $G_{34,1}$ | 124.96734313 |
| $G_{44,1}$ | 1556.4933188 | $G_{15,1}$ | -19.550329381 | $G_{35,1}$ | -46.365430933 |
| $G_{55,1}$ | 2.2943477126 | $G_{23,1}$ | -138.51346896 | $G_{45,1}$ | -41.327661854 |
| $G_{11,2}$ | -503.63310972 | $G_{12,2}$ | 1.0001888071 | $G_{24,2}$ | 171.51519746 |
| $G_{22,2}$ | -222.61985373 | $G_{13,2}$ | -138.51346896 | $G_{25,2}$ | -27.449426141 |
| $G_{33,2}$ | 236.43111660 | $G_{14,2}$ | -91.773348299 | $G_{34,2}$ | 249.93468625 |
| $G_{44,2}$ | 3112.9866377 | $G_{15,2}$ | -5.2660645067 | $G_{35,2}$ | -92.730861866 |
| $G_{55,2}$ | 4.5886954251 | $G_{23,2}$ | 144.51087296 | $G_{45,2}$ | -82.655323709 |
| $G_{11,3}$ | -702.04465645 | $G_{12,3}$ | -131.27287797 | $G_{24,3}$ | -320.46027824 |
| $G_{22,3}$ | -898.95397340 | $G_{13,3}$ | -165.59731645 | $G_{25,3}$ | 31.333170348 |
| $G_{33,3}$ | -523.23234047 | $G_{14,3}$ | -160.23013912 | $G_{34,3}$ | -481.76334899 |
| $G_{44,3}$ | 3369.0067211 | $G_{15,3}$ | 15.666585174 | $G_{35,3}$ | -33.288093328 |
| $G_{55,3}$ | 12.187368640 | $G_{23,3}$ | -331.19463290 | $G_{45,3}$ | -58.146763294 |

Table 5.2: Numerical results of the components of the first derivative of the Green's function $G_{ij,k}(\times 10^{-7})$ at the point $(1, 2, 3)$m.

To overcome this difficulty, some special numerical techniques can be used to evaluate the Green's function and its derivatives by the present novel formulae when the Stroh eigenvalues are identical or very close for the practical interest. One of the numerical techniques is the small perturbation method in which some material constants are modified slightly, i.e., $\Sigma \rightarrow \Sigma(1 + \epsilon)$, where $\Sigma$ is a material constant, and $\epsilon$ is a small perturbation parameter. In the next numerical example, the stability of the formulae with the perturbation method is investigated by the numerical results at field points. The perturbation parameter $\epsilon$ is chosen as $10^{-5}$, the modified material constants are $c_{22}$, $c_{55}$, $\kappa_{22}$ and $\mu_{22}$, and the evaluation points are defined by $(\cos\theta\cos\phi, \cos\theta\sin\phi, \sin\theta), \phi \in [0, 2\pi], \theta \in [0, \pi]$. The geometry of the field points is illustrated in Fig. 3.9. Figs. 5.1-5.10 are the components of the magnetoelectroelastic Green's function and its derivatives at the field points. The Green's function and its derivatives at the considered field points are smooth which indicates that the present novel formulae in conjunction with the perturbation method are stable and therefore suitable for the evaluation of the generally anisotropic magnetoelectroelastic Green's function and its derivatives, even for the degenerate and nearly degenerate cases. Although some material constants are modified slightly, the numerical results are practically identical to that of the original unperturbed magnetoelectroelastic material, since the modification of the constants is very small.

## 5.4 Concluding remarks

In this chapter, the 3D Green's function for generally anisotropic and linear magnetoelectroelastic materials are constructed from the solutions of the 3D Stroh eigenvalue problem in the linear magnetoelectroelasticity and the orthonormal relation of the eigenvectors. With the distinctness assumption on the Stroh eigenvalues, the derivatives of the eigenvectors are expressed as linear combinations of the Stroh eigenvectors, where the coefficients are obtained from the derivatives of the Stroh eigenvalue problem equation

| | | | | | |
|---|---|---|---|---|---|
| $G_{11,11}$ | -84.923711750 | $G_{12,11}$ | -143.43833544 | $G_{24,11}$ | -93.425960108 |
| $G_{22,11}$ | -246.67909237 | $G_{13,11}$ | -199.22866956 | $G_{25,11}$ | 1.2064201003 |
| $G_{33,11}$ | -5.2122015353 | $G_{14,11}$ | -138.48632835 | $G_{34,11}$ | 18.552929152 |
| $G_{44,11}$ | 1136.3796110 | $G_{15,11}$ | -4.6628544565 | $G_{35,11}$ | -32.565220675 |
| $G_{55,11}$ | 2.7269371665 | $G_{23,11}$ | -121.43040120 | $G_{45,11}$ | -31.699237588 |
| $G_{11,22}$ | -35.466694098 | $G_{12,22}$ | -75.130840388 | $G_{24,22}$ | -281.93049213 |
| $G_{22,22}$ | -201.56507722 | $G_{13,22}$ | -35.090598953 | $G_{25,22}$ | 10.091744908 |
| $G_{33,22}$ | -375.49548105 | $G_{14,22}$ | -49.191897767 | $G_{34,22}$ | -300.69031277 |
| $G_{44,22}$ | -123.96151242 | $G_{15,22}$ | 10.311936961 | $G_{35,22}$ | 8.8354100986 |
| $G_{55,22}$ | 4.0247055283 | $G_{23,22}$ | -347.20813583 | $G_{45,22}$ | -2.8139647883 |
| $G_{11,33}$ | 211.55693097 | $G_{12,33}$ | 84.382350809 | $G_{24,33}$ | 111.92891588 |
| $G_{22,33}$ | 338.13045718 | $G_{13,33}$ | 35.419945056 | $G_{25,33}$ | -25.056412010 |
| $G_{33,33}$ | 202.99260238 | $G_{14,33}$ | 55.964457942 | $G_{34,33}$ | 233.85887683 |
| $G_{44,33}$ | -818.83147104 | $G_{15,33}$ | -12.528206005 | $G_{35,33}$ | -16.749738620 |
| $G_{55,33}$ | -3.0993622005 | $G_{23,33}$ | 70.839890112 | $G_{45,33}$ | -3.3693045985 |
| $G_{11,12}$ | -2.6300699248 | $G_{12,12}$ | 18.837268767 | $G_{24,12}$ | -49.191897767 |
| $G_{22,12}$ | 65.677425129 | $G_{13,12}$ | -121.43040120 | $G_{25,12}$ | 10.311936961 |
| $G_{33,12}$ | -246.85551967 | $G_{14,12}$ | -93.425960108 | $G_{34,12}$ | -212.82882795 |
| $G_{44,12}$ | -840.22741562 | $G_{15,12}$ | 1.2064201003 | $G_{35,12}$ | 27.600420516 |
| $G_{55,12}$ | 0.86517890784 | $G_{23,12}$ | -35.090598953 | $G_{45,12}$ | 19.256848533 |
| $G_{11,13}$ | 48.865401622 | $G_{12,13}$ | -76.883986080 | $G_{24,13}$ | 125.11881741 |
| $G_{22,13}$ | 261.72161743 | $G_{13,13}$ | -87.490893614 | $G_{25,13}$ | -3.7660550027 |
| $G_{33,13}$ | 87.497374760 | $G_{14,13}$ | -97.670730413 | $G_{34,13}$ | 52.390013497 |
| $G_{44,13}$ | -856.30380581 | $G_{15,13}$ | 13.783557673 | $G_{35,13}$ | 23.365080503 |
| $G_{55,13}$ | -3.0153301358 | $G_{23,13}$ | 156.21284568 | $G_{45,13}$ | 25.280288077 |
| $G_{11,23}$ | 360.27655919 | $G_{12,23}$ | 43.141344798 | $G_{24,23}$ | 90.007495707 |
| $G_{22,23}$ | 260.89747892 | $G_{13,23}$ | 156.21284568 | $G_{25,23}$ | 8.1344751687 |
| $G_{33,23}$ | 174.99474952 | $G_{14,23}$ | 125.11881741 | $G_{34,23}$ | 104.78002699 |
| $G_{44,23}$ | -1712.6076116 | $G_{15,23}$ | -3.7660550027 | $G_{35,23}$ | 46.730161006 |
| $G_{55,23}$ | -6.0306602716 | $G_{23,23}$ | 146.82837490 | $G_{45,23}$ | 50.560576154 |

Table 5.3: Numerical results of the components of the second derivative of the Green's function $G_{ij,kl}(\times 10^{-7})$ at the point $(1,2,3)$m.

| | $G_{IJ}$ | $G_{IJ,k}$ | $G_{IJ,kl}$ |
|---|---|---|---|
| CPU Time $(10^{-4}$s) | 1.40805340 | 2.18008423 | 7.67242527 |

Table 5.4: The CPU time for the calculation of the Green's function and its derivatives by the novel explicit expressions
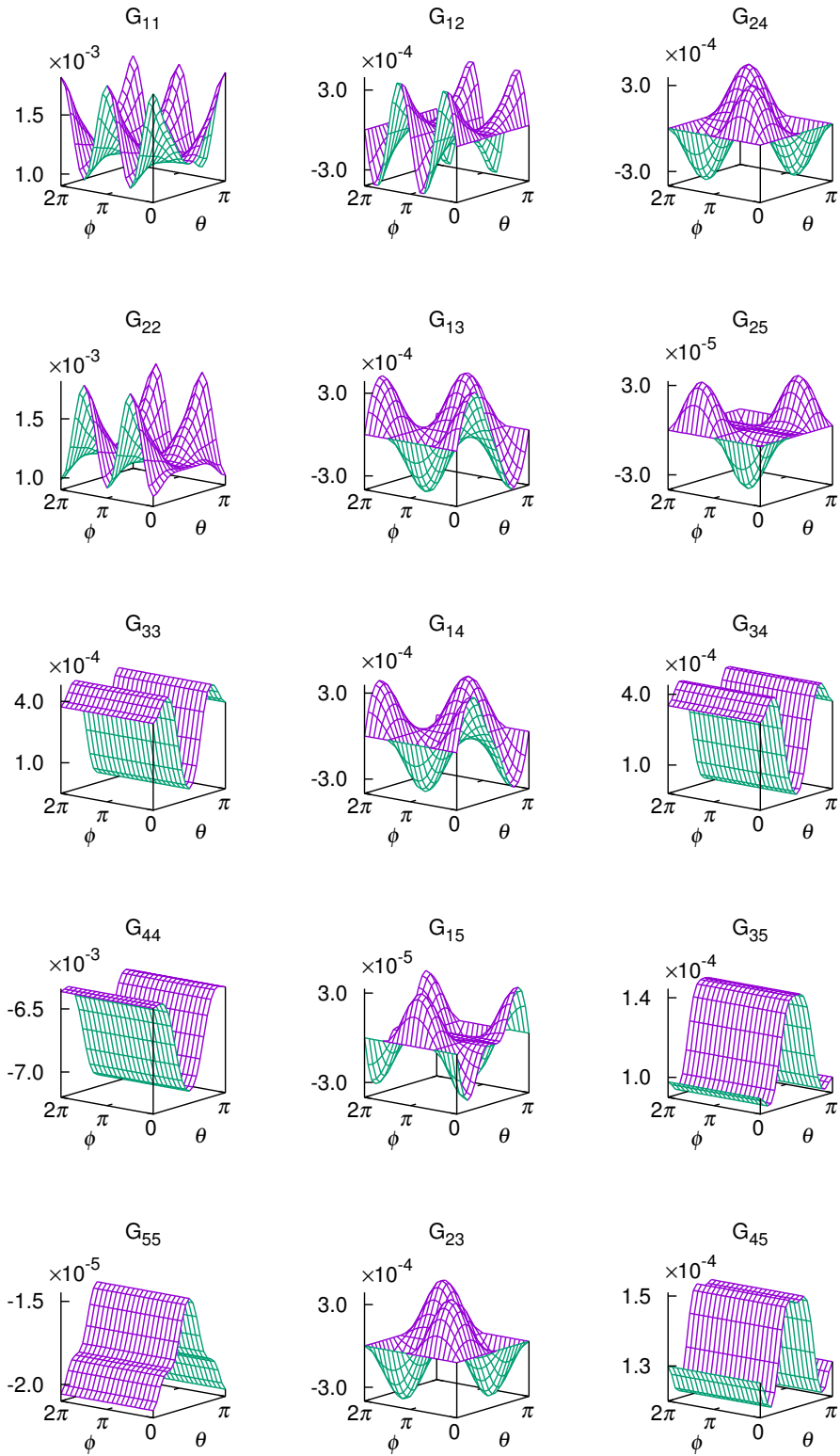
Figure 5.1: Variation of the Green's function $G_{IJ}$ on upper half unit sphere with the source point at the origin.

Figure 5.2: Variation of the first derivative of the Green's function $G_{IJ,1}$ on upper half unit sphere with the source point at the origin.
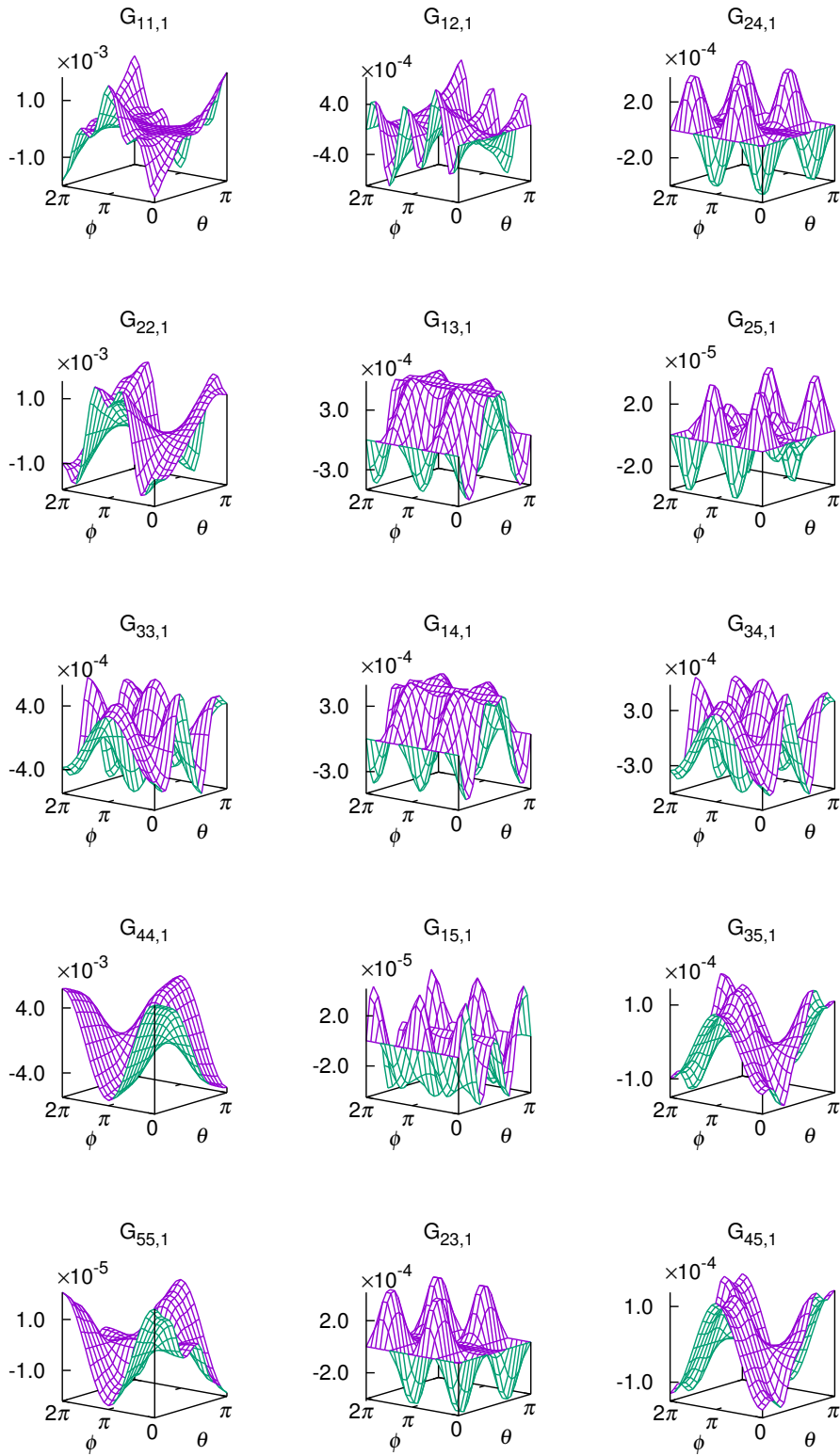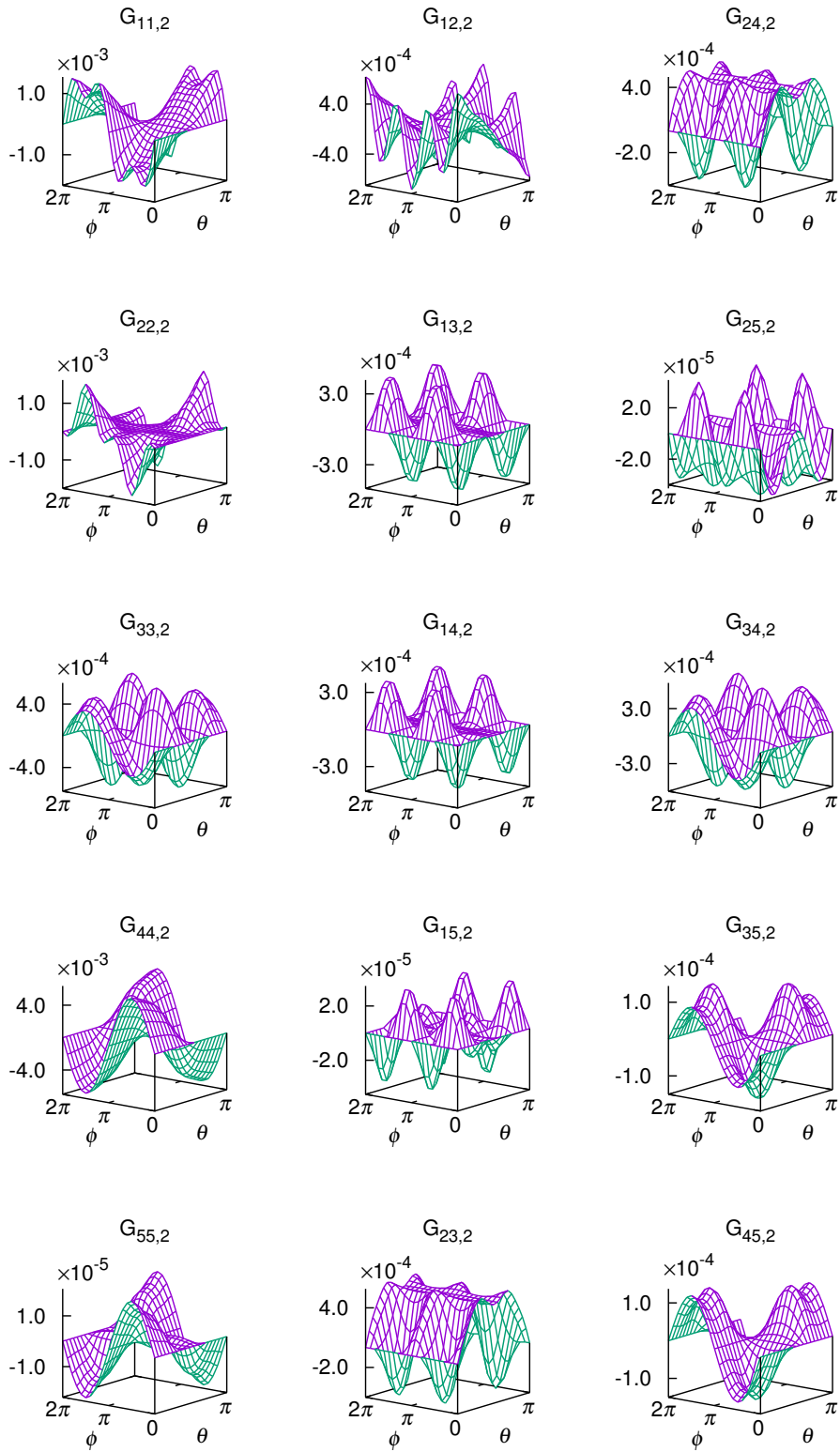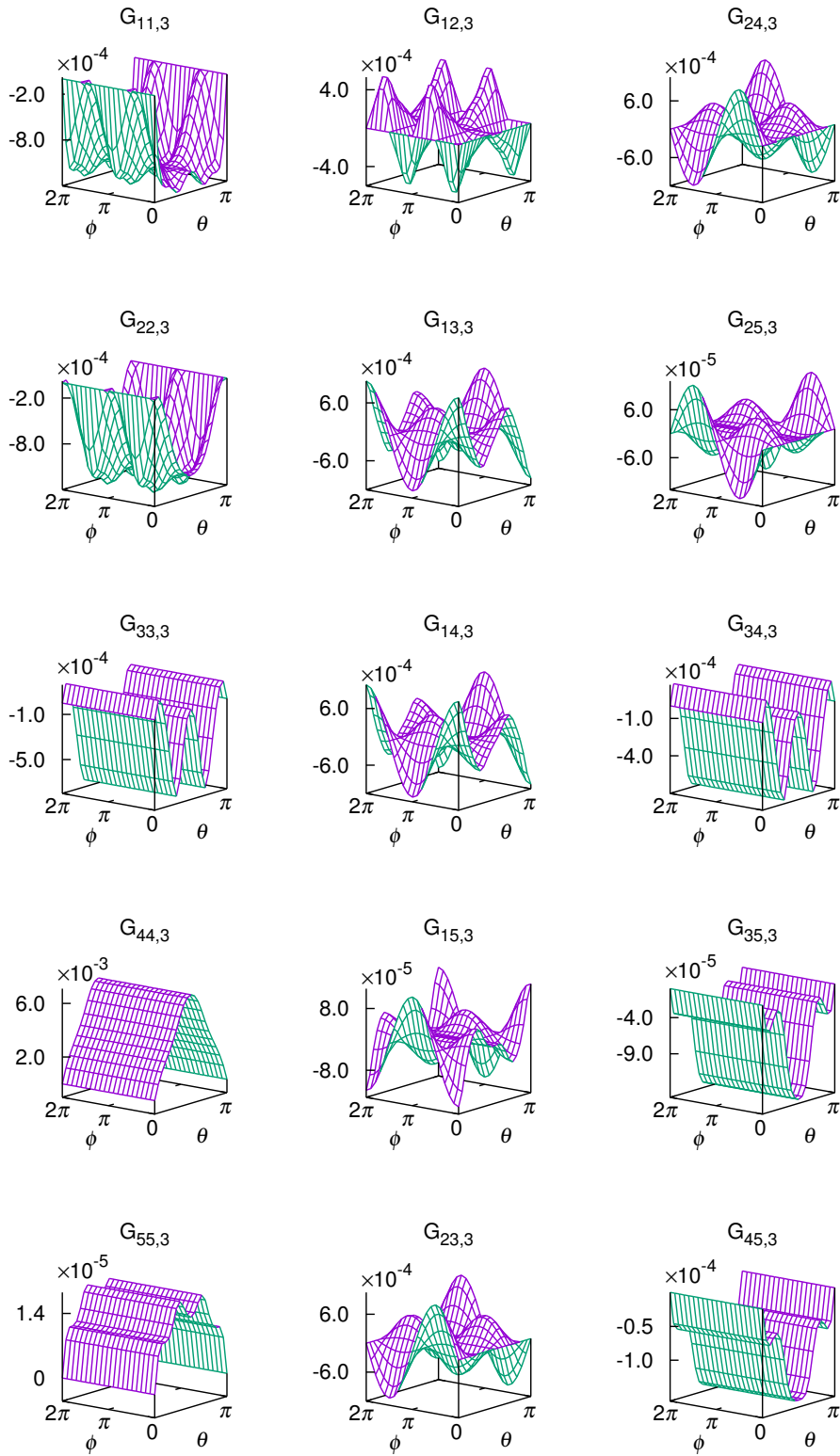
70

Figure 5.3: Variation of the first derivative of the Green's function $G_{IJ,2}$ on upper half unit sphere with the source point at the origin.

Figure 5.4: Variation of the first derivative of the Green's function $G_{IJ,3}$ on upper half unit sphere with the source point at the origin.
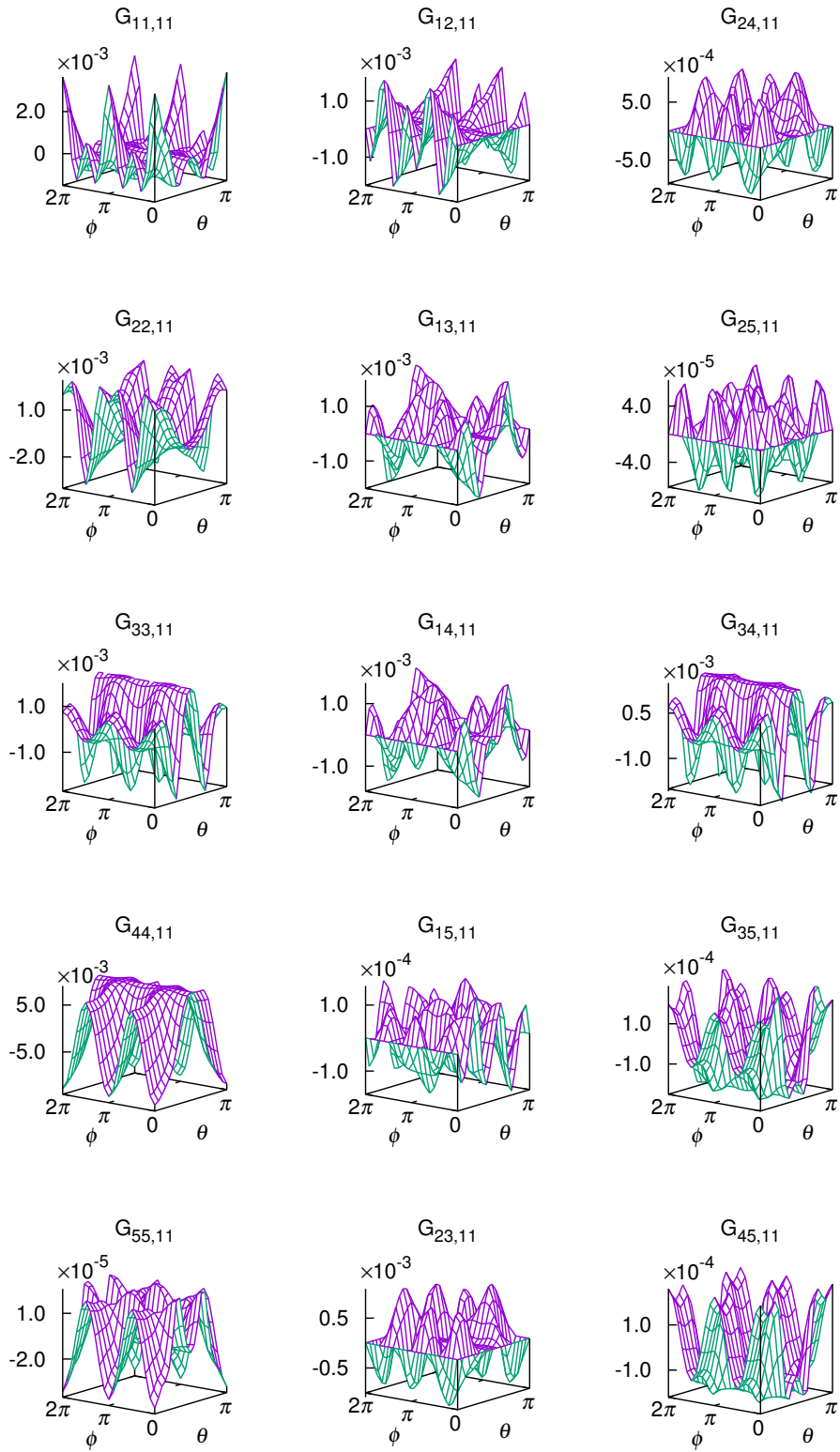
Figure 5.5: Variation of the second derivative of the Green's function $G_{IJ,11}$ on upper half unit sphere with the source point at the origin.
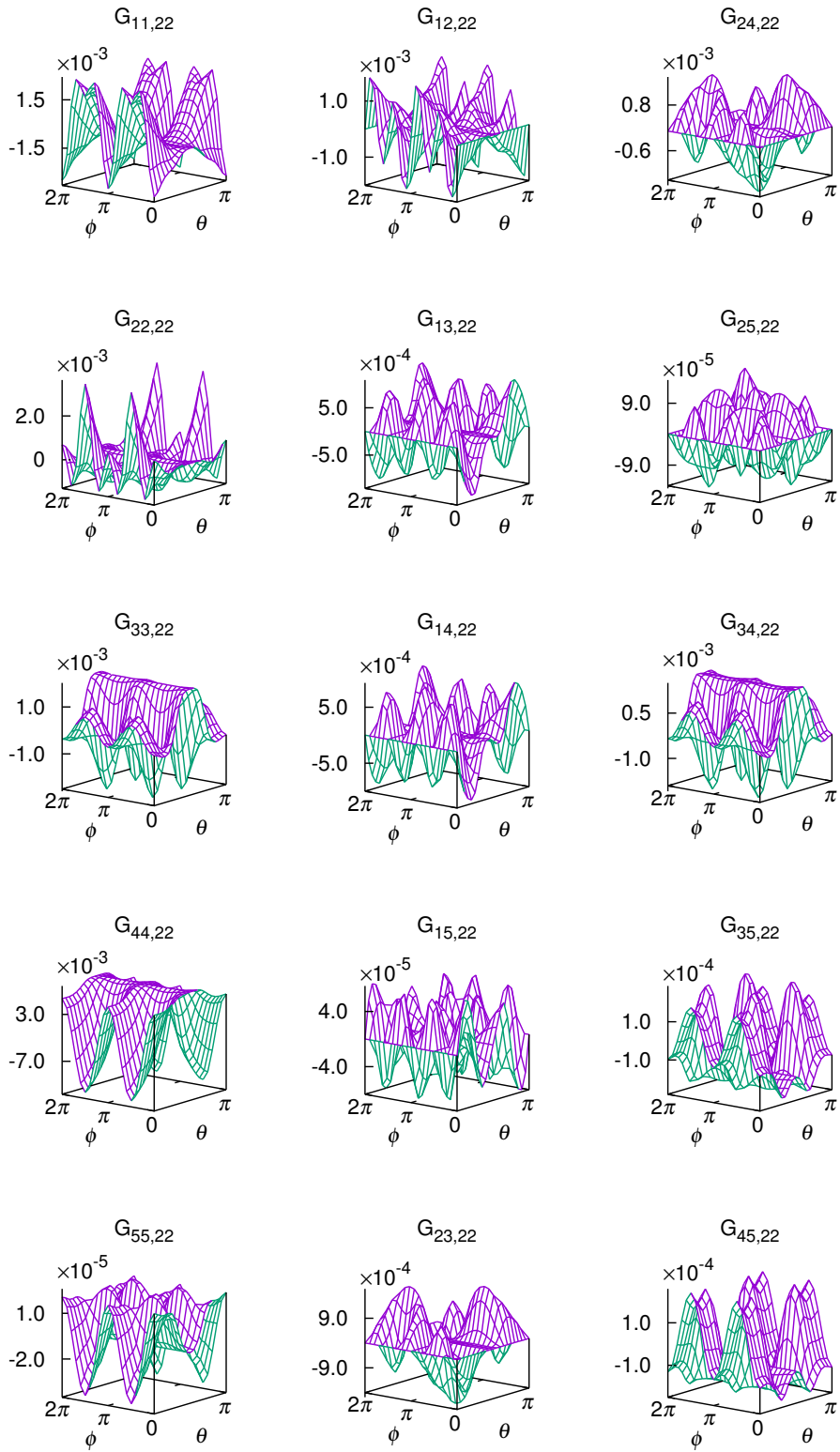
Figure 5.6: Variation of the second derivative of the Green's function $G_{IJ,22}$ on upper half unit sphere with the source point at the origin.
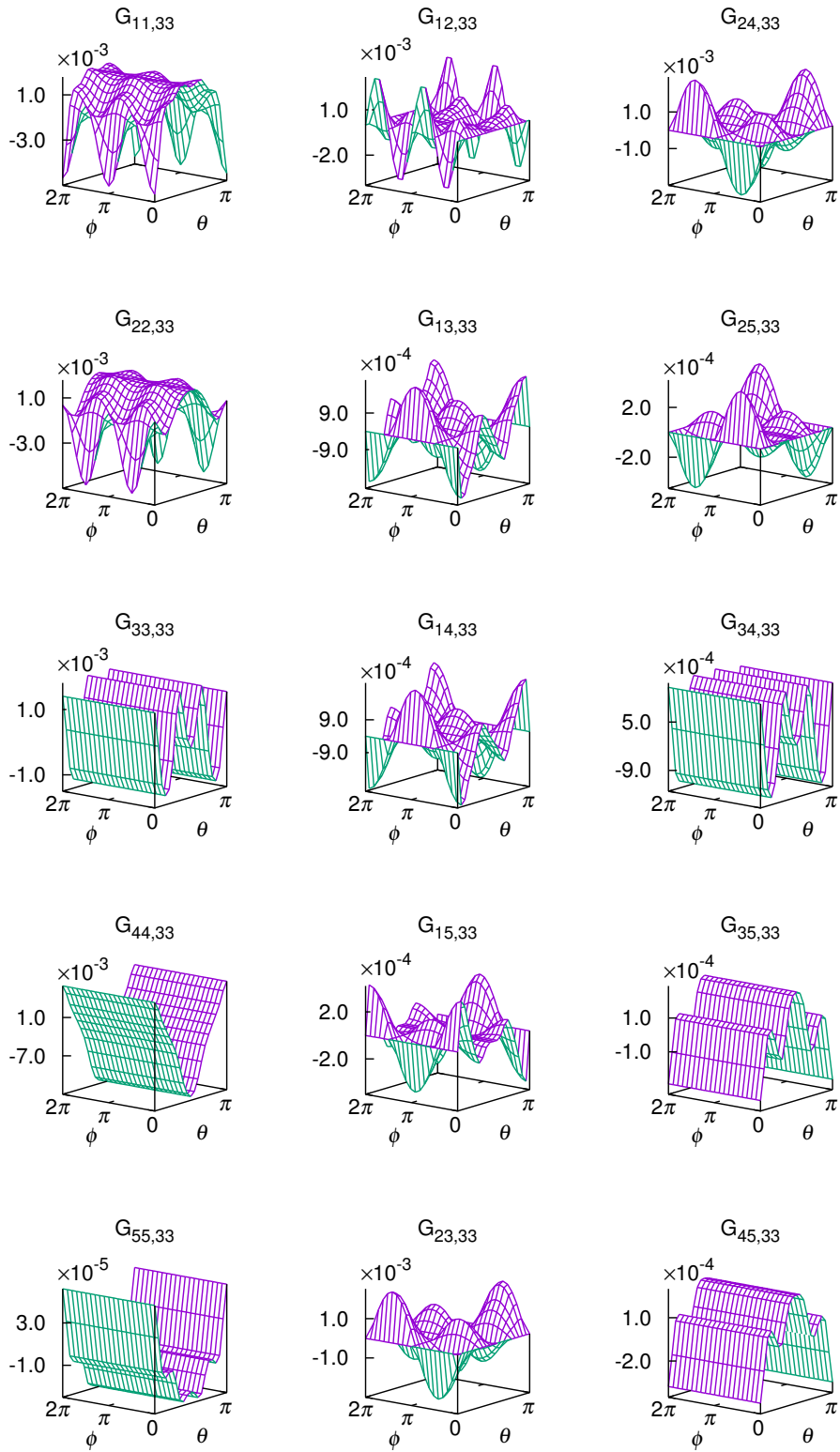
Figure 5.7: Variation of the second derivative of the Green's function $G_{IJ,33}$ on upper half unit sphere with the source point at the origin.

Figure 5.8: Variation of the second derivative of the Green's function $G_{IJ,12}$ on upper half unit sphere with the source point at the origin.
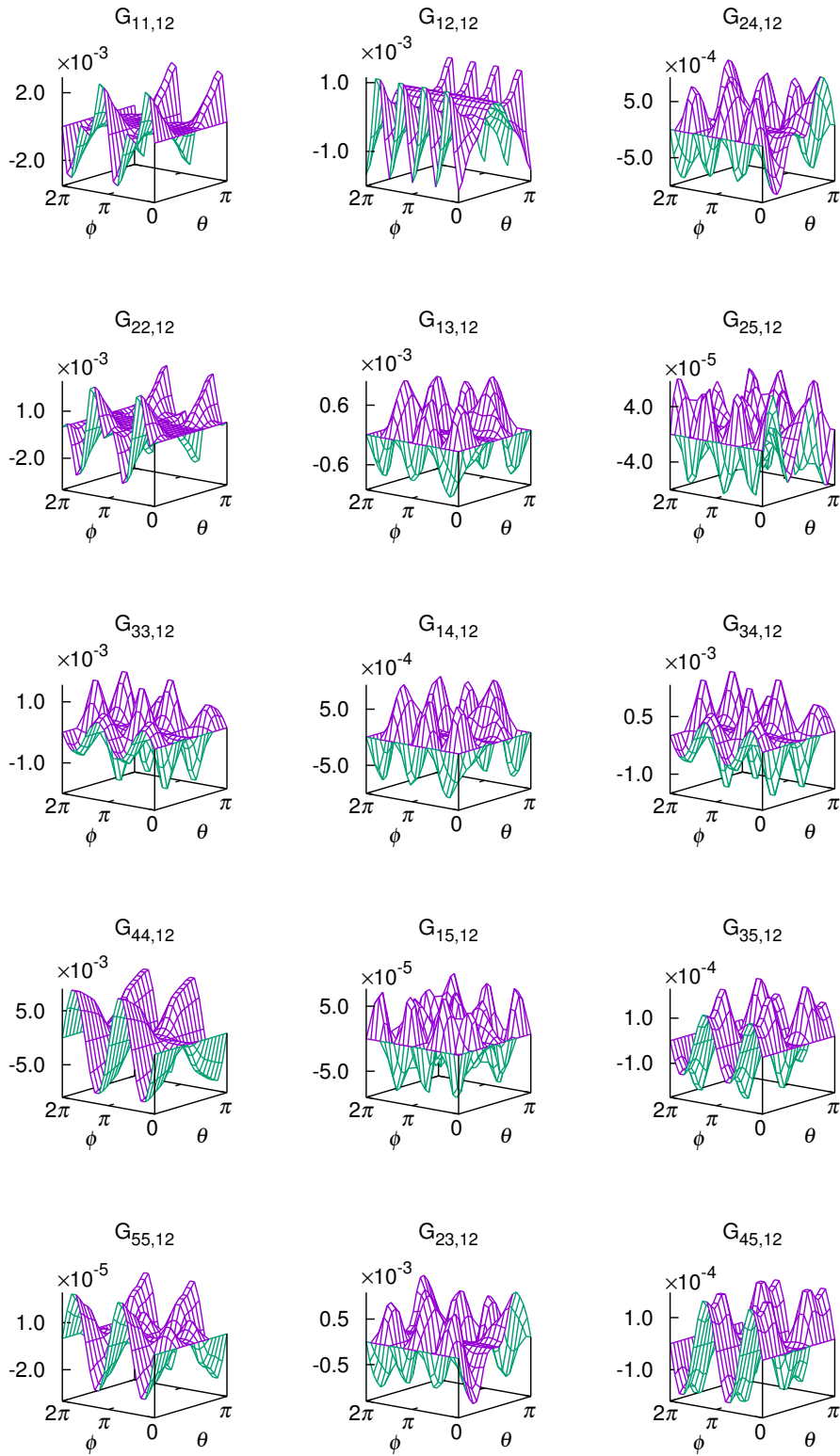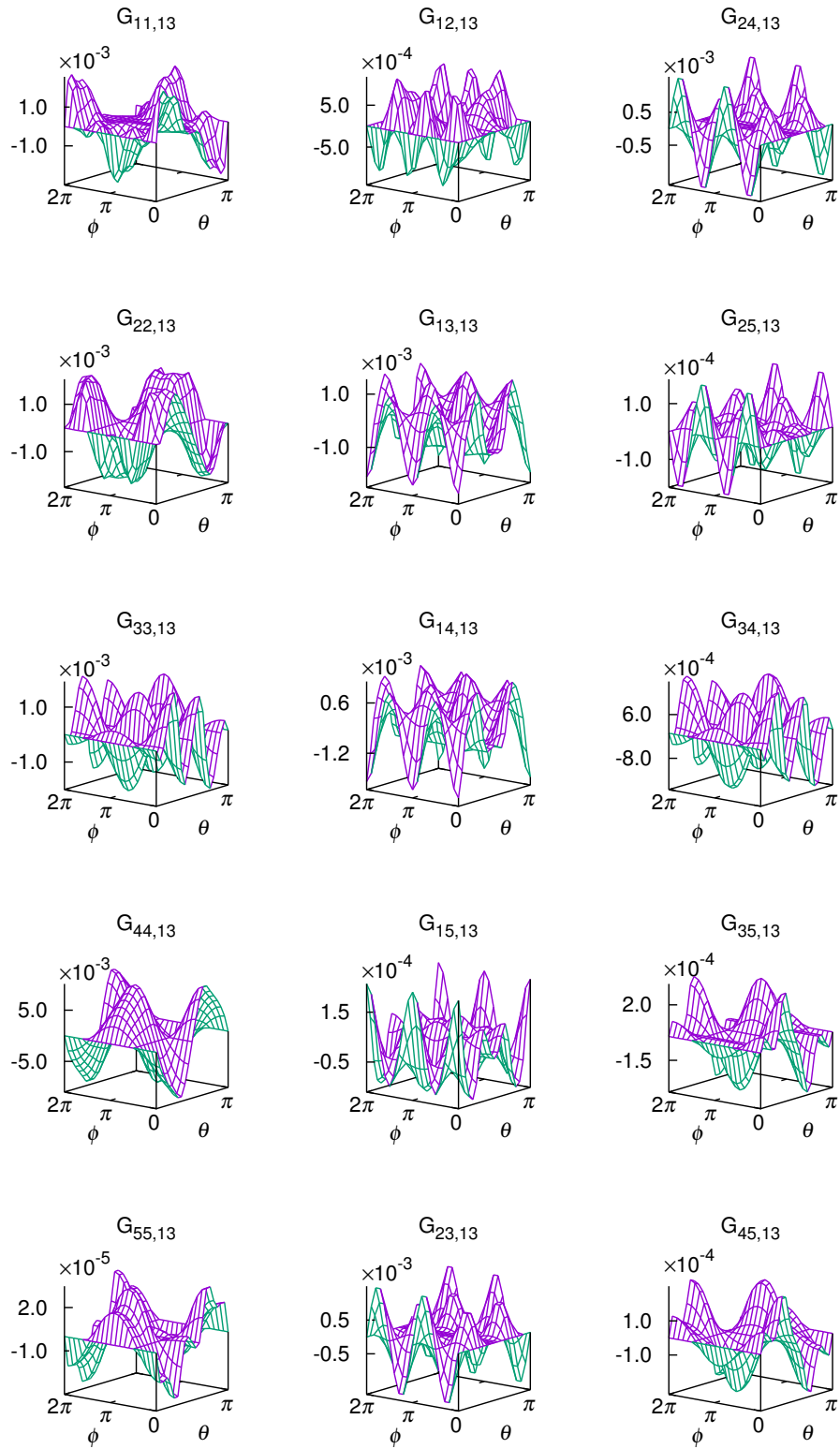
76

Figure 5.9: Variation of the second derivative of the Green's function $G_{IJ,13}$ on upper half unit sphere with the source point at the origin.
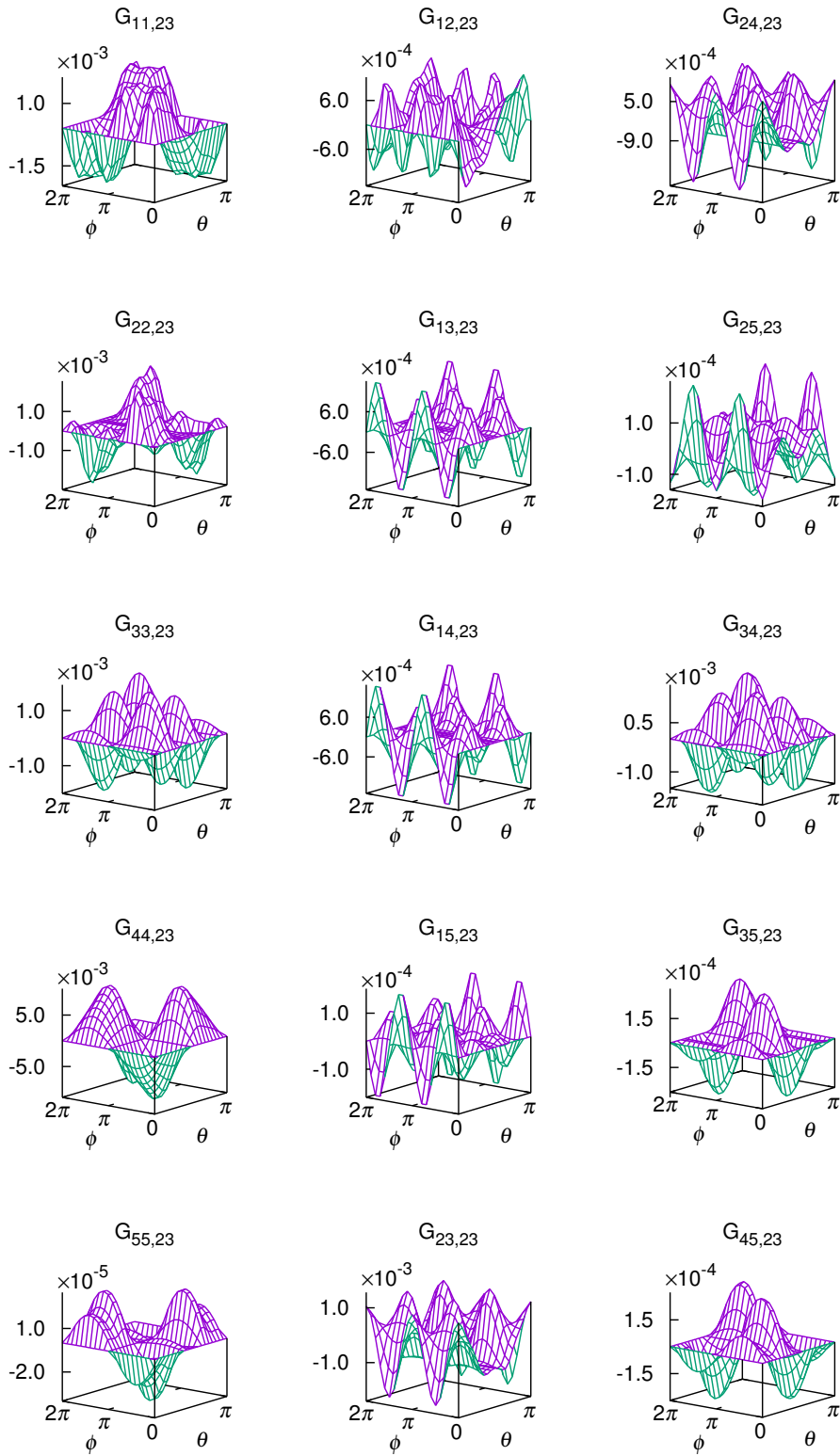
Figure 5.10: Variation of the second derivative of the Green's function $G_{IJ,23}$ on upper half unit sphere with the source point at the origin.

and the orthonormal relation of the eigenvectors. Once the derivatives of the Stroh eigenvectors are determined, the derivatives of the Green's function can be constructed from them. The accuracy of the present novel explicit expressions of the Green's function and its derivatives for generally anisotropic magnetoelectroelastic materials is verified by the analytical solutions for transversely isotropic magnetoelectroelastic materials. The CPU time for the calculation is provided to show the efficiency of the present novel expressions. For evaluation of the Green's function and its derivatives in degenerate (identical eigenvalues) and nearly degenerate (very close eigenvalues) cases, a small perturbation on the material constants is suggested to avoid the presence of the identical or very close Stroh eigenvalues.

# Chapter 6

# Applications of the Green's function and its derivatives in the BEM

## 6.1 Preliminary remarks

The boundary element method (BEM) is a general and efficient numerical method for many practical problems. It is sometimes called the boundary integral equation (BIE) method, because the BEM is based on the discretization of the BIE. Some of the advantages of the BEM are (1) the reduction of the dimension of problems to be solved, from three dimension to two dimension, or from two dimension to one dimension, (2) the accuracy of the BEM due to the nature of integrals used in the formulation, and (3) the easy and accurate modeling for problems in infinite domain without additional conditions at infinity due to the properties of the kernel function or the Green's function.

The BIE method and its numerical evaluation were first formulated to solve the potential problems by Jaswon (1963), Jaswon and Ponter (1963) and Symm (1963). Later Rizzo (1967) extended this method to solve the elastic problems. Following these early works, extensive research efforts had been made to use the BIE method as well as the BEM to solve many problems in applied mechanics and engineering. Among the subsequent contributions, Cruse (1968, 1974), Cruse and Rizzo (1968), Lachat and Watson (1976), Rizzo and Shippy (1977), Wilson and Cruse (1978), Sladek and Sladek (1982), Tanaka et al. (1994), Aliabadi (1997) and Tan et al. (2013) should be mentioned. A comprehensive review with recent advances and some future directions of the BEM was given by Liu et al. (2011). A recent overview of the BEM was given by Mukherjee and Liu (2013). For textbooks on the BEM, readers are referred to Aliabadi (2002) and Gaul et al. (2003).

In this chapter, the Green's function and its derivatives for anisotropic linear elastic materials are implemented into a BEM, which serves as a typical application of the Green's function and its derivatives. Some representative numerical examples are presented to demonstrate the correctness and the accuracy of the developed BEM.

## 6.2 Description of the BEM for anisotropic linear elasticity

For a general problem, the BIE (2.58) is usually solved numerically. The discretization of the boundary $S$ with so-called boundary elements $S^{(e)}$, $S = \sum_{e=1}^{E} S^{(e)}$ where $E$ is the number of elements, is applied to the BIE (2.58), and then point collocation on the nodes of the discretization leads a system of equations for the unknown boundary values. The BIE (2.58) becomes

$$c_{ij}(\boldsymbol{x})u_j(\boldsymbol{x}) = \sum_{n=1}^{E} \int_{S^{(e)}} u_{ij}^G(\boldsymbol{x},\boldsymbol{y})t_j^{(e)}(\boldsymbol{y})dS^{(e)} - \sum_{n=1}^{E} \int_{S^{(e)}} t_{ij}^G(\boldsymbol{x},\boldsymbol{y})u_j^{(e)}(\boldsymbol{y})dS^{(e)}. \qquad (6.1)$$

To simplify the evaluation of the integrals in the BIE (6.1), each boundary element is transformed to a local reference element in the local coordinates $s_1$ and $s_2$, as shown in Fig. 6.1. The field variables, i.e., point coordinates $\boldsymbol{y}$, the displacements $\boldsymbol{u}$ and the
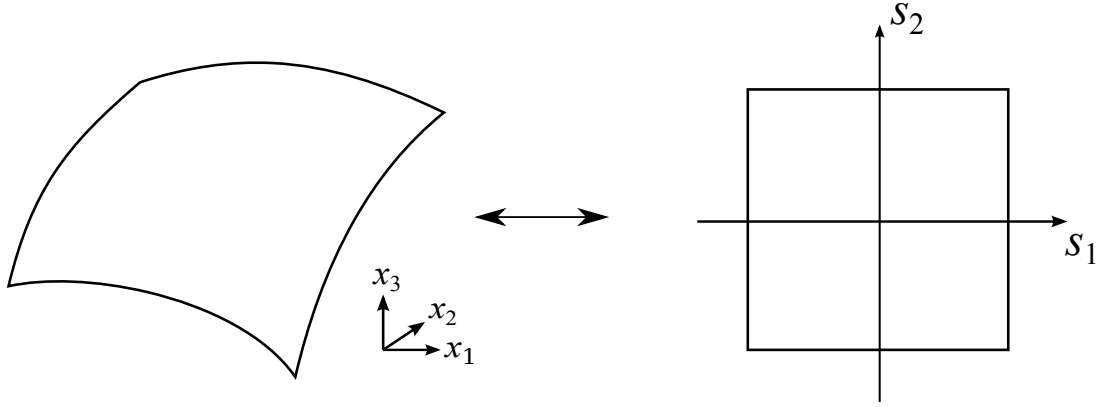


Figure 6.1: Transformation of a boundary element to a local reference element

tractions $\boldsymbol{t}$, inside the boundary element are approximated by the interpolation method. In virtue of the isoparametric concept, the different field variables are approximated by the same interpolation technique

$$\boldsymbol{y}^{(e)}(s_1, s_2) = \sum_{n=1}^{N^{(e)}} \Phi_n(s_1, s_2)\dot{\boldsymbol{y}}_n^{(e)}, \qquad (6.2a)$$

$$\boldsymbol{u}^{(e)}(s_1, s_2) = \sum_{n=1}^{N^{(e)}} \Phi_n(s_1, s_2)\dot{\boldsymbol{u}}_n^{(e)}, \quad \boldsymbol{t}^{(e)}(s_1, s_2) = \sum_{n=1}^{N^{(e)}} \Phi_n(s_1, s_2)\dot{\boldsymbol{t}}_n^{(e)}, \qquad (6.2b)$$

where the matrix notation is used, $N^{(e)}$ is the number of nodes in an element, $\Phi_n(s_1, s_2)$ is the $n$-th shape function, and $\dot{\boldsymbol{y}}_n^{(e)}$, $\dot{\boldsymbol{u}}_n^{(e)}$ and $\dot{\boldsymbol{t}}_n^{(e)}$ are the nodal coordinates, displacements and tractions at the $n$-th node of element $(e)$. Now locating the source point at the $l$-th node of the discretization and substituting Eq. (6.2) into Eq. (6.1), we obtained the BIE in the matrix form

$$\mathbf{c}(\boldsymbol{x}^l)\boldsymbol{u}(\boldsymbol{x}^l) = \sum_{n=1}^{E} \sum_{n=1}^{N^{(e)}} \left( \int_{S^{(e)}} \mathbf{u}^G(\boldsymbol{x}^l, \boldsymbol{y})\Phi_n(\boldsymbol{y})dS^{(e)} \right) \dot{\boldsymbol{t}}_n^{(e)}$$

$$-\sum_{n=1}^{E}\sum_{n=1}^{N^{(e)}}\left(\int_{S^{(e)}}\mathbf{t}^{G}(\boldsymbol{x}^{l},\boldsymbol{y})\Phi_{n}(\boldsymbol{y})dS^{(e)}\right)\dot{\boldsymbol{u}}_{n}^{(e)}. \tag{6.3}$$

The integrands in the above equation are products of the fundamental solutions with the shape functions. Evaluation of the Eq. (6.3) over all $N$ global nodes will set up a system of equations for the unknown boundary values.

Assuming that there are only 3 unknowns at any node (Cruse, 1974), the system contains $3N$ linearly independent equations for the $3N$ unknown boundary variables. By combining the unknowns in a vector $\boldsymbol{x}$, the system yields

$$\mathbf{A}\boldsymbol{x} = \boldsymbol{f}, \tag{6.4}$$

where $\boldsymbol{f}$ contains the products of the coefficients from Eq. (6.3) and the known boundary data. The resulting system can be solved by standard methods, for example, the DGESV subroutine in the library LAPACK (Anderson et al., 1999).

## 6.3    Numerical examples

In this section, the conventional BEM is coded by FORTRAN with the Green's function and its derivatives calculated by the unified explicit expression method (UEEM). The boundary elements are 9-node quadrilaterals. On the numerical calculation of the integrals, the rigid body movement method is applied to calculate the strongly singular integrals; the Lachat-Watson Transformation (Lachat and Watson, 1976) is applied to calculate the weakly singular integrals; and the Gaussian quadrature with $8 \times 8$ nodes is applied to calculate the regular double integrals. The algorithm proposed by Cruse (1974) is used to deal with the discontinuous tractions. And the linear system is solved by the DGESV subroutine in the library LAPACK (Anderson et al., 1999).

### 6.3.1    Cube under tension

This is a test of the BEM program. A cube of length $2a$ is prescribed with uniaxial tension $\sigma^0$. The Fig. 6.2 is one-eighth of the cube. Due to the symmetry of the problem, the symmetric boundary conditions are imposed on the planes $x_1 = 0$, $x_2 = 0$ and $x_3 = 0$ where the normal displacements and the inplane tractions vanish. The boundary is discretized by 6 elements, that is one element per face. The number of nodes is totally 26.

For the demonstration of the applicability of the BEM program for the general anisotropy, the transversely isotropic material Mg is taken for the numerical example. Letting the $x_3$ coordinate axis of the Cartesian coordinate system along with the symmetry axis of the transversely isotropic material, the material constants in Voigt notation are listed in Eqs. (3.5.1). Table 6.1 is the numerical results of the BEM program for the displacements of some points when $a = 1$ m and $\sigma^0 = 1$ GPa. The underlined digits in the table agree exactly with the analytical results. These numerical results show the high accuracy of the BEM program and the calculation of the Green's function and its derivatives.

To give mathematically generally anisotropic materials, the Cartesian coordinates are clockwise rotated about the $x_1$-axis by an angle $\alpha$, about the $x_2$-axis by $\beta$, and about the $x_3$-axis by $\gamma$. The rotations are illustrated in Fig. 6.3. The transformation matrix from
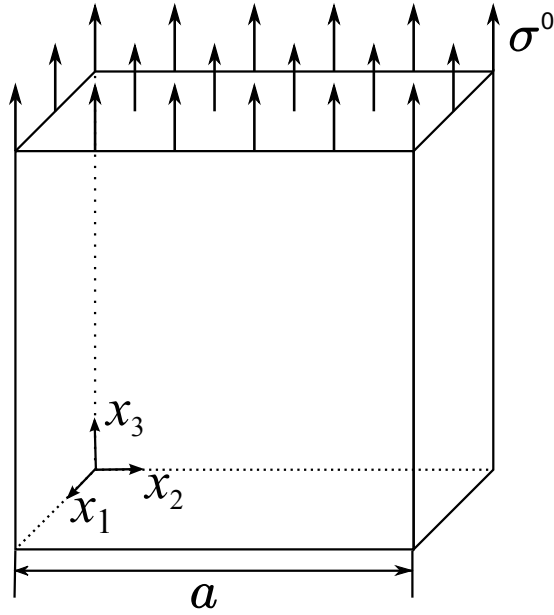
Figure 6.2: One-eighth of a cube under tension

| Points | $u_1$ $(10^{-3}\text{m})$ | $u_2$ $(10^{-3}\text{m})$ | $u_3$ $(10^{-3}\text{m})$ |
|--------|---------------------------|---------------------------|---------------------------|
| $(1.0, 1.0, 1.0)$ | -4.9790686007 | -4.9790686007 | 19.7097507377 |
| $(0.5, 0.5, 1.0)$ | -2.4895346247 | -2.4895346247 | 19.7097333807 |
| $(1.0, 0.5, 0.5)$ | -4.9790717447 | -2.4895319447 | 9.85487006790 |
| $(0.5, 1.0, 0.5)$ | -2.4895319447 | -4.9790717447 | 9.85487006790 |
| $(1.0, 0.5, 1.0)$ | -4.9790705923 | -2.4895335628 | 19.7097415567 |
| $(0.5, 1.0, 1.0)$ | -2.4895335628 | -4.9790705923 | 19.7097415567 |
| $(1.0, 1.0, 0.5)$ | -4.9790558988 | -4.9790558988 | 9.85487214820 |

Table 6.1: Displacements of the cube under tension with transversely isotropic material Mg
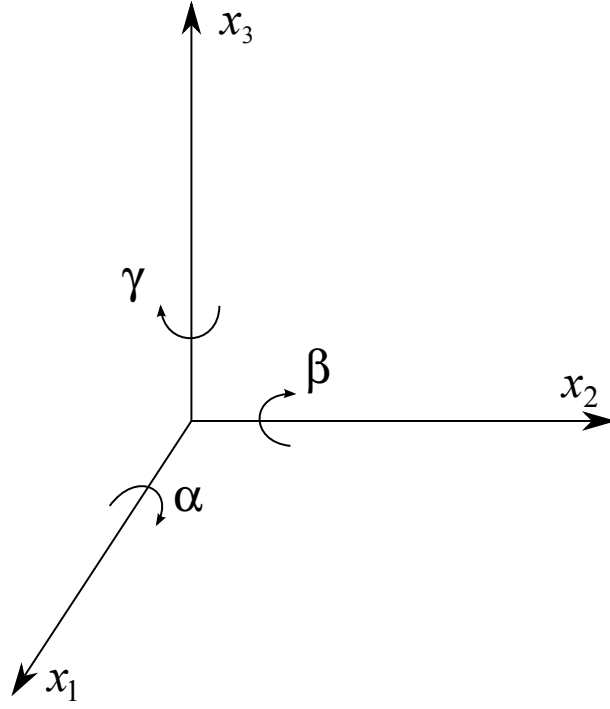
Figure 6.3: Rotations of the coordinates.

the origin system to the new system is

$$\boldsymbol{\Omega} = \begin{bmatrix} \cos\beta\cos\gamma & \sin\alpha\sin\beta\cos\gamma - \cos\alpha\sin\gamma & \cos\alpha\sin\beta\cos\gamma + \sin\alpha\sin\gamma \\ \cos\beta\sin\gamma & \cos\alpha\cos\gamma + \sinh\alpha\sin\beta\sin\gamma & -\sin\alpha\cos\gamma + \cos\alpha\sin\beta\sin\gamma \\ -\sin\beta & \sin\alpha\cos\beta & \cos\alpha\cos\beta \end{bmatrix}. \quad (6.5)$$

Then the elasticity tensor in the new Cartesian coordinate system is

$$c^*_{ijkl} = \Omega_{im}\Omega_{jn}\Omega_{ks}\Omega_{lt}c_{mnst}. \quad (6.6)$$

When the angles, $\alpha$, $\beta$ and $\gamma$, are arbitrary, the material constant matrix in Voigt notation in the new coordinate system is generally anisotropic. However, due to the symmetry required by the analysis, we choose $\alpha = \pi/2$, $\beta = 0$ and $\gamma = 0$. In this case, the material constant matrix is given by

$$\begin{bmatrix} 59.7 & 21.7 & 26.2 & 0 & 0 & 0 \\ & 61.7 & 21.7 & 0 & 0 & 0 \\ & & 59.7 & 0 & 0 & 0 \\ & & & 16.4 & 0 & 0 \\ & \text{Sym.} & & & 16.75 & 0 \\ & & & & & 16.4 \end{bmatrix} \text{(GPa)}. \quad (6.7)$$

Table 6.2 are the numerical results of the BEM program with the rotated material Mg, compared with the results of the software COMSOL. The results are accurate, although the number of the elements is small.

## 6.3.2   Cube with a spheroidal cavity under tension

In this example, we consider a cube of length $2a$ under tension $\sigma^0$ with a small spheroid cavity in the center. Fig. 6.4 (a) is the cube and Fig. 6.4 (b) is one-eighth of it, which

| Points | $u_1|u_1^c$ ($10^{-3}$m) | $u_2|u_2^c$ ($10^{-3}$m) | $u_3|u_3^c$ ($10^{-3}$m) |
|---|---|---|---|
| $(1.0, 1.0, 1.0)$ | -7.8469021\|-7.8468439 | -4.9790358\|-4.9790626 | 22.003965\|22.003902 |
| $(0.5, 0.5, 1.0)$ | -3.9234047\|-3.9234219 | -2.4895393\|-2.4895313 | 22.003853\|22.003902 |
| $(1.0, 0.5, 0.5)$ | -7.8466707\|-7.8468439 | -2.4895052\|-2.4895313 | 11.001962\|11.001951 |
| $(0.5, 1.0, 0.5)$ | -3.9234025\|-3.9234219 | -4.9790578\|-4.9790626 | 11.001947\|11.001951 |
| $(1.0, 0.5, 1.0)$ | -7.8468756\|-7.8468439 | -2.4895172\|-2.4895313 | 22.003957\|22.003902 |
| $(0.5, 1.0, 1.0)$ | -3.9234330\|-3.9234219 | -4.9790884\|-4.9790626 | 22.003913\|22.003902 |
| $(1.0, 1.0, 0.5)$ | -7.8468622\|-7.8468439 | -4.9789869\|-4.9790626 | 11.001973\|11.001951 |

Table 6.2: Displacements of the cube under tension with rotated transversely isotropic material Mg; $u_i$ are the present results; $u_i^c$ are evaluated by COMSOL Multiphysics with 1000 elements.

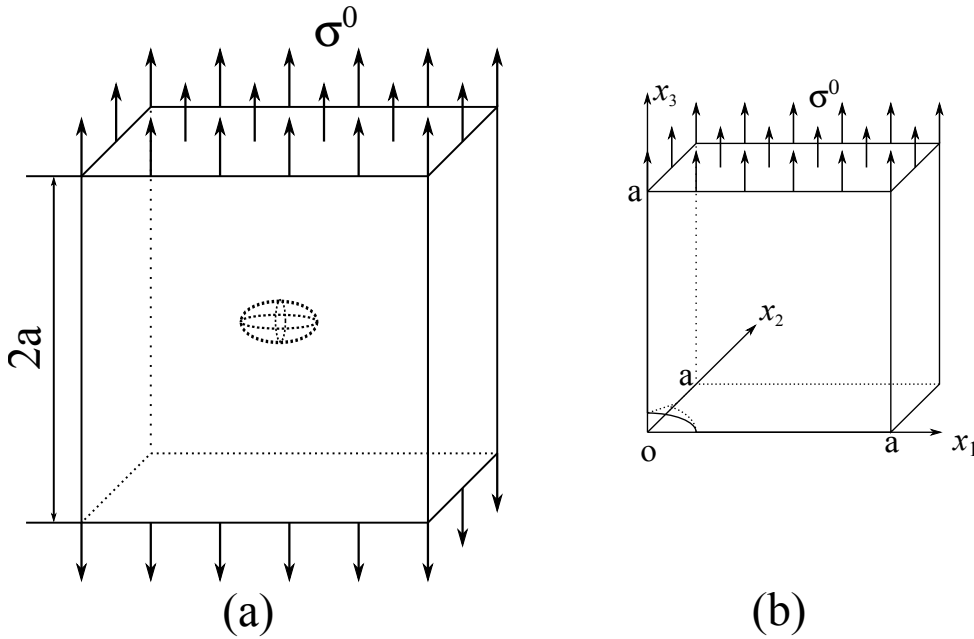is used for the numerical computation. The axes of the Cartesian coordinate system are



Figure 6.4: Model of the cube with a cavity under tension.

along with the axes of the spheroid. We set $a = 10$ m and $\sigma^0 = 1$ GPa. The long axis of the spheroid is 2 m and the short axis 1 m. Thus the equation of the spheroid is

$$(x_1^2 + x_2^2)/4 + x_3^2 = 0. \tag{6.8}$$

The rotated Mg is used for the numerical computation. The material constant matrix is given by Eq. (6.7).

The boundary is discretized by 9-node quadrilaterals. Fig. 6.5 (a) is an illustration of the discretization of the boundary. There are totally 131 elements and 526 nodes. Fig. 6.5 (b) is the mesh of the one-eighth spheroid, the edges of which can be easily described by introducing $\theta$ and $\phi$

$$x_1 = 2\sin\theta\cos\phi, \quad x_2 = 2\sin\theta\sin\phi, \quad x_3 = \cos\theta. \tag{6.9}$$

The edges are respectively represented by $\theta = \pi/2$, $\phi = 0$ and $\phi = \pi/2$.
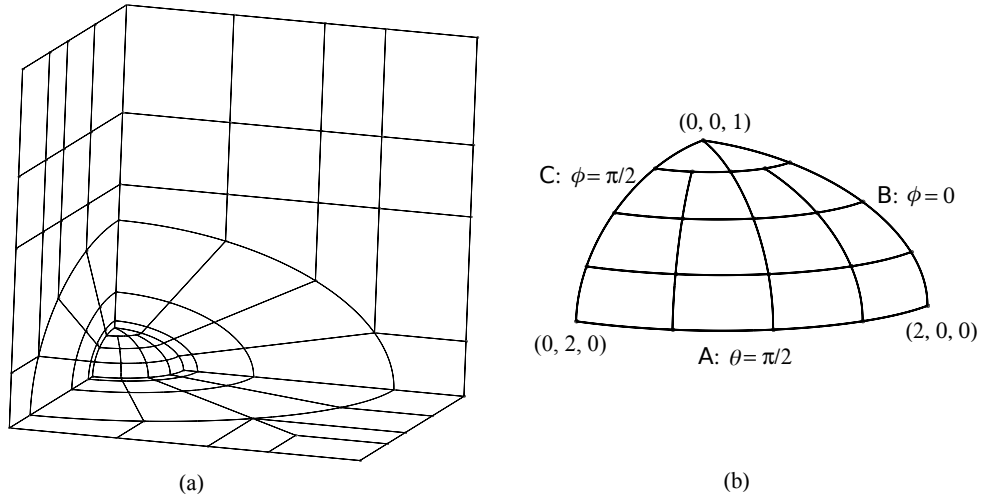
(a)           (b)

Figure 6.5: The mesh of the cube with a spheroidal cavity

As a case study, we investigate the displacements on the edges of the one-eighth spheroid. The numerical results of the present BEM program are compared with the results obtained by the finite element software COMSOL. Figs. 6.6-6.8 show that the displacements on the edges of the one-eighth spheroid obtained with the present BEM program agree well with those obtained by the software COMSOL.
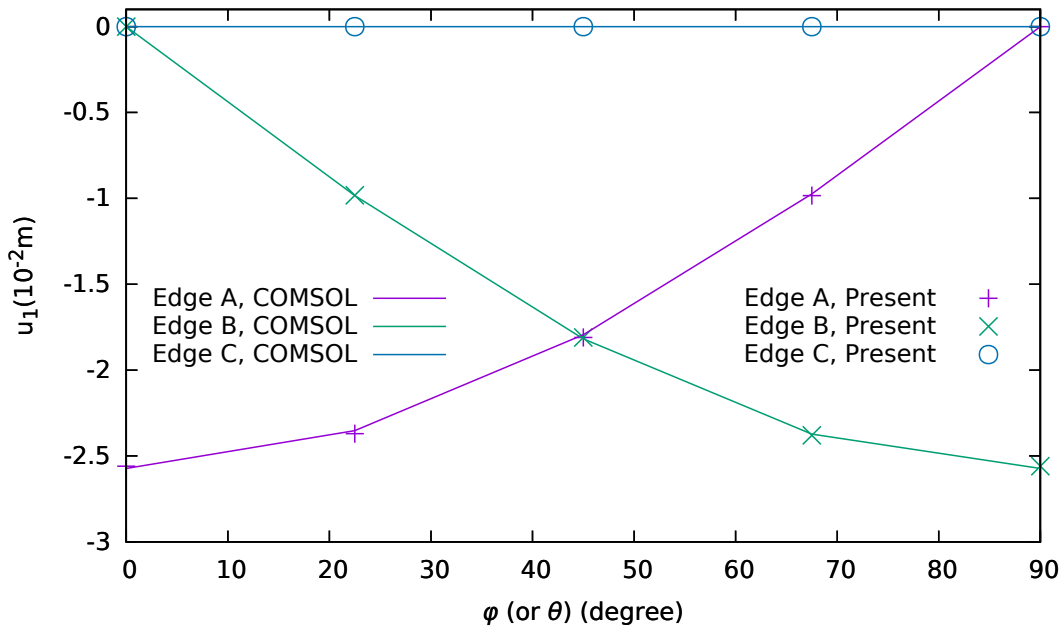


Figure 6.6: The displacement $u_1$ on the edges of the one-eighth spheroid.

## 6.4   Concluding remarks

In this chapter, a boundary element method (BEM) is developed in FORTRAN, in which the Green's function and its derivatives for anisotropic elastic solids are evaluated by the
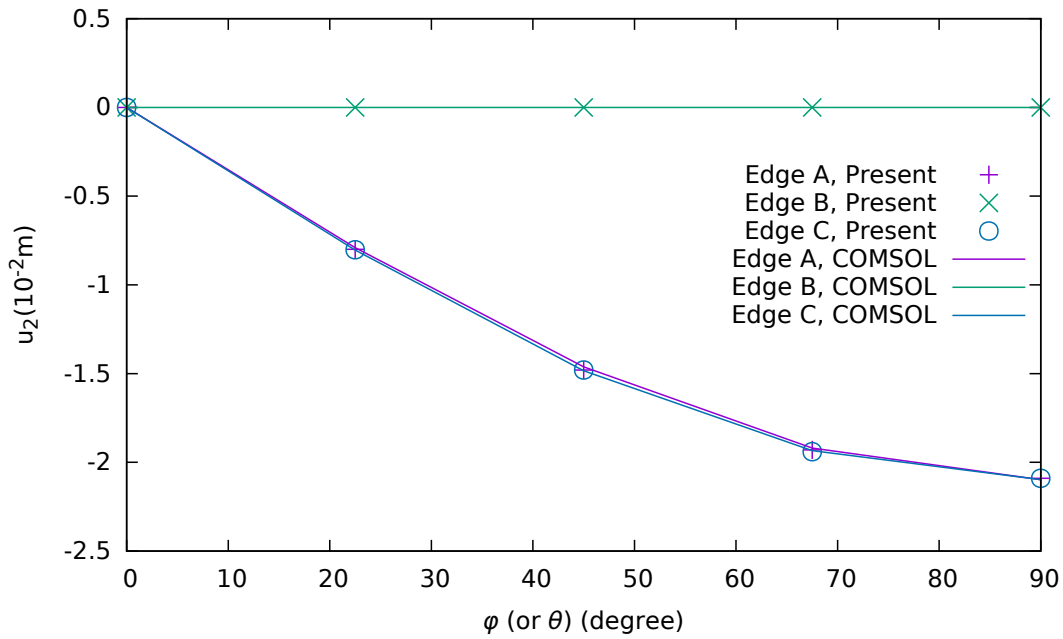
Figure 6.7: The displacement $u_2$ on the edges of the one-eighth spheroid.
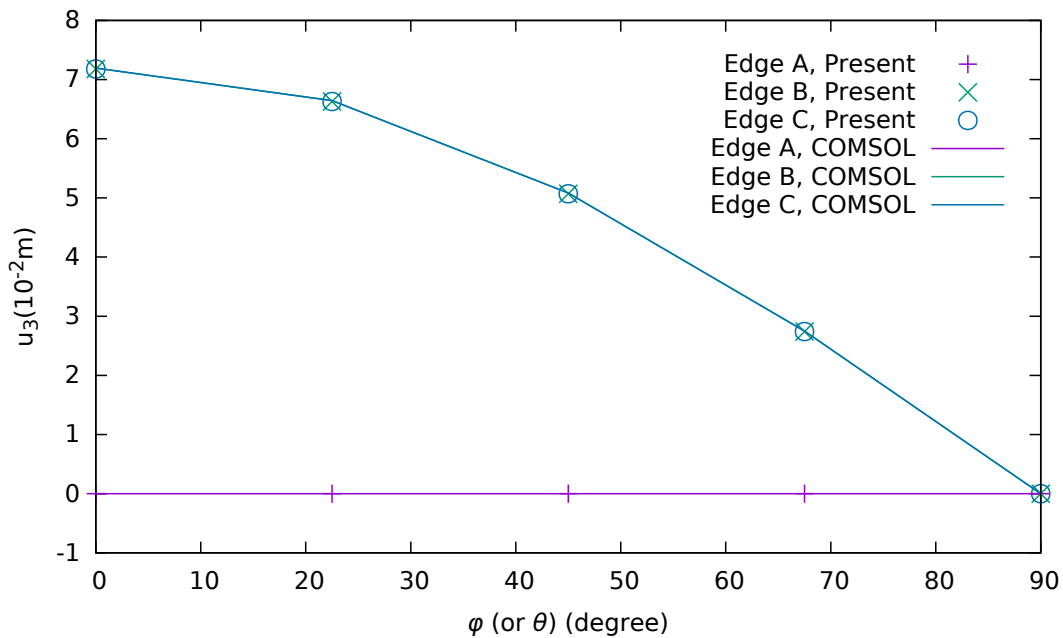


Figure 6.8: The displacement $u_3$ on the edges of the one-eighth spheroid.

unified explicit expressions method (UEEM). The program is tested by a problem which has analytical solutions. The numerical results suggested the correctness of the coded BEM program and therefore the correctness of the Green's function and its derivatives. Then the BEM program is used to solve the problem of a cube with a spheroid cavity in the center under tension. The results agree well with the numerical results by the FEM software COMSOL. So the present BEM can be used for general structural analysis in 3D anisotropic elasticity.

# Chapter 7

# Summary and outlook

Novel explicit expressions of the 3D Green's function and its derivatives for linear elastic, piezoelectric and magnetoelectroelastic materials are presented and investigated in this thesis. The starting point for deriving the explicit expressions of the Green's function and its derivatives is the line integral expression of the Green's function and its derivatives, which can be derived by applying the Fourier transform or Radon transform followed by some elementary mathematical manipulations to the governing equations for the Green's function. A straightforward way to derive the explicit expressions is applying the residue calculus to the line integrals, which is referred to as the residue calculus method (RCM) in this thesis. An alternative way is to construct the explicit expressions in terms of the solutions of a standard eigenvalue problem, or Stroh eigenvalue problem. This method is referred to as the Stroh formalism method (SFM) in this thesis. However, the numerical evaluation of the RCM and SFM has some troubles in the degenerate and nearly degenerate cases when the Stroh eigenvalues or the roots of the characteristic equation are identical or very close to each other. By a proper rewritten of the explicit expressions resulting from the residue calculus, novel unified explicit expressions of the Green's function and its derivatives are obtained. Here, unified means that the explicit expressions keep the same form and are applicable for all cases including non-degenerate, nearly degenerate and degenerate cases. The serious difficulty arising in the numerical evaluation of the RCM and SFM doesn't occur in the numerical evaluation of the unified explicit expressions. This method is referred to as unified explicit expression method (UEEM) in this thesis.

The derivations of the explicit expressions of the Green's function and its derivatives for anisotropic linear elastic materials by the three methods as well as the numerical integration method (NIM) are presented in Chapter 3. For the numerical computation, the RCM and SFM require a small perturbation on the material constants to avoid the nearly degenerate and degenerate cases in order to keep a general evaluation procedure for the Green's function and its derivatives, while the UEEM does not has such a requirement. The accuracy and efficiency of the three methods, as well as the NIM, are compared with each other. It is shown that the UEEM exhibits the highest accuracy and efficiency for the numerical evaluation of the Green's function and its derivatives for the anisotropic linear elastic materials. However, due to the mathematical complexity, the UEEM is difficult to be extended directly to the derivative evaluations of the Green's function for the linear piezoelectric and magnetoelectroelastic materials. For this reason, in Chapter 4, only the RCM and SFM are directly extended to derive the explicit expressions of the Green's func-

tion and its derivatives for the anisotropic linear piezoelectric materials. By the numerical evaluations of these two methods, it is shown that 1) if similar accuracy is required, the SFM is more efficient than the RCM, and 2) to retain a generally valid evaluation procedure, the required perturbation of the material constants by the SFM is smaller than that by the RCM. Thus, only the SFM is extended to derive the explicit expressions of the Green's function and its derivatives for the anisotropic linear magnetoelectroelastic materials in Chapter 5. As representative applications, the UEEM is implemented into a boundary element method (BEM) FORTRAN-program for anisotropic linear elastic materials. The numerical examples by using the developed BEM program in Chapter 6 show the correctness and accuracy of the implemented BEM program in this work. Therefore, the potential applications of the UEEM in the BEM programming are demonstrated.

As future research works, the UEEM should be extended to the linear piezoelectric and magnetoelectroelastic materials, because it is in all likelihood the most efficient and accurate one among the three aforementioned methods with explicit expressions. Besides, the implementations of different explicit expressions of the Green's function and its derivatives for linear piezoelectric and magnetoelectroelastic materials into the BEM should be conducted in future.

# Appendix A

# Residue calculus of an improper line integral

In the complex analysis, the Cauchy residue theorem is a powerful tool to calculate the contour integrals, i.e., the line integrals defined over closed curves; it can be used to evaluate real integrals as well. In the complex plane, the equation of Cauchy residue theorem is

$$\oint_\gamma f(z)dz = 2\pi i \sum \text{Res}(f, p_k), \tag{A.1}$$

where $\gamma$ is a closed curve, variables $p_k$ are poles of the function $f(z)$ inside the curve $\gamma$, and $\text{Res}(f, p_k)$ is the residue of the function $f(z)$ at a pole $p_k$. If $p_k$ is a pole of $m$-order, then

$$\text{Res}(f, p_k) = \frac{1}{(m-1)!} \lim_{p \to p_k} \frac{d^{m-1}}{dp^{m-1}} [(p - p_k)^m f(p)]. \tag{A.2}$$

The integral

$$\int_{-\infty}^{+\infty} f(x)dx, \tag{A.3}$$

where $f(x) = \sum_{k=0}^m b_k x^k / \sum_{k=0}^n a_k x^k$ with $a_n \neq 0$ and $n > m$, arises in the study of the Green's function for the general anisotropic materials. It resists the techniques of elementary calculus but can be evaluated as a limit of a contour integral in the complex plane. As illustrated in Fig. A.1, the contour goes along the real line from A to B, and then counterclockwise along a semicircle centered at the origin from B to A through C. The radius $\xi$ of the semicircle is large enough to allow the semicircle includes all poles with positive imaginary parts. The contour integral is $\oint_\Gamma f(z)dz$. Since the contour can be divided into a straight line AB and an arc BCA, we have

$$\oint_\Gamma f(z)dz = \int_{AB} f(z)dz + \int_{BCA} f(z)dz = 2\pi i \sum \text{Res}(f, p_k), \quad \text{Im}(p_k) > 0. \tag{A.4}$$

When $z$ is on the straight line AB, the integral on the line is

$$\int_{AB} f(z)dz = \int_{-\xi}^{+\xi} f(x)dx \tag{A.5}$$

When $z$ is on the arc BCA, substitution of $z = x + yi = \xi e^{i\theta}$ into $f(z)$ leads to

$$\int_{BCA} f(z)dz = \int_0^\pi \frac{\sum_{k=0}^m b_k \xi^k e^{k\theta i}}{\sum_{k=0}^n a_k \xi^k e^{k\theta i}} d\theta. \tag{A.6}$$
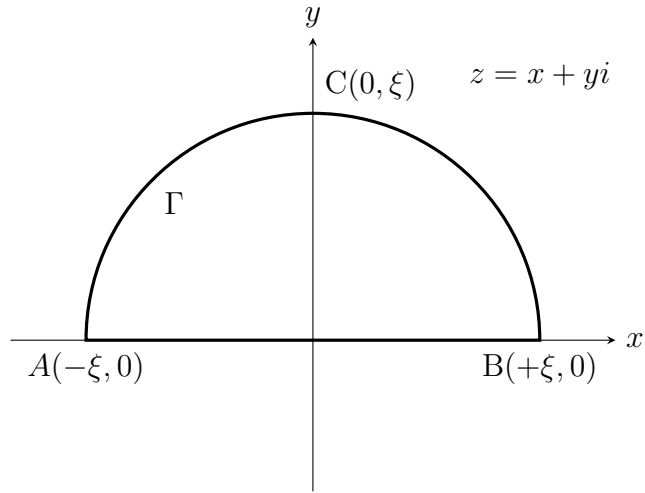
Figure A.1: The contour $\Gamma$.

When $\xi \to \infty$, the integrand of the right integral in Eq. (A.6) vanish since $n > m$ while $\theta$ is independent of $\xi$. Therefore $\lim_{\xi \to \infty} \int_{BCA} f(z)dz = 0$. Then we have

$$\int_{-\infty}^{+\infty} f(x)dx = 2\pi i \sum \text{Res}(f, p_k), \quad \text{Im}(p_k) > 0. \tag{A.7}$$

Some literature on the explicit evaluation of the Green's function by the residue calculus had directly given the above equation. We give the proof here for the reader's convenience to understand Eq. (A.7), which will be used in the following chapters.

# Appendix B

# Explicit expressions of $\mathbf{N}_{,i}$ and $\mathbf{N}_{,ij}$

In this appendix, the derivatives of $\mathbf{N}$ for elastic, piezoelectric and magnetoelectroelastic materials are presented in a unified form.

Given any two orthogonal unit vectors $\boldsymbol{n}$ and $\boldsymbol{m}$ on the oblique plane perpendicular to $\boldsymbol{x}$, $\mathbf{N}$ is defined as

$$\mathbf{N} = \begin{pmatrix} \mathbf{N}_1 & \mathbf{N}_2 \\ \mathbf{N}_3 & \mathbf{N}_1^T \end{pmatrix}, \tag{B.1}$$

$$\mathbf{N}_1 = -\mathbf{T}^{-1}\mathbf{R}^T, \quad \mathbf{N}_2 = \mathbf{T}^{-1} = \mathbf{N}_2^T, \quad \mathbf{N}_3 = \mathbf{R}\mathbf{T}^{-1}\mathbf{R}^T - \mathbf{Q},$$

with

$$Q_{IJ} = C_{kIJl}n_k n_l, \quad R_{IJ} = C_{kIJl}n_k m_l, \quad T_{IJ} = C_{kIJl}m_k m_l, \tag{B.2}$$

where the repeated lowercase letters denote summation from 1 to 3, and the capital letters $I$ and $J$ are from 1 to 3 in elasticity, from 1 to 4 in piezoelectricity, and from 1 to 5 in magnetoelectroelasticity. In the program, it is convenience to note that

$$\mathbf{N}_2 = \mathbf{T}^{-1}, \quad \mathbf{N}_1 = -\mathbf{N}_2\mathbf{R}^T, \quad \mathbf{N}_3 = -\mathbf{R}\mathbf{N}_1 - \mathbf{Q}. \tag{B.3}$$

The derivatives of $\mathbf{N}$ mainly consist of the derivatives of $\mathbf{N}_1$, $\mathbf{N}_2$ and $\mathbf{N}_3$. Since $(\mathbf{T}^{-1})_{,i} = -\mathbf{T}^{-1}\mathbf{T}_{,i}\mathbf{T}^{-1}$, which can be obtained by taking the derivative of $\mathbf{T}^{-1}\mathbf{T} = \mathbf{I}$, the first derivatives of $\mathbf{N}_1$, $\mathbf{N}_2$ and $\mathbf{N}_3$ are

$$\mathbf{N}_{2,i} = -\mathbf{N}_2\mathbf{T}_{,i}\mathbf{N}_2, \quad \mathbf{N}_{1,i} = -\mathbf{N}_{2,i}\mathbf{R}^T - \mathbf{N}_2\mathbf{R}_{,i}^T, \quad \mathbf{N}_{3,i} = -\mathbf{R}_{,i}\mathbf{N}_1 - \mathbf{R}\mathbf{N}_{1,i} - \mathbf{Q}_{,i}. \tag{B.4}$$

The second derivative is obtained by taking an additional the derivative of the first derivative, i.e.,

$$\begin{aligned}
\mathbf{N}_{2,ij} &= -\mathbf{N}_{2,j}\mathbf{T}_{,i}\mathbf{N}_2 - \mathbf{N}_2\mathbf{T}_{,ij}\mathbf{N}_2 - \mathbf{N}_2\mathbf{T}_{,i}\mathbf{N}_{2,j}, \\
\mathbf{N}_{1,ij} &= -\mathbf{N}_{2,ij}\mathbf{R}^T - \mathbf{N}_{2,i}\mathbf{R}_{,j}^T - \mathbf{N}_{2,j}\mathbf{R}_{,i}^T - \mathbf{N}_2\mathbf{R}_{,ij}^T, \\
\mathbf{N}_{3,ij} &= -\mathbf{R}_{,ij}\mathbf{N}_1 - \mathbf{R}_{,i}\mathbf{N}_{1,j} - \mathbf{R}_{,j}\mathbf{N}_{1,i} - \mathbf{R}\mathbf{N}_{1,ij} - \mathbf{Q}_{,ij}.
\end{aligned} \tag{B.5}$$

The derivatives of $\mathbf{Q}$, $\mathbf{R}$ and $\mathbf{T}$ are expressed in terms of $\boldsymbol{n}$ and $\boldsymbol{m}$ and their derivatives which are presented in the following after a proper choice of $\boldsymbol{n}$ and $\boldsymbol{m}$.

For any point except $x_1 = x_2 = 0$, $\boldsymbol{n}$ and $\boldsymbol{m}$ are chosen as

$$\boldsymbol{n} = \frac{1}{\rho}\left[-x_2, x_1, 0\right], \quad \boldsymbol{m} = \frac{1}{\rho r}\left[-x_1 x_3, -x_2 x_3, x_1^2 + x_2^2\right], \tag{B.6a}$$

where

$$\rho = \sqrt{x_1^2 + x_2^2}, \quad r = \sqrt{x_1^2 + x_2^2 + x_3^2}. \tag{B.6b}$$

The non-zero derivatives of $\rho$ and $r$ are

$$\rho_{,i} = x_i/\rho, \quad \rho_{,ij} = (\delta_{ij} - \rho_{,i}\rho_{,j})/\rho, \quad i, j \neq 3,$$
$$r_{,i} = x_i/r, \quad r_{,ij} = (\delta_{ij} - r_{,i}r_{,j})/r. \tag{B.7}$$

Introducing

$$\hat{\boldsymbol{n}} = [-x_2, x_1, 0], \quad \hat{\boldsymbol{m}} = \left[-x_1x_3, -x_2x_3, x_1^2 + x_2^2\right], \tag{B.8}$$

the derivatives of $\boldsymbol{n}$ and $\boldsymbol{m}$ are given by

$$\boldsymbol{n}_{,i} = (\hat{\boldsymbol{n}}_{,i} - \rho_{,i}\boldsymbol{n})/\rho,$$
$$\boldsymbol{n}_{,ij} = -(\rho_{,ij}\boldsymbol{n} + \rho_{,i}\boldsymbol{n}_{,j} + \rho_{,j}\boldsymbol{n}_{,i})/\rho,$$
$$\boldsymbol{m}_{,i} = [\hat{\boldsymbol{m}}_{,i} - (\rho r)_{,i}\boldsymbol{m}]/(\rho r),$$
$$\boldsymbol{m}_{,ij} = [\hat{\boldsymbol{m}}_{,ij} - (\rho r)_{,ij}\boldsymbol{m} - (\rho r)_{,i}\boldsymbol{m}_{,j} - (\rho r)_{,j}\boldsymbol{m}_{,i}]/(\rho r), \tag{B.9a}$$

where

$$(\rho r)_{,i} = \rho_{,i}r + \rho r_{,i},$$
$$(\rho r)_{,ij} = \rho_{,ij}r + \rho_{,i}r_{,j} + \rho_{,j}r_{,i} + \rho r_{,ij},$$
$$\hat{\boldsymbol{n}}_{,i} = [-\delta_{2i}, \delta_{1i}, 0], \quad \hat{\boldsymbol{n}}_{,ij} = 0,$$
$$\hat{\boldsymbol{m}}_{,i} = [-\delta_{1i}x_3 - \delta_{3i}x_1, -\delta_{2i}x_3 - \delta_{3i}x_2, 2x_1\delta_{1i} + 2x_2\delta_{2i}],$$
$$\hat{\boldsymbol{m}}_{,ij} = [-\delta_{1i}\delta_{3j} - \delta_{3i}\delta_{1j}, -\delta_{2i}\delta_{3j} - \delta_{3i}\delta_{2j}, 2\delta_{1i}\delta_{1j} + 2\delta_{2i}\delta_{2j}]. \tag{B.9b}$$

Another possible choice for the orthogonal vectors $\boldsymbol{n}$ and $\boldsymbol{m}$ is

$$\boldsymbol{n} = \frac{1}{\rho}[-x_3, 0, x_1], \quad \boldsymbol{m} = \frac{1}{\rho r}\left[-x_1x_2, x_1^2 + x_3^2, -x_2x_3\right], \tag{B.10a}$$

where

$$\rho = \sqrt{x_1^2 + x_3^2}, \quad r = \sqrt{x_1^2 + x_2^2 + x_3^2}. \tag{B.10b}$$

Note that this choice is applicable everywhere except on the line $x_1 = x_3 = 0$, and we apply it at points $x_1 = x_2 = 0$, $x_3 \neq 0$ which are excluded in the previous choice for vectors $\boldsymbol{n}$ and $\boldsymbol{m}$. Following the previous procedure, when $x_1 = x_2 = 0$, most components of the derivatives of $\boldsymbol{n}$ and $\boldsymbol{m}$ are zero except the following ones

$$n_{3,1} = 1/|x_3|, \quad n_{1,11} = \text{sgn}(x_3)/x_3^2,$$
$$n_{3,13} = n_{3,31} = -\text{sgn}(x_3)/x_3^2,$$
$$m_{3,2} = -1/x_3, \quad m_{1,12} = m_{1,21} = -1/x_3^2,$$
$$m_{2,22} = -1/x_3^2, \quad m_{3,23} = m_{3,32} = 1/x_3^2. \tag{B.11}$$

By using the above given relations, the explicit expressions for the derivatives of $\mathbf{N}$ can be obtained.

# Appendix C

# Auxiliary functions $F_m^{(n)}$ for the second derivative of the Green's function

The functions $F_m^{(\alpha)}(...)$ for $m = 4, 5, ..., 11$ and $\alpha = 0, 1$ arising in Eq. (3.81) are given in the following.

$$F_4^{(0)}(x_1, \ldots, x_7) = \left[\prod_{i=3}^{7}(x_1 - x_i)(x_2 - x_i)\right]^{-1} \times$$

$$[y_1^4 + y_2^2 - y_1^3 y_3 - y_2 y_4 + y_1^2(-3y_2 + y_4) + y_1(2y_2 y_3 - y_5) + y_6],$$

$$F_5^{(0)}(x_1, \ldots, x_7) = \left[\prod_{i=4}^{7}(x_1 - x_i)(x_2 - x_i)(x_3 - x_i)\right]^{-1}$$

$$[y_2^3 + y_3^2 + y_2^2(-y_1 y_4 + y_4^2 - 2y_5) + y_3 y_4(y_1^2 - y_1 y_4 + y_5) - 2y_3 y_6$$
$$+ y_6(-y_1(y_1^2 - y_1 y_4 + y_5) + y_6) - (y_1^2 - y_1 y_4 + y_5)y_7$$
$$+ y_2(y_3 y_4 + y_1^2 y_5 + y_5^2 - y_1(2y_3 + y_4 y_5 - 3y_6) - 2y_4 y_6 + y_7)],$$

$$F_m^{(1)}(x_1, \ldots, x_7) = F_{m-2}^{(0)}(x_1, \ldots, x_6) + x_7 F_m^{(0)}(x_1, \ldots, x_7), \quad m = 4, 5. \qquad \text{(C.1)}$$

In Eq. (C.1), $y_i$ in $F_4^{(0)}(x_1, \ldots, x_7)$ are defined by

$$y_i = \begin{cases} e_i(x_1, x_2), & i = 1, 2, \\ e_{i-2}(x_3, \ldots, x_7), & i = 3, 4, \ldots, 7, \end{cases} \qquad \text{(C.2)}$$

and $y_i$ in $F_5^{(0)}(x_1, \ldots, x_7)$ are defined by

$$y_i = \begin{cases} e_i(x_1, x_2, x_3), & i = 1, 2, 3, \\ e_{i-3}(x_4, \ldots, x_7), & i = 4, 5, \ldots, 7. \end{cases} \qquad \text{(C.3)}$$

Here and in what follows, $e_i(\ldots)$ is the elementary symmetric polynomial defined by Eq. (3.72).

$$F_6^{(0)}(x_1, \ldots, x_8) = \left[\prod_{i=3}^{8}(x_1 - x_i)(x_2 - x_i)\right]^{-1} \times$$

$$[y_1^5 - y_1^4 y_3 + y_1^3(-4y_2 + y_4) + y_1^2(3y_2 y_3 - y_5)$$
$$+ y_2(-y_2 y_3 + y_5) + y_1(3y_2^2 - 2y_2 y_4 + y_6) - y_7], \tag{C.4a}$$

$$F_7^{(0)}(x_1, \ldots, x_8) = \left[ \prod_{i=4}^{8} (x_1 - x_i)(x_2 - x_i)(x_3 - x_i) \right]^{-1} \times$$

$$[y_2^4 + y_3^2 y_4^2 + y_2^3(-y_1 y_4 + y_4^2 - 2y_5) - y_3^2 y_5 + y_3 y_5 y_6 + y_1^4 y_7 - 2y_3 y_4 y_7$$
$$+ y_2^2(y_3 y_4 + y_1^2 y_5 + y_5^2 - y_1(3y_3 + y_4 y_5 - 3y_6) - 2y_4 y_6 + 2y_7) + y_3 y_8$$
$$+ y_1^3(y_8 - y_3 y_5 - y_4 y_7) + y_1^2(y_3^2 + y_3 y_4 y_5 + y_5 y_7 - y_4 y_8) - y_6 y_8$$
$$+ y_7^2 - y_1(2y_3^2 y_4 + y_3(y_5^2 - 3y_7) + y_6 y_7 - y_5 y_8) + y_2(2y_3^3 - 2y_5 y_7$$
$$+ y_3(2y_1(y_1 - y_4)y_4 + (2y_1 + y_4)y_5 - 3y_6) + y_6^2 + y_1^2(y_4 y_6 - 4y_7)$$
$$- y_1(y_5 y_6 - 3y_4 y_7 + 2y_8) - y_1^3 y_6 + y_4 y_8)], \tag{C.4b}$$

$$F_8^{(0)}(x_1, \ldots, x_8) = \left[ \prod_{i=5}^{8} (x_1 - x_i)(x_2 - x_i)(x_3 - x_i)(x_4 - x_i) \right]^{-1} \times$$

$$[y_3^3 + y_2^2 y_4 y_5 - y_4^2 y_5 + y_2 y_4 y_5^3 - 2y_2 y_4 y_5 y_6 + y_4 y_5 y_6^2 - y_2^3 y_7 + 2y_2 y_4 y_7$$
$$- y_2^2 y_5^2 y_7 - y_4 y_5^2 y_7 + 2y_2^2 y_6 y_7 - 2y_4 y_6 y_7 + 2(y_4 y_5 + (-y_2 + y_6)y_7)y_8$$
$$- y_3^2(y_2 y_5 - y_1 y_5^2 + y_5^3 + 2y_1 y_6 - 3y_5 y_6 + 3y_7) - y_2 y_6^2 y_7 + 2y_2 y_5 y_7^2$$
$$+ y_1^2(y_4(y_5 y_6 - 2y_7) - y_7(y_2 y_6 + y_5 y_7) + (y_5(y_2 + y_6) + y_7)y_8) - y_7^3$$
$$+ y_1(y_4^2 - y_4 y_5(y_5(y_2 + y_6) - 3y_7) + y_7(y_2^2 y_5 + y_2 y_5 y_6 - 3y_2 y_7 + y_6 y_7)$$
$$- 2y_4 y_8 - (y_2^2 + y_2(y_5^2 - 2y_6) + y_6^2 + y_5 y_7)y_8 + y_8^2) + y_3(-y_4 y_5^2 + y_2^2 y_6$$
$$+ 2y_4 y_6 + y_6^3 - 3y_5 y_6 y_7 + 3y_7^2 - y_2(2y_4 + y_1 y_5 y_6 - y_5^2 y_6 + 2y_6^2 - 3y_1 y_7$$
$$+ y_5 y_7 - 2y_8) + 2y_5^2 y_8 - 2y_6 y_8 + y_1^2(y_6^2 - 2y_5 y_7 + y_8)$$
$$+ y_1(y_4 y_5 + 2y_5^2 y_7 + y_6 y_7 - y_5(y_6^2 + 3y_8))) - y_5 y_8^2 + y_1^3(y_7^2 - y_6 y_8)], \tag{C.4c}$$

$$F_m^{(1)}(x_1, \ldots, x_8) = F_{m-2}^{(0)}(x_1, \ldots, x_7) + x_8 F_m^{(0)}(x_1, \ldots, x_8), \quad m = 6, 7,$$
$$F_8^{(1)}(x_1, \ldots, x_8) = F_5^{(0)}(x_5, x_6, x_7, x_1, \ldots, x_4) + x_8 F_8^{(0)}(x_1, \ldots, x_8). \tag{C.4d}$$

In Eq. (C.4), $y_i$ in $F_6^{(0)}(x_1, \ldots, x_8)$ are defined by

$$y_i = \begin{cases} e_i(x_1, x_2), & i = 1, 2, \\ e_{i-2}(x_3, \ldots, x_8), & i = 3, 4, \ldots, 8, \end{cases} \tag{C.5}$$

$y_i$ in $F_7^{(0)}(x_1, \ldots, x_8)$ are defined by

$$y_i = \begin{cases} e_i(x_1, x_2, x_3), & i = 1, 2, 3, \\ e_{i-3}(x_4, \ldots, x_8), & i = 4, 5, \ldots, 8, \end{cases} \tag{C.6}$$

and $y_i$ in $F_8^{(0)}(x_1, \ldots, x_8)$ are defined by

$$y_i = \begin{cases} e_i(x_1, \ldots, x_4), & i = 1, 2, 3, 4, \\ e_{i-4}(x_5, \ldots, x_8), & i = 5, 6, 7, 8. \end{cases} \tag{C.7}$$

$$F_9^{(0)}(x_1,\ldots,x_9) = \left[\prod_{i=3}^{9}(x_1-x_i)(x_2-x_i)\right]^{-1} \times$$

$$[y_1^6 - y_1^5 y_3 + y_1^4(-5y_2+y_4) + y_1^3(4y_2 y_3 - y_5) + y_1^2(6y_2^2 - 3y_2 y_4 + y_6)$$
$$- y_2(y_2^2 - y_2 y_4 + y_6) - y_1(3y_2^2 y_3 - 2y_2 y_5 + y_7) + y_8], \tag{C.8a}$$

$$F_{10}^{(0)}(x_1,\ldots,x_9) = \left[\prod_{i=4}^{9}(x_1-x_i)(x_2-x_i)(x_3-x_i)\right]^{-1} \times$$

$$[y_2^5 + y_3^3 y_4 + y_2^4(y_4^2 - y_1 y_4 - 2y_5) + y_3^2 y_5^2 - y_3^2 y_4 y_6 - y_3^2 y_7 + y_3 y_6 y_7 + y_8^2$$
$$+ y_2^3(y_3 y_4 + y_1^2 y_5 + y_5^2 - y_1(4y_3 + y_4 y_5 - 3y_6) - 2y_4 y_6 + 2y_7) - y_1^5 y_8$$
$$- 2y_3 y_5 y_8 - y_7 y_9 + y_1^2(y_3^2(y_4^2 + y_5) + y_3(y_5 y_6 - 4y_8) + y_6 y_8 - y_5 y_9)$$
$$+ y_2^2(3y_3^2 + y_3(3y_1(y_1 - y_4)y_4 + (4y_1 + y_4)y_5 - 3y_6) - y_1^3 y_6 + y_6^2$$
$$+ y_1^2(y_4 y_6 - 4y_7) - 2y_5 y_7 + 2y_4 y_8 - y_1(y_5 y_6 - 3y_4 y_7 + 5y_8) - y_9)$$
$$- y_1^3(y_3 y_4(y_3 + y_6) + y_5 y_8 - y_4 y_9) + y_1^4(y_3 y_6 + y_4 y_8 - y_9) + y_3 y_4 y_9$$
$$- y_1(2y_3^3 + y_3^2(2y_4 y_5 - 3y_6) + y_7 y_8 - y_6 y_9 + y_3(y_6^2 - 3y_4 y_8 + 2y_9))$$
$$+ y_2(y_3^2(2y_4^2 - 3y_5) + y_1^4 y_7 + y_7^2 - y_1^3(2y_3 y_5 + y_4 y_7 - 5y_8) - 2y_6 y_8$$
$$+ y_5 y_9 + y_1^2(3y_3^2 + 2y_3 y_4 y_5 - 3y_3 y_6 + y_5 y_7 - 4y_4 y_8 + 3y_9)$$
$$- y_1(4y_3^2 y_4 + 2y_3(y_5^2 - y_4 y_6 - 2y_7) + y_6 y_7 - 3y_5 y_8 + 2y_4 y_9)$$
$$+ y_3(y_5 y_6 - 3y_4 y_7 + 4y_8))], \tag{C.8b}$$

$$F_{11}^{(0)}(x_1,\ldots,x_9) = \left[\prod_{i=5}^{9}(x_1-x_i)(x_2-x_i)(x_3-x_i)(x_4-x_i)\right]^{-1} \times$$

$$[y_3^4 - y_4^3 + y_1^2 y_4^2 y_5^2 - y_1 y_4^2 y_5^3 - y_1^2 y_4^2 y_6 + y_1 y_4^2 y_5 y_6 + y_4^2 y_5^2 y_6 - y_4^2 y_6^2$$
$$- 2y_4^2 y_5 y_7 + y_1^3 y_4 y_6 y_7 - y_1^2 y_4 y_5 y_6 y_7 + y_1 y_4 y_6^2 y_7 - y_4 y_6 y_7^2 + 3y_4^2 y_8$$
$$- y_3^3(y_2 y_5 - y_1 y_5^2 + y_5^3 + 2y_1 y_6 - 3y_5 y_6 + 3y_7) + y_2^4 y_8 + 2y_1^2 y_4 y_5^2 y_8$$
$$+ y_1^2 y_4 y_6 y_8 - 3y_1 y_4 y_5 y_6 y_8 + y_4 y_6^2 y_8 + 2y_4 y_5 y_7 y_8 + y_1^4 y_8^2 - 3y_4 y_8^2$$
$$- y_1 y_7 y_8^2 + y_8^3 + (-y_1^4 y_7 + y_1^3(y_4 + y_5 y_7 + y_8) - y_1^2(3y_4 y_5 + y_6 y_7$$
$$+ y_5 y_8) + y_1(y_4(2y_5^2 + y_6) + y_7^2 + y_6 y_8) - 2(y_4 y_5 y_6 - y_4 y_7 + y_7 y_8))y_9$$
$$+ (y_1^2 - y_1 y_5 + y_6)y_9^2 + y_2^3(y_5(-y_1 + y_5)y_8 - y_6(y_4 + 2y_8) + y_1 y_9)$$
$$+ y_2^2(y_4^2 + y_4 y_6((y_1 - y_5)y_5 + 2y_6) - 3y_4 y_8 + y_8(y_6(y_1^2 - y_1 y_5 + y_6)$$
$$+ (3y_1 - 2y_5)y_7 + 2y_8) + y_1(-y_1 y_5 + y_5^2 - 2y_6)y_9) + y_3^2(-y_4 y_5^2 + y_2^2 y_6$$
$$+ 2y_4 y_6 + y_6^3 - 3y_5 y_6 y_7 + 3y_7^2 - y_2(3y_4 + y_1 y_5 y_6 - y_5^2 y_6 + 2y_6^2 - 3y_1 y_7$$
$$+ y_5 y_7 - 4y_8) + 3y_5^2 y_8 - 3y_6 y_8 + y_1^2(y_6^2 - 2y_5 y_7 + 2y_8) - 2y_5 y_9$$
$$+ y_1(y_4 y_5 + 2y_5^2 y_7 + y_6 y_7 - y_5(y_6^2 + 5y_8) + 3y_9)) + y_2(y_8(y_7^2 - 2y_6 y_8)$$
$$+ y_1^2(3y_4 y_8 - y_4 y_6^2 + y_5 y_7 y_8 - 4y_8^2 - y_5 y_6 y_9 + 3y_7 y_9) + y_1^3(y_6 y_9 - y_7 y_8)$$
$$- y_4(y_6^3 + 2y_5^2 y_8 - 2y_6(y_5 y_7 + y_8)) + y_4^2 y_5^2 + y_1(y_4 y_5 y_6^2 - y_6 y_7 y_8$$
$$- 2y_4^2 y_5 - 3y_4 y_6 y_7 + y_4 y_5 y_8 + 3y_5 y_8^2 + (y_4 + y_6^2 - 2y_5 y_7 - 3y_8)y_9)$$
$$- y_9^2 + 2y_5 y_8 y_9) + y_3(y_4 y_5 y_6^2 - y_4^2 y_5 - y_2^3 y_7 - 2y_4 y_5^2 y_7 - y_4 y_6 y_7 - y_7^3$$

99

$$+ 4y_4y_5y_8 + 3y_6y_7y_8 - 3y_5y_8^2 + 3y_5y_6y_9 - 2(y_4 + y_6^2 - y_5y_7 - y_8)y_9$$
$$+ y_2^2(2y_4y_5 - y_5^2y_7 + 2y_6y_7 + y_5y_8 - 2y_9) + y_1^3(y_7^2 - 2y_6y_8 + y_5y_9)$$
$$+ y_2(2y_5y_7^2 - y_6^2y_7 + y_4(2y_5^3 - 5y_5y_6 + 3y_7) + y_5y_6y_8 - 5y_7y_8 - 2y_5^2y_9$$
$$+ 4y_6y_9) + y_1^2(y_4y_5y_6 - 3y_4y_7 - y_2y_6y_7 - y_5y_7^2 + 3y_2y_5y_8 + 2y_5y_6y_8$$
$$+ y_7y_8 - (2y_2 + y_5^2 + 2y_6)y_9) + y_1(2y_4^2 + y_6y_7^2 + y_2^2(y_5y_7 - 4y_8)$$
$$- 2y_6^2y_8 - y_5y_7y_8 + 4y_8^2 - y_4(2y_2(y_5^2 - y_6) + y_5^2y_6 - 5y_5y_7 + 6y_8)$$
$$- 4y_7y_9 + y_2(y_5y_6y_7 - 3y_7^2 - 3y_5^2y_8 + 4y_6y_8 + 3y_5y_9)))$$
$$+ y_1y_4^2y_7 - 2y_1^3y_4y_5y_8 - y_1^3y_5y_8^2 + y_1^2y_6y_8^2]$$

$$F_m^{(1)}(x_1, \ldots, x_9) = F_{m-3}^{(0)}(x_1, \ldots, x_8) + x_9 F_m^{(0)}(x_1, \ldots, x_9), \quad m = 9, 10, 11. \tag{C.9}$$

In Eq. (C.9), $y_i$ in $F_9^{(0)}(x_1, \ldots, x_9)$ are defined as

$$y_i = \begin{cases} e_i(x_1, x_2), & i = 1, 2, \\ e_{i-2}(x_3, \ldots, x_9), & i = 3, 4, \ldots, 9, \end{cases} \tag{C.10}$$

$y_i$ in $F_{10}^{(0)}(x_1, \ldots, x_9)$ are defined as

$$y_i = \begin{cases} e_i(x_1, x_2, x_3), & i = 1, 2, 3, \\ e_{i-3}(x_4, \ldots, x_9), & i = 4, 5, \ldots, 9, \end{cases} \tag{C.11}$$

and $y_i$ in $F_{11}^{(0)}(x_1, \ldots, x_9)$ are defined as

$$y_i = \begin{cases} e_i(x_1, \ldots, x_4), & i = 1, 2, 3, 4, \\ e_{i-4}(x_5, \ldots, x_9), & i = 5, 6, \ldots, 9. \end{cases} \tag{C.12}$$

It should be mentioned here that $y_i$ in different $F_m^{(\alpha)}(...)$ have different definitions.

# Appendix D

# Explicit expression of the Stroh eigenvector $\boldsymbol{\xi}$

In this appendix, we list the explicit expressions of the Stroh eigenvectors $\boldsymbol{\xi}$, i.e., $\boldsymbol{a}$ and $\boldsymbol{b}$. Note that the notations in this appendix follow those in Ref. Hwu (2010). For more details, please refer to Ref. Hwu (2010).

The explicit expressions of $\boldsymbol{a}$ and $\boldsymbol{b}$ are given by

$$\boldsymbol{a} = \begin{Bmatrix} a_1 \\ a_2 \\ a_3 \\ a_4 \end{Bmatrix} = \begin{Bmatrix} p_1 b_2 + q_1 b_3 + r_1 b_4 \\ \left( p_2 b_2 + q_2 b_3 + r_2 b_4 \right)/\mu \\ \left( p_4 b_2 + q_4 b_3 + r_4 b_4 \right)/\mu \\ p_4 b_2 + q_7 b_3 + r_7 b_4 \end{Bmatrix}, \tag{D.1a}$$

where

$$\begin{aligned} p_j &= \mu^2 \hat{S}'^D_{j1} + \hat{S}'^D_{j2} - \mu \hat{S}'^D_{j6}, \\ q_j &= \hat{S}'^D_{j4} - \mu \hat{S}'^D_{j5}, \\ r_j &= \hat{S}'^D_{j8} - \mu \hat{S}'^D_{j7}, \quad j = 1, 2, 4, 7, \end{aligned} \tag{D.1b}$$

and

$$\boldsymbol{b} = \begin{Bmatrix} b_1 \\ b_2 \\ b_3 \\ b_4 \end{Bmatrix} = c \begin{Bmatrix} \mu l_4^* \\ -l_4^* \\ l_3^* \\ m_3^* \end{Bmatrix}, \quad \text{or} \quad c \begin{Bmatrix} \mu l_3^* \\ -l_3^* \\ l_2^* \\ m_2^* \end{Bmatrix}, \quad \text{or} \quad c \begin{Bmatrix} \mu m_3^* \\ -m_3^* \\ m_2^* \\ \rho_2^* \end{Bmatrix}. \tag{D.2}$$

In Eq. (D.2),

$$\begin{aligned} l_2^* &= l_4 \rho_2 - m_3^2, & l_3^* &= m_2 m_3 - l_3 \rho_2, & l_4^* &= l_2 \rho_2 - m_2^2, \\ m_2^* &= l_3 m_3 - l_4 m_2, & m_3^* &= l_3 m_2 - l_2 m_3, & \rho_2^* &= l_2 l_4 - l_3^2, \end{aligned} \tag{D.3}$$

where

$$\begin{aligned} l_2 &= \hat{S}'^D_{55} \mu^2 - 2 \hat{S}'^D_{45} \mu + \hat{S}'^D_{44}, \\ l_3 &= \hat{S}'^D_{15} \mu^3 - \left( \hat{S}'^D_{14} + \hat{S}'^D_{56} \right) \mu^2 + \left( \hat{S}'^D_{25} + \hat{S}'^D_{46} \right) \mu - \hat{S}'^D_{24}, \\ l_4 &= \hat{S}'^D_{11} \mu^4 - 2 \hat{S}'^D_{16} \mu^3 + \left( 2 \hat{S}'^D_{12} + \hat{S}'^D_{66} \right) \mu^2 - 2 \hat{S}'^D_{26} \mu + \hat{S}'^D_{22}, \\ m_2 &= \hat{g}'_{15} \mu^2 - \left( \hat{g}'_{14} + \hat{g}'_{25} \right) \mu + \hat{g}'_{24}, \end{aligned}$$

101

$$m_3 = \hat{g}'_{11}\mu^3 - \left(\hat{g}'_{21} + \hat{g}'_{16}\right)\mu^2 + \left(\hat{g}'_{12} + \hat{g}'_{26}\right)\mu - \hat{g}'_{22},$$
$$\rho_2 = -\hat{\beta}'^{\sigma}_{11}\mu^2 + 2\hat{\beta}'^{\sigma}_{12}\mu - \hat{\beta}'^{\sigma}_{22}. \tag{D.4}$$

In the above equations, $\hat{S}'^D_{ij}$, $\hat{g}'_{ij}$ and $\hat{\beta}'^{\sigma}_{ij}$ are the reduced piezoelectric compliances, and $\mu$ represents the Stroh eigenvalues which are the roots of

$$l_2 l_4 \rho_2 + 2 l_3 m_2 m_3 - l_2 m_3^2 - l_4 m_2^2 - \rho_2 l_3^2 = 0. \tag{D.5}$$

In Eq. (D.2) $c$ is the scaling factor. To have a unique value for the eigenvectors, for each Stroh eigenvalue $\mu_k$ the scaling factor $c_k$ is determined by

$$c_k^2 = \frac{1}{2(a_{1k}b_{1k} + a_{2k}b_{2k} + a_{3k}b_{3k} + a_{4k}b_{4k})}, \quad k = 1, 2, 3, 4, \tag{D.6}$$

where $a_{jk}$ and $b_{jk}$ are the components of $\boldsymbol{a}$ and $\boldsymbol{b}$ before scaling.

# Bibliography

M. Akamatsu and K. Tanuma. Green's function of anisotropic piezoelectricity. *Proceedings of the Royal Society of London A: Mathematical, Physical and Engineering Sciences*, 453(1958):473–487, 1997.

M. H. Aliabadi. A new generation of boundary element methods in fracture mechanics. *International Journal of Fracture*, 86(1-2):91–125, 1997.

M. H. Aliabadi. *The Boundary Element Method: Applications in Solids and Structures, Vol. 2.* John Wiley & Sons, New York, 2002.

V. I. Alshits, A. N. Darinskii, and J. Lothe. On the existence of surface waves in half-infinite anisotropic elastic media with piezoelectric and piezomagnetic properties. *Wave Motion*, 16(3):265–283, 1992.

E. Anderson, Z. Bai, C. Bischof, S. Blackford, J. Demmel, J. Dongarra, J. Du Croz, A. Greenbaum, S. Hammerling, A. McKenney, et al. *LAPACK Users' Guide*, volume 9. SIAM, 1999.

D. M. Barnett. The precise evaluation of derivatives of the anisotropic elastic Green's functions. *Physica Status Solidi (b)*, 49(2):741–748, 1972.

D. M. Barnett and J. Lothe. Dislocations and line charges in anisotropic piezoelectric insulators. *Physica Status Solidi (b)*, 67(1):105–111, 1975.

Y. Benveniste. Magnetoelectric effect in fibrous composites with piezoelectric and piezomagnetic phases. *Physical Review B*, 51(22):16424, 1995.

F. C. Buroni and A. Sáez. Three-dimensional Green's function and its derivative for materials with general anisotropic magneto-electro-elastic coupling. *Proceedings of the Royal Society A: Mathematical, Physical and Engineering Science*, 466(2114):515–537, 2010.

F. C. Buroni and A. Sáez. Unique and explicit formulas for Green's function in three-dimensional anisotropic linear elasticity. *ASME Journal of Applied Mechanics*, 80: 051018–1–14, 2013.

F. C. Buroni, J. E. Ortiz, and A. Sáez. Multiple pole residue approach for 3D BEM analysis of mathematical degenerate and non-degenerate materials. *International Journal for Numerical Methods in Engineering*, 86(9):1125–1143, 2011.

T. Chen. Green's functions and the non-uniform transformation problem in a piezoelectric medium. *Mechanics Research Communications*, 20:271–278, 1993.

T. Chen and F.-Z. Lin. Numerical evaluation of derivatives of the anisotropic piezoelectric Green's functions. *Mechanics Research Communications*, 20:501–506, 1993.

M. Chung and T. Ting. The Green function for a piezoelectric piezomagnetic magneto-electric anisotropic elastic medium with an elliptic hole or rigid inclusion. *Philosophical Magazine Letters*, 72(6):405–410, 1995.

T. A. Cruse. *The Direct Potential Method in Three Dimensional Elastostatics*. Carnegie-Mellon University, Carnegie Institute of Technology, Department of Mechanical Engineering, 1968.

T. A. Cruse. An improved boundary-integral equation method for three dimensional elastic stress analysis. *Computers and Structures*, 4(4):741–754, 1974.

T. A. Cruse and F. J. Rizzo. A direct formulation and numerical solution of the general transient elastodynamic problem. i. *Journal of Mathematical Analysis and Applications*, 22(1):244–259, 1968.

P. H. Dederichs and G. Liebfried. Elastic Green's function for anisotropic cubic crystals. *Physical Review*, 188:1175–1183, 1969.

W. F. J. Deeg. *The Analysis of Dislocation, Crack, and Inclusion Problems in Piezoelectric Solids*. PhD thesis, Standford University, 1980.

H. Ding and A. Jiang. Fundamental solutions for transversely isotropic magneto-electro-elastic media and boundary integral formulation. *Science in China Series E: Technological Sciences*, 46(6):607–619, 2003.

H. Ding, J. Liang, and B. Chen. Fundamental solutions for transversely isotropic piezoelectric media. *Science in China Series A*, 7:009, 1996.

M. L. Dunn. Electroelastic Green's functions for transversely isotropic piezoelectric media and their application to the solution of inclusion and inhomogeneity problems. *International Journal of Engineering Science*, 32:119–131, 1994.

M. L. Dunn and H. A. Wienecke. Green's functions for transversely isotropic piezoelectric solids. *International Journal of Solids and Structures*, 33(30):4571–4581, 1996.

W. Eerenstein, N. D. Mathur, and J. F. Scott. Multiferroic and magnetoelectric materials. *nature*, 442(7104):759–765, 2006.

J. D. Eshelby, W. T. Read, and W. Shockley. Anisotropic elasticity with applications to dislocation theory. *Acta Metallurgica*, 1(3):251–259, 1953.

R. Fitzpatrick. *Maxwell's Equations and the Principles of Electromagnetism*. INFINITY SCIENCE PRESS LLC, Hingham, 2008.

I. Fredholm. Sur les équations de l'équilibre d'un corps solide élastique. *Acta Mathematica*, 23(1):1–42, 1900.

L. Gaul, M. Kógl, and M. Wagner. *Boundary Element Methods for Engineers and Scientists*. Springer-Verlag Berlin Heidelberg New York, 2003.

L. J. Gray, D. Ghosh, and T. Kaplan. Evaluation of the anisotropic Green's function in three dimensional elasticity. *Computational Mechanics*, 17:253–261, 1996.

S. A. Gundersen and J. Lothe. A new method for numerical calculations in anisotropic elasticity problems. *Physica Status Solidi (b)*, 143(1):73–85, 1987.

J. H. Huang and W.-s. Kuo. The analysis of piezoelectric/piezomagnetic composite materials containing ellipsoidal inclusions. *Journal of Applied Physics*, 81(3):1378–1386, 1997.

C. Hwu. *Anisotropic Elastic Plates*. Springer, New York, 2010.

M. A. Jaswon. Integral equation methods in potential theory. i. *Proceedings of the Royal Society of London A: Mathematical, Physical and Engineering Sciences*, 275(1360):23–32, 1963.

M. A. Jaswon and A. R. Ponter. An integral equation solution of the torsion problem. *Proceedings of the Royal Society of London A: Mathematical, Physical and Engineering Sciences*, 273(1353):237–246, 1963.

M. A. Jenkins. Algorithm 493: Zeros of a real polynomial [c2]. *ACM Transactions on Mathematical Software (TOMS)*, 1(2):178–189, 1975.

M. A. Jenkins and J. F. Traub. A three-stage algorithm for real polynomials using quadratic iteration. *SIAM Journal on Numerical Analysis*, 7(4):545–566, 1970.

R. M. Jones. *Mechanics of composite materials*. Crc Press, 1998.

J. C. Lachat and J. O. Watson. Effective numerical treatment of boundary integral equations: a formulation for three-dimensional elastostatics. *International Journal for Numerical Methods in Engineering*, 10(5):991–1005, 1976.

A. M. Lavagnino. *Selected Static and Dynamic Problems in Anisotropic Linear Elasticity*. PhD thesis, Stanford University, Stanford, 1995.

V.-G. Lee. Explicit expression of derivatives of elastic Green's functions for general anisotropic materials. *Mechanics Research Communications*, 30(3):241–249, 2003.

V.-G. Lee. Derivatives of the three-dimensional Green's functions for anisotropic materials. *International Journal of Solids and Structures*, 46(18):3471–3479, 2009.

J. Y. Li and M. L. Dunn. Anisotropic coupled-field inclusion and inhomogeneity problems. *Philosophical Magazine A*, 77(5):1341–1350, 1998.

K.-H. C. Lie and J. Koehler. The elastic stress field produced by a point force in a cubic crystal. *Advances in Physics*, 17(67):421–478, 1968.

I. M. Lifshitz and L. N. Rozenzweig. Construction of the Green tensor for the fundamental equation of elasticity theory in the case of unbounded elastically anisotropic medium. *Zh. Eksp. Teor. Fiz*, 17:783–791, 1947.

J. Liu, X. Liu, and Y. Zhao. Green's functions for anisotropic magnetoelectroelastic solids with an elliptical cavity or a crack. *International Journal of Engineering Science*, 39 (12):1405–1418, 2001.

Y. J. Liu, S. Mukherjee, N. Nishimura, M. Schanz, W. Ye, A. Sutradhar, E. Pan, N. A. Dumont, A. Frangi, and A. Saez. Recent advances and emerging applications of the boundary element method. *Applied Mechanics Reviews*, 64(3):030802, 2011.

K. Malén. A unified six-dimensional treatment of elastic Green's functions and dislocations. *Physica Status Solidi (b)*, 44(2):661–672, 1971.

S. Mukherjee and Y. Liu. The boundary element method. *International Journal of Computational Methods*, 10(06):1350037, 2013.

T. Mura. *Micromechanics of Defects in Solids*. Kluwer Academic Pub, 1987.

T. Mura and N. Kinoshita. Green's functions for anisotropic elasticity. *Phys. Status Solidi B*, 47:607–618, 1971.

G. Nakamura and K. Tanuma. A formula for the fundamental solution of anisotropic elasticity. *Quartely Journal of Mechanics and Applied Mathematics*, 50:179–194, 1997.

R. B. Nelson. Simplified calculation of eigenvector derivatives. *AIAA journal*, 14(9): 1201–1205, 1976.

E. Pan. Three-dimensional Green's functions in anisotropic magneto-electro-elastic bimaterials. *Zeitschrift für angewandte Mathematik und Physik ZAMP*, 53(5):815–838, 2002.

E. Pan and W. Chen. *Static Green's Functions in Anisotropic Media*. Cambridge University Press, 2015.

E. Pan and F. Tonon. Three-dimensional Green's functions in anisotropic piezoelectric solids. *International Journal of Solids and Structures*, 37(6):943–958, 2000.

E. Pan and F. G. Yuan. Boundary element analysis of three-dimensional cracks in anisotropic solids. *International Journal for Numerical Methods in Engineering*, 48: 211–237, 2000.

Y.-C. Pan and T.-W. Chou. Point force solution for an infinite transversely isotropic solid. *Journal of Applied Mechanics*, 43(4):608–612, 1976.

A.-V. Phan, L. J. Gray, and T. Kaplan. On the residue calculus evaluation of the 3D anisotropic elastic Green's function. *Communications in Numerical Methods in Engineering*, 20(5):335–341, 2004.

A.-V. Phan, L. J. Gray, and T. Kaplan. Residue approach for evaluating the 3D anisotropic elastic Green's function: Multiple roots. *Engineering Analysis with Boundary Elements*, 29(6):570–576, 2005.

W. H. Press. *Numerical Recipes 3rd Edition: The Art of Scientific Computing*. Cambridge University Press, 2007.

Q.-H. Qin. Green's functions of magnetoelectroelastic solids with a half-plane boundary or bimaterial interface. *Philosophical Magazine Letters*, 84(12):771–779, 2004.

Q.-H. Qin. *Green's Function and Boundary Elements of Multifield Materials*. Elsevier, 2010.

F. J. Rizzo. An integral equation approach to boundary value problems of classical elastostatics. *Quart. Appl. Math*, 25(1):83–95, 1967.

F. J. Rizzo and D. J. Shippy. An advanced boundary integral equation method for three-dimensional thermoelasticity. *International Journal for Numerical Methods in Engineering*, 11(11):1753–1768, 1977.

M. A. Sales and L. J. Gray. Evaluation of the anisotropic Green's function and its derivatives. *Computers and Structures*, 69:247–254, 1998.

Y. C. Shiah, C. L. Tan, and R. F. Lee. Internal point solutions for displacements and stresses in 3D anisotropic elastic solids using the boundary element method. *Computer Modeling in Engineering and Sciences*, 69(2):167–179, 2010.

Y. C. Shiah, C. L. Tan, and C. Y. Wang. Efficient computation of the Green's function and its derivatives for three-dimensional anisotropic elasticity in BEM analysis. *Engineering Analysis with Boundary Elements*, 36:1746–1755, 2012.

V. Sladek and J. Sladek. Three dimensional crack analysis for an anisotropic body. *Applied Mathematical Modelling*, 6(5):374–380, 1982.

A. K. Soh, J.-X. Liu, and K. H. Hoon. Three-dimensional Green's functions for transversely isotropic magnetoelectroelastic solids. *International Journal of Nonlinear Sciences and Numerical Simulation*, 4(2):139–148, 2003.

G. Srinivasan. Magnetoelectric composites. *Annual Review of Materials Research*, 40: 153–178, 2010.

A. N. Stroh. Dislocations and cracks in anisotropic elasticity. *Philosophical Magazine*, 3 (30):625–646, 1958.

A. N. Stroh. Steady state problems in anisotropic elasticity. *J. Math. Phys*, 41(2):77–103, 1962.

G. T. Symm. Integral equation methods in potential theory. ii. *Proceedings of the Royal Society of London A: Mathematical, Physical and Engineering Sciences*, 275(1360):33–46, 1963.

J. L. Synge. *The Hypercircle in Mathematical Physics*. University Press Cambridge, 1957.

C. L. Tan, Y. C. Shiah, and C. Y. Wang. Boundary element elastic stress analysis of 3D generally anisotropic solids using fundamental solutions based on fourier series. *International Journal of Solids and Structures*, 50:2701–2711, 2013.

M. Tanaka, V. Sladek, and J. Sladek. Regularization techniques applied to boundary element methods. *Applied Mechanics Reviews*, 47(10):457–499, 1994.

T. C. T. Ting. *Anisotropic Elasticity: Theory and Applications*. Oxford University Press, USA, 1996.

T. C. T. Ting and V.-G. Lee. The three-dimensional elastostatic Green's function for general anisotropic linear elastic solids. *The Quarterly Journal of Mechanics and Applied Mathematics*, 50(3):407–426, 1997.

J. van Suchtelen. Product properties: A new application of composite materials. *Philips Res. Rep*, 27(1):28–37, 1972.

S. M. Vogel and F. J. Rizzo. An integral equation formulation of three dimensional anisotropic elastostatic boundary value problems. *Journal of Elasticity*, 3(3):203–216, 1973.

C. Y. Wang. Elastic fields produced by a point source in solids of general anisotropy. *Journal of Engineering Mathematics*, 32(1):41–52, 1997.

X. Wang and Y.-P. Shen. The general solution of three-dimensional problems in magneto-electroelastic media. *International Journal of Engineering Science*, 40(10):1069–1080, 2002.

J. R. Willis. The elastic interaction energy of dislocation loops in anisotropic media. *The Quarterly Journal of Mechanics and Applied Mathematics*, 18(4):419–433, 1965.

R. B. Wilson and T. A. Cruse. Efficient implementation of anisotropic three dimensional boundary-integral equation stress analysis. *International Journal for Numerical Methods in Engineering*, 12(9):1383–1397, 1978.

L. Xie, C. Zhang, Y. Wan, and Z. Zhong. On explicit expressions of 3D elastostatic Green's functions and their derivatives for anisotropic solids. In A. Sellier and M. H. Aliabadi, editors, *Advances in Boundary Element & Meshless Techniques XIV*, pages 286–291. EC, Ltd, UK, 2013.

L. Xie, C. Hwu, and C. Zhang. Advanced methods for calculating Green's function and its derivatives for three-dimensional anisotropic elastic solids. submitted for publication, 2015a.

L. Xie, C. Zhang, C. Hwu, J. Sladek, and V. Sladek. On two accurate methods for computing 3D Green's function and its first and second derivatives in piezoelectricity. *Engineering Analysis With Boundary Elements*, 61:183–193, 2015b.

# Curriculum Vitae

## Personal

- Name: Longtao Xie
- Chinese Citizen

## Education

- **PhD**, Structural Mechanics, University of Siegen, Germany, 2011.12 – 2016.08
    - Thesis: *Three-Dimensional Green's Function and Its Derivatives for Anisotropic Elastic, Piezoelectric and Magnetoelectroelastic Materials*
    - Advisor: Prof. Dr.-Ing. habil. Dr. h.c. Chuanzeng Zhang

- **Master**, Solid Mechanics, Tongji University, China, 2008 – 2011
    - Thesis: *Micromechanical Model for Cellular Polymer Electrets (in Chinese)*
    - Advisor: Prof. Yongping Wan

- **Bachelor**, Engineering Mechanics, Sichuan University, China, 2003 – 2007

## Funding

2011.12–2015.11, China Scholarship Council, No. 2011626148